The *C. elegans* PHR protein RPM-1: Deciphering the molecular mechanisms of neuronal development by examining a central regulatory molecule

A DISSERTATION
SUBMITTED TO THE FACULTY OF
UNIVERSITY OF MINNESOTA
BY

SCOTT BAKER

IN PARTIAL FULFILLMENT OF THE REQUIREMENTS
FOR THE DEGREE OF
DOCTOR OF PHILOSOPHY

ADVISOR: DR. BROCK GRILL

December 2015

Acknowledgements

I would first like to thank my mentor, Dr. Brock Grill, for believing in me and offering me the opportunity to pursue my Ph.D. in Pharmacology. I couldn't have asked for a better advisor, and don't think there has been a person more instrumental in my growth as a scientist.

Secondly, I would like to thank my graduate committee: Dr. Kevin Wickman, Dr. Daniel Romero, and Dr. Jocelyn Shaw. Without their input and guidance, I never would have been able to get to the point I am at today. I greatly appreciate the time they put into serving on my committee, especially given the long distance setting.

Thirdly, thank you to everyone who has ever been in the Grill lab, especially our technician Karla Opperman. She is a worm wizard and her technical support and suggestions helped make my science better.

Lastly, thank you to my family and friends who have always been there to support me and listen to me complain about my every day life as a graduate student. A special thank you to my girlfriend Chrissy, who takes the brunt of my complaints when an experiment doesn't work. Her continual support and ability to pick my spirits up kept me on the right path.

Table of Contents

List of Figures

1 Introduction

1.1 Overview of neuronal development

The central nervous system (CNS) is a massive network of neurons that communicate with each other through specialized cell-cell connections, called synapses. The brain contains billions of neurons, some forming thousands of synaptic connections with other neurons. The critical feature of the nervous system is its ability to propagate information, which requires well-controlled, reproducible organization of synaptic structures at precise locations. This suggests that explicit cellular properties must exist that create the identity and connectivity of each neuron in the brain.

In order to understand how neurons generate functional circuits, it is crucial to first determine where, when, and how synapse formation occurs. Our knowledge of how synapse formation is regulated is critical to understanding the underlying complexity of neural networks. This knowledge is also of great importance clinically, as abnormalities in synapse formation, and loss of synaptic connectivity are associated with numerous neurological disorders such as Alzheimer's disease, Parkinson's disease, and Huntington's disease. Furthermore, understanding what molecules can promote the formation of synapses and/or prevent loss of connections could lead to pharmaceutical interventions for many neurodegenerative diseases where synaptic loss occurs.

Chemical synapses are cellular specializations that mediate information flow between neurons and their target cells. These asymmetric cellular junctions

are composed of both a pre- and postsynaptic terminal, separated by a synaptic cleft filled with fibrous material consisting of soluble and membrane bound proteins, carbohydrates, and varying amounts of neurotransmitters (Scheiffele, 2003). Presynaptic terminals exist either at the ends of a terminally branched axon, or along the axon shaft if synapses are formed *en passant*. The presynaptic terminal is defined by the presence of synaptic vesicles (SV) clustered around an electron-dense region of the membrane referred to as the active zone. The active zone is also the physiologically defined site where synaptic vesicle fusion (exocytosis) and neurotransmitter release occur (Couteaux, 1963). The main function of the active zone is to convert a presynaptic action potential from the soma of the neuron into a neurotransmitter signal. The post-synaptic specialization contains receptors, ion channels, and associated proteins that together transduce the neurotransmitter signal.

Many of the molecular components that define the active zone are evolutionarily conserved and typically consist of several core proteins: RIM, Munc13, Piccolo, Bassoon, CASK, Velis, Mints, ELKs, and Liprins (Jin and Garner, 2008; Sudhof, 2012). In order for the active zone to function properly several events must occur. First, synaptic components are synthesized primarily in the neuronal cell body, and need to be transported down the axon (Hannah et al., 1999). This synaptic material is often present in axons well before the onset of synapse formation as well, to permit rapid and timely formation of synapses as axonal growth and extension occurs (Ziv and Garner, 2004). Piccolo and

Bassoon define transport vesicles that deliver active zone components to the presynaptic terminal (Shapira et al., 2003; Ziv and Garner, 2004). Additionally, the kinesin-3 family of motor proteins is specifically involved in transporting SV precursors (Pack-Chung et al., 2007). SVs from the reserve pool are translocated to the readily releasable pool, which includes SVs that are docked at the plasma membrane. SVs are docked through binding of SV proteins, such as Rab3a, with the active zone component RIM. SVs are then primed into the SNARE complex by RIM, Munc13, and Munc18 in preparation for Ca^{2+} triggered fusion (Jin and Garner, 2008). The core active zone components also recruit Ca^{2+} channels to the site of exocytosis, and through cell adhesion molecules position the active zone in apposition to the post-synaptic specialization (Sudhof, 2012).

Before a synapse forms, a neuron has to extend an axon outward and the axon needs to migrate toward the correct target. The highly dynamic tip of an extending axon, the growth cone, navigates by responding to a variety of extracellular cues and mediates migration to distant target cells where synaptic connections will be built (Dontchev and Letourneau, 2003). The most prominent and well understood guidance molecules are highly conserved and include netrins, slits, semaphorins, and ephrins (Dickson, 2002). These extracellular signals are diffusible, or anchored in the extracellular matrix or on the surface of guidepost cells. Guidance cues can be attractive or repulsive for the axonal growth cone (Kolodkin, 1996). Additionally, morphogens previously identified for controlling cell fate and tissue patterning, such as Wnts and Bone Morphogenic

Proteins, are secreted signaling molecules that act as guidance cues (Charron and Tessier-Lavigne, 2005). Membrane-bound receptors act as growth cone sensors and recognize external cues to regulate growth cone adhesion, and translate information through signaling molecules to the actin and microtubule cytoskeleton. Following guidance receptor stimulation, intracellular signaling cascades lead to localized cytoskeletal modifications that allow the axon to extend, turn or be repulsed, and ultimately navigate to a specific target (Dickson and Senti, 2002). In addition to their role in axon guidance, guidepost cells and their cues have been shown to help determine the location of synaptic sites, and regulate pre- and post-synaptic differentiation (Chen and Cheng, 2009). The ability of guidance cues to define the microenvironment for both axon guidance and synapse formation suggests that these events are coordinated on a molecular level.

Once the axon reaches the correct target, the synaptic machinery must be assembled and oriented in the correct location, and the pre- and postsynaptic cells must recognize each other. This is essential for proper synapse formation. Cell adhesion molecules (CAMs) are membrane-anchored proteins that help hold the pre- and postsynaptic cells together. These molecules originally were characterized for their function in axon outgrowth and fasciculation, but later were shown to be important for maintaining the integrity of the synaptic junction and promoting the stability of the synapse (Yamagata et al., 2003). CAMs are also expressed at mature synapses, where they have been shown to regulate

synaptic plasticity and consequently contribute to a variety of cognitive functions (Arikkath and Reichardt, 2008; Benson and Huntley, 2012; Hirano and Takeichi, 2012; McGeachie et al., 2011; Sudhof, 2008). A variety of synaptic CAMs have been identified in the CNS and these include: neuroligins, neurexins, cadherins, and integrins. CAMs are classified according to the type of interaction partners they bind across the synaptic cleft, and are either homophillic or heterophilic. One of the best studied cadherins in the CNS, N-cadherin, is expressed at both excitatory and inhibitory synapses during development but later enriches at excitatory synapses (Fannon and Colman, 1996). This represents a homophilic synaptic CAM that participates in synapse formation, and also functions at mature synapses. The best-known heterophilic CAMs include the presynaptic neurexins and their postsynaptic partners, the neuroligins (Shen and Scheiffele, 2010; Siddiqui and Craig, 2011). This highly diverse interaction is thought to provide synapse specificity (Shen and Scheiffele, 2010). It was further established that each partner can trigger formation of a hemisynapse, with neuroligins and neurexins causing pre- and post-synaptic differentiation respectively (Craig and Kang, 2007). Together, CAMs mediate the interaction between the pre- and postsynaptic cell by regulating formation, differentiation, and plasticity of synapses.

Efficient wiring of the brain requires several developmental events during maturation of the nervous system. Neurons send out their projections, which must be guided accurately and precisely over long distances to their target sites

(Bashaw and Klein, 2010; Kolodkin and Tessier-Lavigne, 2011). Once long-range navigation is complete, the neuron must transition from exclusively outgrowth to a combination of short-range growth and synaptogenesis (Po et al., 2010). Further, synapses need to form in the correct density and location (Shen and Scheiffele, 2010). Finally, axons must terminate their growth in a spatially and temporally precise manner (Feldheim and O'Leary, 2010). While these developmental events typically have been looked at independently of one another, several studies suggest that the molecular mechanisms that govern them are interrelated. For instance, in cultured hippocampal neurons, synapse assembly rapidly takes places upon axodendritic contact (Friedman et al., 2000). At the fly NMJ, synapses form within a tight transition period after the growth cone reaches its target muscle (Yoshihara et al., 1997), and new synapses are added at the tip of growing axons (Zito et al., 1999). Live *in vivo* imaging using developing retinal ganglion cells of zebrafish shows that synaptogenesis guides axon arbor growth by promoting branch extension and then stabilizing certain branches (Meyer and Smith, 2006). Similarly, in invertebrates and zebrafish, synaptic activity is linked with axon outgrowth and branching (Ben Fredj et al., 2010; Budnik et al., 1990; Hua et al., 2005; Zhao and Nonet, 2000). Numerous studies in both invertebrates and vertebrates have shown that guidance cues, adhesion molecules, and various morphogens function in both axon guidance and synapse formation as well (Shen and Cowan, 2010). Despite evidence that the molecular mechanisms between axon outgrowth, synapse formation, and

termination of outgrowth are integrated during development, the identities of intracellular signaling proteins that coordinate these events remain unclear.

In the past decade, the Pam/Highwire/RPM-1 (PHR) proteins have emerged as key intracellular regulators of axon guidance, axon termination, and synapse formation. A common theme elucidated is that these proteins are likely to mediate the coordinated switch between axon growth and the formation of synapses (Po et al., 2010). Despite significant progress numerous key questions remain unanswered: Are there upstream regulators of PHR proteins? Is the localization of PHR proteins regulated? How do PHR proteins integrate information and regulate multiple signaling pathways? Do functionally relevant *in vivo* targets of PHR protein function remain to be discovered? This dissertation aims to answer some of these questions by focusing on the identification of several downstream molecules and pathways that mediate the function of the Regulator of Presynaptic Morphology 1 (RPM-1), the PHR protein in the nematode *Caenorhabditis elegans*.

1.2 PHR proteins: important regulators of neuronal development

The PHR proteins are a highly conserved family of large signaling proteins that have E3 ubiquitin ligase activity. PHR proteins have emerged as central regulators of multiple aspects of axon development. The founding member of this family, human Pam (protein associated with Myc), was identified for its ability to interact with the proto-oncogene Myc (Guo et al., 1998). Other members of the

PHR family include: mouse Phr1, zebrafish Esrom*, Drosophila* Highwire (HIW) and *C. elegans* RPM-1. Loss-of-function mutations in PHR proteins affect the development of synapses and axons (Bloom et al., 2007; Culican et al., 2009; D'Souza et al., 2005; Lewcock et al., 2007; Schaefer et al., 2000; Wan et al., 2000; Zhen et al., 2000). The original function of PHR proteins in neuronal development first emerged from three independent genetic screens looking for abnormal axon and/or synapse morphology. These screens elucidated *C. elegans rpm-1* (Schaefer et al., 2000; Zhen et al., 2000*)* and *Drosophila Highwire* (Wan et al., 2000) as regulators of synapse development. Later, studies in vertebrate PHRs revealed a prominent role for Phr1 in axon navigation and outgrowth during development (Burgess et al., 2004; D'Souza et al., 2005).

Invertebrate systems have proven invaluable in our understanding of the PHR proteins. In *C. elegans*, RPM-1 regulates synapse formation in motor neurons (Nakata et al., 2005; Zhen et al., 2000), and mechanosensory neurons (Grill et al., 2007; Schaefer et al., 2000). In the mechanosensory neurons, failed synapse formation results in retraction of the synaptic branch (Schaefer et al., 2000). In GABAeric motor neurons, *rpm-1* mutants show fewer presynaptic specializations, and synaptic organization is abnormal (Zhen et al., 2000). These neurons also have abnormal presynaptic terminals with aggregated active zones (Zhen et al., 2000). *rpm-1* mutants have severe axon termination defects in both the motor neurons and mechanosensory neurons (Grill et al., 2007; Opperman and Grill, 2014; Schaefer et al., 2000). Axon termination defects occur when

axons grow past precise anatomical locations where outgrowth is normally halted.

Highwire (Hiw) regulates axon branching, axon length, and synapse formation of fly motor neurons (Collins et al., 2006; Wan et al., 2000). In *hiw* mutants, long-range motor axon pathfinding is normal, but excessive axon branching occurs, and is accompanied by abnormally long axonal processes (Wan et al., 2000). Synapse formation is also abnormal with higher numbers of glutamatergic presynaptic terminals forming, but with drastically reduced size (Wan et al., 2000). While these synapses are ultrastructurally normal, they have impaired synaptic transmission. The extensive increase in motor axon length in *hiw* mutants suggests that these animals have defects in axon termination that accompany synapse formation defects. This is further supported by recent work in fly sensory neurons that shows Hiw regulates axon termination (Kim et al., 2013).

Despite differences in the presentation of synapse formation defects in worms and flies lacking PHR protein function, both HIW and RPM-1 function cell-autonomously in motor neurons to regulate axon termination and synapse formation, often in the same cell (Opperman and Grill, 2014; Schaefer et al., 2000; Zhen et al., 2000). Similarly, RPM-1 functions cell autonomously in mechanosensory neurons to regulate synapse formation and axon termination in individual cells (Opperman and Grill, 2014; Schaefer et al., 2000). These results are consistent with RPM-1 being localized to distinct subcellular compartments,

the mature axon tip, and the presynaptic terminal in both motor neurons and mechanosensory neurons (Abrams et al., 2008; Opperman and Grill, 2014; Zhen et al., 2000). Studies focused on the PLM mechanosensory neurons, which show severe and highly frequent axon termination defects in *rpm-1* mutants, have shown that once termination fails in *rpm-1* mutants that Slit and Netrin are the attractive guidance cues that facilitate excess axon outgrowth (Li et al., 2008). Very little is known about the extracellular cues that trigger PLM axon termination, but a recent study has suggested a modest role for two Wnts, LIN-44 and EGL-20 (Tulgren et al., 2014).

With regard to vertebrates, mice lacking *Phr1* function have motor neurons with synapse formation defects (Bloom et al., 2007; Burgess et al., 2004). In *Phr1*$^{-/-}$ mice, the phrenic nerve fails to properly innervate the diaphragm. This defect coupled to the possibility of impaired synaptic function is thought to explain why these mice die shortly after birth. Similar to the synaptic defects observed in both *Hiw* and *rpm-1* mutants, presynaptic terminal morphology is severely disrupted in the motor neurons of mice lacking Phr1 (Burgess et al., 2004). More specifically, the size of the presynaptic terminals is reduced, and orphan presynaptic terminals are present that lack postsynaptic partners (Bloom et al., 2007; Burgess et al., 2004). Further, NMJs made by the phrenic nerve display abnormally long terminals that could suggest defects in axon termination or axonal pruning.

While early studies on invertebrate PHR proteins identified roles in synapse formation and axon termination, later studies on vertebrate PHRs demonstrated a prominent role for PHR proteins in axon guidance and outgrowth in both the peripheral and central nervous system. In mice with targeted disruption of *Phr1*, there is a severe reduction of axon tracts in the brain, as well as an overall decrease of neurites in the cerebral cortex (Bloom et al., 2007). Motor axon guidance and extension is also impaired in the motor neurons in the hind limb (Lewcock paper 2007). In Zebrafish *Esrom* mutants, bundling of retinal axons is disrupted and incorrect targeting of these axons causes ectopic arborization (D'Souza et al., 2005). These navigation defects are likely to result in part from abnormal microtubule dynamics (Hendricks and Jesuthasan, 2009). While axon guidance and extension defects are prominent in *Phr1*$^{-/-}$ mice, the sensory neurons of these animals do have axon termination defects in the periphery and in the spinal column (Burgess et al., 2004; Holland et al., 2011; Lewcock et al., 2007). Thus, PHR proteins play a conserved functional role in axon termination from worms to mammals, but neuronal context and the extracellular environment seem likely to dictate whether a PHR protein will figure more prominently in axon extension and guidance versus axon termination.

Systemic defects in axon guidance and extension are not observed in invertebrates lacking PHR protein function. However, results from the worm on the AVM mechanosensory neuron showed that RPM-1 does regulate axon guidance in the context of sensitizing backgrounds, such as loss of function in

the *unc-5* Netrin receptor or the *sax-3* Robo receptor (Li et al., 2008). Analysis of double mutants of *rpm-1* and the active zone regulator *syd-2/liprin* showed that RPM-1 not only regulates axon termination, but can affect axon extension in motor neurons (Opperman and Grill, 2014). Thus, while RPM-1 is not a primary regulator of axon extension and guidance, it does function in these processes.

Loss of PHR protein function results in varied combinations of defects in axon guidance and extension, axon termination, and synapse formation during maturation of the nervous system in different organisms. This diverse range of phenotypes is likely to result from PHR proteins regulating multiple signaling pathways as well as the cell type, developmental stage, and surrounding extracellular cues that a given neuron experiences. Nonetheless, a likely unifying theme for these phenotypic observations is that PHR proteins regulate the transition between important events in neuronal development (Po et al., 2010).

1.3 PHR proteins function as signaling hubs

PHR proteins are gigantic proteins with multiple conserved domains (Figure 1-1A), which lends to their involvement in multiple aspects of neuronal development. PHR proteins contain an RCC1-like domain, two PHR protein-specific repeats, a Myc-binding region (that is only partially conserved in RPM-1 and Hiw), and a RING-H2 zinc finger domain that confers E3 ubiquitin ligase activity (Guo et al., 1998; Wan et al., 2000; Zhen et al., 2000). Many of the loss-of-function alleles in both vertebrate and invertebrate PHR mutants encode

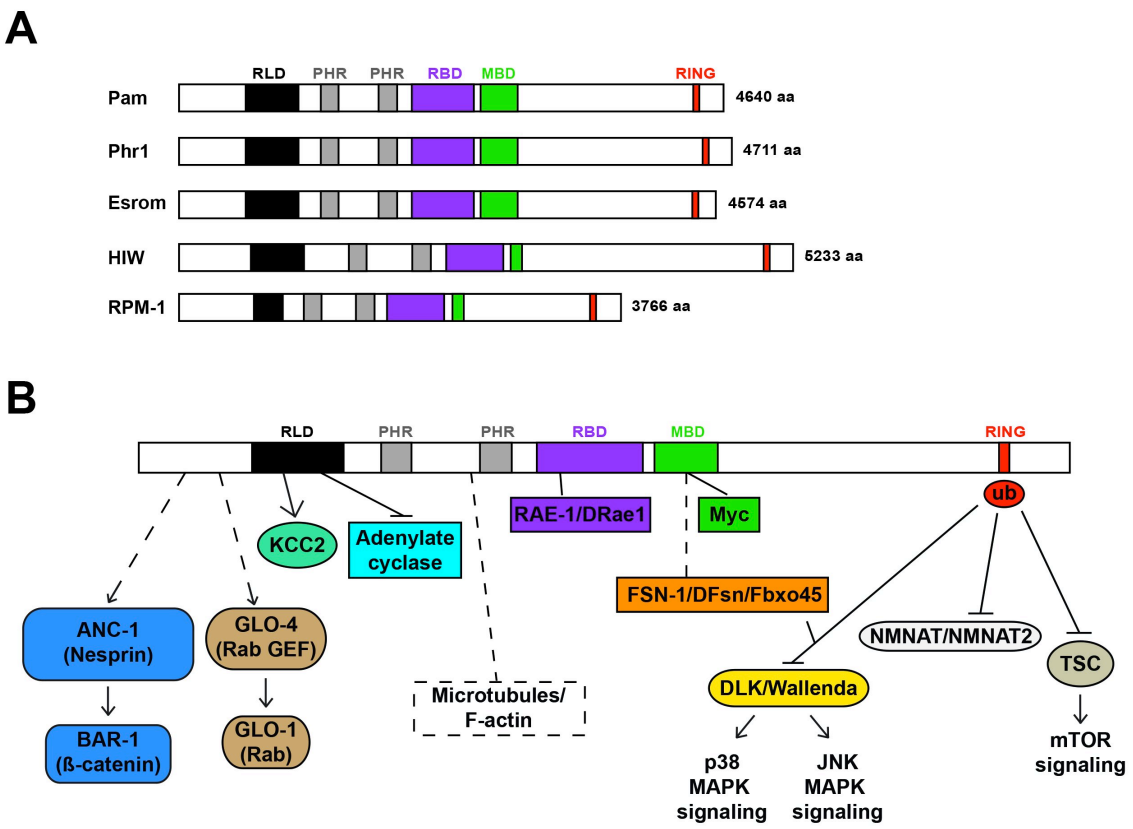

Figure 1-1. PHR protein signaling in vertebrates and invertebrates.
(A) Diagram of the conserved protein domains of the PHR proteins Pam, Phr1, Esrom, HIW, and RPM-1: RCC1 like domain (RLD), two PHR family specific domains (PHR), RAE-1 binding domain (RBD), Myc binding domain (MBD), and RING-H2 ubiquitin ligase domain (RING). *(B)* PHRs function through both positive and negative signaling mechanisms to regulate different aspects of neuronal development. PHRs interact with the F-box proteins (FSN-1/DFsn/Fbxo45) to downregulate DLK/Wallenda activity through ubiquitination (RPM-1/HIW/Phr1). This negative regulation of DLK/Wallenda results in inhibition of p38 and JNK MAP kinase signaling. PHRs also ubiquitinate NMNAT/NMNAT2 (HIW/Phr1), and TSC which inhibits mTOR signaling (Phr1/Pam/Esrom). PHR proteins have also been shown to bind to Myc (Pam), RAE-1/DRae-1 (RPM-1/HIW), GLO-4 (RPM-1), ANC-1 (RPM-1), KCC2 (PAM), and Adenylate cyclase (Phr1). They also associate with polymerized microtubules and F-actin (Pam/Phr1/Esrom). Dashed lines indicate unknown domain of binding, while connected lines indicate direct binding to a specific domain.

premature stop codons or missense mutations that affect the RCC1-like and RING-H2 domains, highlighting the functional importance of these domains (D'Souza et al., 2005; Wan et al., 2000; Zhen et al., 2000). Recently, another conserved domain called the RAE-1 binding domain was also discovered (Grill et

al., 2012). Over the past decade, a combination of genetic and biochemical evidence has revealed that the PHR proteins exert both positive and negative activity through several functionally conserved signaling pathways (Figure 1-1B). Because PHR proteins, and in particular RPM-1, function through such a diverse array of downstream signaling activities it has prompted the proposal that PHR proteins function as intracellular signaling hubs that regulate neuronal development (Cherra and Jin, 2015)

Previous studies in *C. elegans*, *Drosophila*, and mice have shown that PHR proteins function as E3 ubiquitin ligases that negatively regulate p38 and JNK MAP kinase signaling (Collins et al., 2006; Klinedinst et al., 2013; Lewcock et al., 2007; Nakata et al., 2005; Yan et al., 2009). PHRs interact with the FSN-1/DFsn/Fbxo45 F-box proteins, and function as a complex to ubiquitinate and degrade the DLK/Wallenda MAP3K (Liao et al., 2004; Saiga et al., 2009; Wu et al., 2007). By regulating DLK, PHR proteins impact p38 and JNK MAP kinase signaling cascades (see Figure 1-1B).

The ubiquitin ligase function of the PHR proteins not only regulates MAP kinase cascades, but also affects mTOR signaling via ubiquitination and degradation of the Tuberous Sclerosis Complex (Han et al., 2012; Han et al., 2008; Murthy et al., 2004). PHR control of the activity and levels of the axon survival molecule NMNAT takes place through ubiquitination as well, and this regulation likely balances axonal maintenance and degeneration (Babetto et al., 2013; Xiong et al., 2012).

Ubiquitin ligase activity is not the sole biochemical function of the PHR proteins. PHR proteins bind to several proteins that are not targeted for ubiquitination and degradation. These PHR binding proteins include Myc (Guo et al., 1998), a Rab GEF GLO-4 (Grill et al., 2007), a microtubule binding protein RAE-1 (Grill et al., 2012), and the Nesprin ANC-1 (Tulgren et al., 2014) (see Figure 1-1B). Further, the RCC1-like domain of Phr1 inhibits adenylate cyclase (Scholich et al., 2001), and promotes the activity of the neuronal K^+CL^- transporter KCC2 (Garbarini and Delpire, 2008). PHR proteins also associate with polymerized microtubules (Lewcock et al., 2007) and polymerized F-actin (Pierre et al., 2008). Together, these studies show that through both positive and negative signaling, PHR proteins function in variety of processes including: endosomal trafficking or formation (Grill et al., 2007), receptor trafficking and endocytosis (Holland et al., 2011; Li et al., 2008; Park et al., 2009), microtubule dynamics (Hendricks and Jesuthasan, 2009; Lewcock et al., 2007), and gene transcription (Collins et al., 2006; Han et al., 2008; Murthy et al., 2004; Nakata et al., 2005).

1.4 Postdevelopmental function of PHR proteins

In addition to regulating the developing nervous system, the PHR proteins were recently shown to function in mature, adult neurons. Axon degeneration occurs frequently in many types of neurodegenerative diseases and in injuries to axons as a result of trauma (Coleman and Perry, 2002; Raff et al., 2002). This leads to

loss of neuronal function through an apoptosis-independent mechanism. Research on Wallerian degeneration, a process that involves the degeneration of distal axons after nerve injury, is the simplest and fastest physiological model of axon degeneration available (George and Griffin, 1994). Using this model, inhibition of the ubiquitin proteasome system was shown to profoundly delay axon degeneration (Zhai et al., 2003). However, it remained unclear which E3 ubiquitin ligases impacted axon degeneration. A recent study showed that Hiw promotes Wallerian degeneration by negatively regulating the NAD+ biosynthetic enzyme Nmnat (Xiong et al., 2012). Previous studies on Wallerian degeneration established a role for NMNAT in protecting severed axons from degeneration (Coleman and Perry, 2002; Feng et al., 2010b; Zhai et al., 2008). Because Hiw targets ectopically expressed NMNAT2 from the mouse, this function was potentially conserved (Xiong et al., 2012). Indeed, Phr1 was shown to be a key component of the axonal degeneration program that regulates the availability of NMNAT2 (Babetto et al., 2013). Increased levels of NMNAT2 in Phr1 genetically ablated mice delays axon degeneration and leads to long-term preservation of peripheral and central nervous systems axons and synapses (Babetto et al., 2013). In addition to targeting NMNAT, Hiw and Phr1 also downregulate the MAP3K Wnd/DLK as a secondary mechanism to promote Wallerian degeneration (Miller et al., 2009; Xiong and Collins, 2012; Xiong et al., 2012). Notably, Wnd function is not required for Hiw to regulate Nmnat, as both Wnd and Nmnat protect axons independently of one another (Xiong et al., 2012).

Injury studies in flies revealed that neurons regenerate faster when excess Dlk/Wnd signaling is present (Xiong et al., 2010). In worms, DLK-1 is necessary and sufficient for axon regeneration in motor neurons and mechanosensory neurons following injury (Hammarlund et al., 2009; Yan et al., 2009). Importantly, DLK functions as a conserved regulator of axon regeneration in mammals (Itoh et al., 2009; Shin et al., 2012). Overall, this body of work suggests that PHR proteins regulate a core axon regeneration and degeneration program that balances axon survival and loss (Babetto et al., 2013).

Axonopathy is a major component of many neuropathies and neurological diseases, which remain largely untreatable. Mammalian Phr1 is a potentially attractive therapeutic target for pharmacological agents that would broadly reduce axon degeneration and/or improve axon regeneration. The challenge will be to develop specific inhibitors of the PHR ubiquitin ligase complex. While drugs targeting global protein degradation have been discovered, efforts on targeting enzymes upstream of the proteasome, such as E3 ubiquitin ligases, remain in their infancy (Zhao and Sun, 2013).

1.5 The PHR ubiquitin ligase complex

Negative regulation of the MAP3K Dlk/Wnd by PHR proteins is mediated by a conserved biochemical mechanism. PHR proteins function through an ubiquitin ligase complex that includes an F-box protein: FSN-1 in *C.* elegans (Liao et al., 2004), DFsn in *Drosophila* (Wu et al., 2007*)*, and Fbxo45 in mammals (Saiga et

al., 2009) (see Figure 1-1B). Despite this progress, the large size of the PHR proteins has hindered structure-function analysis, and we know relatively little about how the PHR proteins interact with these F-box proteins. Some progress was made with the discovery that Fbxo45 binds to the same very large region in human PAM where Myc binds, which is referred to as the Myc binding domain (MBD) (Saiga et al., 2009) (see Figure 1-1A). The MBD of Phr1 contains a conserved N-terminal region and a C-terminal region that is not conserved. Proteomic screens for proteins that bind to the invertebrate PHRs have not identified Myc (Grill et al., 2007; Tian et al., 2011). This suggests that Myc most likely binds to the C-terminal region of the MBD that is only present in vertebrate PHR proteins. In one chapter of this dissertation, we focus on a detailed structure-function analysis of RPM-1 and FSN-1. We provide evidence that the conserved N-terminal portion of the MBD in RPM-1 mediates binding to FSN-1. More importantly, our biochemical and genetic analysis has led to the identification of an *in vivo* inhibitor of the RPM-1/FSN-1 ubiquitin ligase complex. This represents the first inhibitor of a PHR ubiquitin ligase complex that has been identified to date. On a pharmacological level, a small molecule that specifically blocks the formation or function of the PHR ubiquitin ligase complex might be valuable for improving axon regeneration following trauma, or slowing the onset of axon degeneration in a range of neurodegenerative diseases.

1.6 *C. elegans* RPM-1

As previously mentioned, *C. elegans* RPM-1 was first identified in independent genetic screens looking for axon/synaptic morphology defects (Schaefer et al., 2000; Zhen et al., 2000). In one of these studies, RPM-1 was also shown to regulate axon termination. Subsequent work has identified an array of downstream signaling mechanisms that mediate RPM-1 function in axon termination and synapse formation (Figure 1-2). RPM-1 forms an SCF-like ubiquitin ligase complex with the F-box protein FSN-1 (Liao et al., 2004), and through the RING-H2 domain ubiquitinates the MAP3K DLK-1 to target it for proteasomal degradation (Nakata et al., 2005). DLK-1 is the most upstream kinase in a p38 MAP kinase cascade, and a combination of genetic suppressor experiments and biochemistry showed that RPM-1 negatively regulates this pathway (Nakata et al., 2005). Proteomic screens for RPM-1 binding proteins have identified several molecules and pathways that mediate RPM-1 function. 1) GLO-4, a guanine nucleotide exchange factor that regulates GLO-1, a Rab GTPase (Grill et al., 2007). RPM-1 positively regulates this pathway to regulate late endosome trafficking or biogenesis (Grill et al., 2007). 2) The microtubule binding protein RAE-1, which colocalizes with RPM-1 at the presynaptic terminals of motor neurons (Grill et al., 2012). This finding established a novel post-mitotic function for RAE-1 in neuronal development. 3) The Nesprin ANC-1, which functions in a non-canonical β-catenin pathway (Tulgren et al., 2014). This study highlights an unexpected mechanism by which RPM-1 functions, as it is

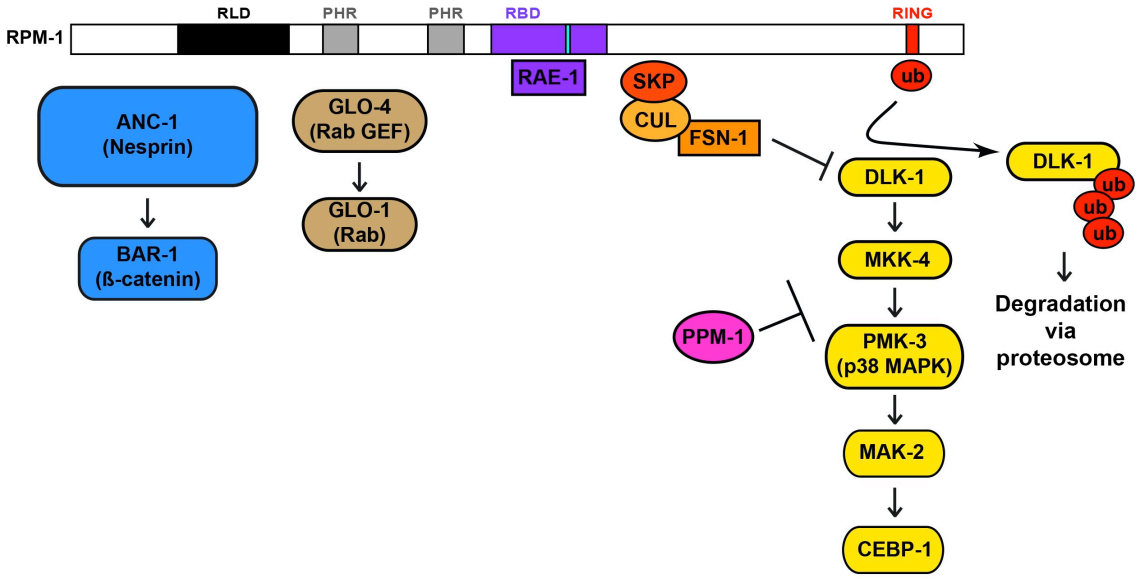

Figure 1-2. RPM-1 signaling in *C. elegans*.
RPM-1 functions through an array of downstream signaling mechanisms to regulate neuronal development. It positively regulates the GLO-4 pathway consisting of the GEF GLO-4 and the Rab GTPase GLO-1. Additionally it positively regulates the Nesprin ANC-1, which functions in a non-canonical β-catenin pathway with BAR-1. RPM-1 forms an SCF-like ubiquitin ligase complex with the F-box protein FSN-1 and together they target the MAP3K DLK-1 for proteasomal degradation via ubiquitination. In this way, RPM-1 negatively regulates the DLK-1 pathway, which consists of the MAP3K DLK-1, the MAP2K MKK-4, the p38 MAP kinase PMK-3, the MAPKAP kinase MAK-2, and the C/EBP bZip factor (CEBP-1). The PP2C phosphatase PPM-1 negatively regulates the DLK-1 pathway, most likely at the level of PMK-3. RPM-1 also binds to the microtubule binding protein RAE-1. The small box in the RBD represents a conserved motif that is necessary and sufficient for RAE-1 binding to RPM-1.

the first genetic link between RPM-1 and a pathway that is regulated by extracellular signals, such as Wnts (Tulgren et al., 2014). 4) A PP2C family phosphatase, PPM-2, was also identified as an RPM-1 binding protein in this proteomic screen. Chapter two of this dissertation will describe our work characterizing how PPM-2 binds to RPM-1 and mediates RPM-1 function in axon termination and synapse formation.

1.7 PP2C family phosphatases

Several studies suggest that MAP kinases are negatively regulated by phosphatases including MAP kinase-specific phosphatases, and broad-acting Protein Phosphatase 2C (PP2C)/ Protein Phosphatase Mg/Mn dependent (PPM) family phosphatases (Bermudez et al., 2010; Lu and Wang, 2008; Shi, 2009). While MAP kinases are known to function in neurons (Ji et al., 2009; Samuels et al., 2009), very little is known about the negative regulatory mechanisms that control MAP kinase signaling pathways *in vivo*. I have already touched on PHR proteins functioning as ubiquitin ligases to regulate MAP kinase cascades *in vivo*. Here, I will discuss what is known about PP2C phosphatase function *in vivo* in the nervous system.

PP2C/PPM family phosphatases are single subunit enzymes with serine/threonine phosphatase activity. Biochemical experiments *in vitro* and in mammalian cell culture systems have shown that PP2Cα and PP2Cβ can dephosphorylate and negatively regulate MKKKs, MKKs, and MAPKs (Hanada et al., 2001; Takekawa et al., 1998). Yeast Hog1, the homolog of the p38 MAPK, is negatively regulated by homologs of PP2Cα (Jacoby et al., 1997; Maeda et al., 1994; Nguyen and Shiozaki, 1999; Saito and Tatebayashi, 2004). Additionally, PP2Cα functions in mammalian neurons to control calcium flux (Li et al., 2005), which suggests that PPC2 phosphatases could affect neuronal function. We recently provided evidence that PPM-1, a PP2C phosphatase homologous to human PP2Cα (PPM1A) and PP2Cβ (PPM1B), acts as a negative regulatory

mechanism to inhibit the DLK-1 pathway (Tulgren et al., 2011). This negative regulation is most likely the result of PPM-1 acting at the level of the p38 MAPK PMK-3 (Figure 1-2). In doing so, PPM-1 functions cell autonomously in the motor neurons and mechanosensory neurons to regulate axon termination and synapse formation. This study provided the first evidence that PP2C phosphatases regulate neuronal development *in vivo*.

As mentioned earlier, another PP2C phosphatase, PPM-2, was identified in a proteomic screen for RPM-1 binding proteins. Experiments performed as part of my dissertation work will show that PPM-2 binds to RPM-1, is positively regulated by RPM-1, and functions downstream of RPM-1 to regulate axon termination and synapse formation. Further, I will present biochemical and genetic data suggesting that PPM-2 functions to directly dephosphorylate and inhibit DLK-1. An implication of our findings is that RPM-1 acts as an ubiquitin ligase to regulate long-term stability and turnover of DLK-1, and uses PPM-2 as an independent mechanism to inhibit DLK-1 activity. These results point towards the PHR proteins as particularly sophisticated regulators of DLK-1 signaling.

1.8 The MLK-1 MAP Kinase Pathway

In *C. elegans*, RPM-1 regulates neuronal development by inhibiting the MAP kinase pathway composed of DLK-1, MKK-4, PMK-3, MAK-2, and CEBP-1 (Nakata et al., 2005; Yan et al., 2009). Studies in worms, flies, and mice have shown that DLK/Wallenda kinase is required for axon regeneration (Hammarlund

et al., 2009; Shin et al., 2012; Xiong et al., 2010; Yan et al., 2009). A second MAP kinase pathway, composed of MLK-1, MEK-1 and the KGB-1 JNK, is also required for axon regeneration in worms (Nix et al., 2011). The role of the MLK-1 pathway in neuronal development remains unknown. This dissertation describes our study showing that the MLK-1 pathway regulates synapse formation and axon termination. The MLK-1 pathway, like the DLK-1 pathway, is negatively regulated by RPM-1. Unlike axon regeneration, our results indicate that the MLK-1 pathway plays a secondary role to the DLK-1 pathway in neuronal development. We also explore whether the PP2C phosphatases PPM-1 and PPM-2 regulate the MLK-1 pathway. These findings further expand our understanding of the signaling mechanisms that mediate RPM-1 function in neurons.

1.9 The nematode *C. elegans*: an ideal model system for studying neuronal development *in vivo*

In the later half of the twentieth century, Sydney Brenner introduced a free-living microscopic nematode, *C. elegans*, as a genetic model to study development and neurobiology (Brenner, 1974). For this work, Dr. Brenner was awarded the Nobel Prize. Today, *C. elegans* is used to study a plethora of biological processes including apoptosis, cell signaling, gene regulation, metabolism, aging, and sex determination (Riddle et al., 1997). Several discoveries have highlighted the value of the worm for understanding the conserved molecular and

genetic mechanisms underlying several diseases, such as type 2 Diabetes (Ogg et al., 1997), depression (Ranganathan et al., 2001), Alzheimer' disease (Sundaram and Greenwald, 1993), and Parkinson's disease (Berkowitz et al., 2008; Caldwell and Caldwell, 2008; Locke et al., 2008). Comparison of the complete worm and human genome have also revealed that a large number of genes and pathways, particularly those relevant for function of the nervous system, are conserved between humans and *C. elegans* (Bargmann, 1998; Consortium, 1998; Lander et al., 2001; Venter et al., 2001)

C. elegans is a powerful model system for several reasons. It is easy to cultivate due to its simple diet of bacteria, it can reproduce as a self-fertilizing hermaphrodite facilitating genetic analysis, and the worm has a rapid life cycle developing from egg to adult within 3 days. *C. elegans* has a transparent body, which allows for simple visualization of numerous features in the living animal, a characteristic that is highlighted by the Nobel Prize winning work of Dr. Martin Chalfie (Chalfie et al., 1994). Of particular relevance to neurobiology, *C. elegans* is the only metazoan in which the connectome is known, *i.e.* electron microscopy has been used to map the complete network of chemical and electrical synapses that connect all 302 neurons of the worm nervous system (White, 1986). This work also showed that the position and connectivity of neurons in the worm is invariant. Further, a majority of the known molecules that regulate neuronal development in the worm are conserved with higher organisms (Margeta et al., 2008). Along with powerful genetics, rapid transgenics, and a growing

biochemical toolkit, *C. elegans* has become a tremendous model system for studying multiple aspects of biology, but most importantly for our lab and this dissertation, studying the development of the nervous system.

2 RPM-1 Uses Both Ubiquitin Ligase and Phosphatase-Based Mechanisms to Regulate DLK-1 during Neuronal Development

Content adapted from published article: **Baker ST**, Opperman KJ, Tulgren ED, Turgeon SM, Bienvenut W, Grill B (2014) RPM-1 Uses Both Ubiquitin Ligase and Phosphatase-Based Mechanisms to Regulate DLK-1 during Neuronal Development. PLoS Genet 10(5): e1004297. doi:10.1371/journal.pgen.1004297

2.1 Introduction

As a neuron develops, its axon must execute several important tasks. Initially, the axon extends toward target cells by sensing extracellular guidance cues. Upon reaching its target, the axon detects guidepost signals and makes presynaptic connections with its postsynaptic partner(s) to form synapses (Jin and Garner, 2008; Kolodkin and Tessier-Lavigne, 2011; O'Donnell et al., 2009). At some point during these events, an axon must terminate outgrowth in a spatially and anatomically accurate manner. At present, we know little about how axon termination is governed, and even less about how this process is integrated with synapse formation.

While axon extension, synapse formation, and termination of axon outgrowth are often analyzed individually, there is substantial evidence suggesting that these events are coordinated and integrated during development. Elegant live imaging studies using developing retinal ganglion cells (RGC) in Xenopus and zebrafish showed there is a tight temporal and spatial link between axon outgrowth and synapse formation (Alsina et al., 2001; Ben Fredj et al., 2010; Meyer and Smith, 2006; Ruthazer et al., 2006). In cultured neurons, synaptogenesis proceeds rapidly upon contact between an actively growing axon and its dendritic partner (Ahmari et al., 2000; Friedman et al., 2000). At the Drosophila neuromuscular junction (NMJ), synapse formation displays tight temporal linkage with axon outgrowth (Yoshihara et al., 1997), and new synapses are formed at the terminal tips of growing axons (Zito et al., 1999).

Studies in *C. elegans*, Drosophila, and zebrafish have also shown a link between synaptic activity, and axon outgrowth and branching (Ben Fredj et al., 2010; Budnik et al., 1990; Hua et al., 2005; Zhao and Nonet, 2000). Finally, studies in invertebrate and vertebrate systems have shown that morphogens, axon guidance cues, and cell adhesion molecules function in both axon outgrowth and synapse formation (Shen and Cowan, 2010). This functional promiscuity is likely to reflect, in part, that extracellular signals take on different roles during development, and in different types of neurons. However, some of these observations also highlight a potential role for extracellular signals in coordinating axon outgrowth and termination with synapse formation. Two cases of particular note from *C. elegans* where guidance cues regulate both axon guidance and synapse formation in a single type of neuron are the role of UNC-6 (Netrin) in the RIA and AIY neurons (Colon-Ramos et al., 2007), and studies on UNC-6 and Wnts on the DA9 neuron (Hedgecock et al., 1990; Klassen and Shen, 2007; Poon et al., 2008).

At present, the identity of intracellular signaling proteins that may coordinate axon outgrowth, synapse formation, and termination of outgrowth remain unclear. Nonetheless, such coordinators would be likely to meet several criteria. 1) They would need to be evolutionarily conserved, and function in multiple events during the development of an individual neuron. 2) They would need to be signaling molecules that function intracellularly and cell autonomously. 3) Their activity would need to be regulated by upstream,

presumably extracellular, signals. 4) They would need to regulate multiple downstream signaling pathways, and do so both positively and negatively. 5) They would need to regulate downstream signaling pathways in a relatively precise and accurate manner, most likely to control both gene transcription and short-term/local signaling events.

Members of the PHR protein family meet several of these criteria, and have been put forward as candidate molecules that may coordinate different events during neuronal development (Li et al., 2008; Po et al., 2010). The PHR proteins are highly conserved with a single family-member in worms, flies, fish, mice, and humans (Po et al., 2010). The PHR proteins function in a range of developmental events playing roles in axon extension (Bloom et al., 2007; Burgess et al., 2004; Lewcock et al., 2007), axon guidance (Bloom et al., 2007; Culican et al., 2009; D'Souza et al., 2005; Hendricks and Jesuthasan, 2009; Li et al., 2008; Shin and DiAntonio, 2011), axon termination (Kim et al., 2013; Lewcock et al., 2007; Schaefer et al., 2000), and synapse formation (Burgess et al., 2004; Schaefer et al., 2000; Wan et al., 2000; Zhen et al., 2000). Importantly, studies on the mechanosensory neurons of *C. elegans* and the motor neurons of Drosophila have shown that the PHR proteins function cell autonomously to regulate synapse formation, as well as axon termination and branching in individual neurons (Schaefer et al., 2000; Wan et al., 2000). The functional importance of the PHR protein family is further highlighted by studies showing that they regulate axon regeneration (Hammarlund et al., 2009; Xiong et al.,

2010), axon degeneration (Babetto et al., 2013; Xiong et al., 2012), and aversive long-term memory (Huang et al., 2012).

While our picture of the mechanism for PHR protein function is incomplete, previous studies have established that PHR proteins regulate multiple intracellular signaling pathways both negatively and positively (Collins et al., 2006; Grill et al., 2007; Grill et al., 2012; Lewcock et al., 2007; Murthy et al., 2004; Nakata et al., 2005; Pierre et al., 2004; Scholich et al., 2001; Tian et al., 2011; Yan et al., 2009). Through these signaling mechanisms, the PHR proteins function in late endosome/lysosome trafficking or formation (Grill et al., 2007), receptor trafficking and endocytosis (Holland et al., 2011; Li et al., 2008; Park et al., 2009), microtubule dynamics (Hendricks and Jesuthasan, 2009; Lewcock et al., 2007), and gene transcription (Collins et al., 2006; Han et al., 2008; Murthy et al., 2004; Nakata et al., 2005). The human PHR protein called Protein Associated with Myc (Pam) or Myc binding protein 2 (MYCBP2) also binds to F-actin (Pierre et al., 2008), which suggests a further link between the PHR proteins and the cytoskeleton. While our knowledge of how the PHR proteins function has grown rapidly, it remains unclear if the PHR proteins have the potential to meet two important criteria as candidate coordinators of neuronal development. Are the PHR proteins regulated by upstream signals that are triggered by extracellular guidance cues, adhesion molecules, or morphogens? Do the PHR proteins have the potential to precisely and accurately control the signaling pathways they regulate?

An important, conserved function of the PHR proteins is to ubiquitinate and negatively regulate MAP kinase kinase kinase (MAP3K) signaling. The ubiquitin ligase activity of the PHR proteins requires an F-box protein called F-box Synaptic protein 1 (FSN-1) in *C. elegans* and Drosophila (Liao et al., 2004; Wu et al., 2007) and Fbxo45 in mice (Saiga et al., 2009). One MAP3K target of the PHR proteins is DLK (Collins et al., 2006; Huntwork-Rodriguez et al., 2013; Lewcock et al., 2007; Nakata et al., 2005). Mammalian DLK (also called MAP3K12) has functional orthologs in *C. elegans* (DLK-1), and Drosophila (Wallenda). PHR proteins also use ubiquitination to negatively regulate the TSC complex (Han et al., 2008; Murthy et al., 2004) and NMNAT (Babetto et al., 2013; Xiong et al., 2012).

DLK plays an important and conserved function in neuronal development by regulating synapse formation, axon extension, and termination of axon outgrowth (Collins et al., 2006; Eto et al., 2010; Grill et al., 2007; Hirai et al., 2006; Nakata et al., 2005; Wang et al., 2013). In mature neurons, DLK is critical for axon regeneration (Hammarlund et al., 2009; Itoh et al., 2009; Shin et al., 2012; Watkins et al., 2013; Xiong et al., 2010; Yan et al., 2009), and also functions in axon degeneration (Ghosh et al., 2011; Miller et al., 2009).

Progress has been made in understanding how DLK is regulated. Studies using cell lines and *in vitro* biochemical methods have shown that DLK is phosphorylated, self-dimerizes, and autophosphorylates (Daviau et al., 2009; Mata et al., 1996; Nihalani et al., 2001). JNK Interacting Proteins (JIP) bind to

DLK potentially acting as scaffolds to regulate DLK activity or localization (Ghosh et al., 2011; Nihalani et al., 2001). In Drosophila, the cytoskeletal regulatory protein Spectraplakin inhibits DLK (Valakh et al., 2013). Pharmacological studies have suggested that the phosphatase calcineurin (Mata et al., 1996) and the kinase Src (Daviau et al., 2009) may regulate DLK, but evidence that these molecules regulate DLK in neurons is absent. Finally, work in *C. elegans* has shown that calcium signaling functions upstream of DLK-1 (Ghosh-Roy et al., 2010) to regulate binding of a short, inhibitory isoform of DLK-1 (DLK-1S) to full length DLK-1 (DLK-1L) (Yan and Jin, 2012).

Here, we show that RPM-1 (the *C. elegans* PHR protein) employs a phosphatase-based mechanism to inhibit DLK-1. Using a combination of proteomics and genetics, we show that RPM-1 binds to and positively regulates Protein Phosphatase Magnesium/Manganese dependent 2 (PPM-2), a member of the PP2C phosphatase family. We provide genetic, transgenic, and biochemical evidence showing that PPM-2 negatively regulates DLK-1L by direct dephosphorylation at a specific serine residue that is implicated in binding to DLK-1S. Our findings demonstrate that RPM-1 harnesses two independent mechanisms to negatively regulate DLK-1, ubiquitination and PPM-2 phosphatase activity. These results suggest that RPM-1 may function through ubiquitin ligase activity to regulate long-term DLK-1 signaling and through the phosphatase PPM-2 to regulate short-term/local DLK-1 signaling. Thus, PHR

proteins may be more accurate and precise regulators of DLK than originally thought.

2.2 Results

2.2.1 Identification of PPM-2 as an RPM-1 binding protein

To better understand the mechanism of how RPM-1 regulates neuronal development, we previously purified RPM-1 and used mass spectrometry to identify RPM-1 binding proteins (Grill et al., 2007). In brief, a fusion protein of RPM-1 and GFP (RPM-1::GFP) was transgenically expressed in *C. elegans* using the native *rpm-1* promoter, which is expressed in neurons. An anti-GFP antibody was used to immunoprecipitate RPM-1::GFP from whole worm lysates, and RPM-1 binding proteins were identified using mass spectrometry and *de novo* peptide sequencing. Using this approach, we previously identified GLO-4 and RAE-1 as functional RPM-1 binding proteins (Grill et al., 2007; Grill et al., 2012). This proteomic screen also identified a phosphatase, PPM-2 (*T23F11.1*).

PPM-2 is in the Protein Phosphatase 2C (PP2C) family, which is also called the Protein Phosphatase Mg/Mn dependent (PPM) family. PP2C phosphatases are single subunit enzymes with serine/threonine phosphatase activity. Previous studies have shown that PPM-2 (also called PP2Cg2) has orthologs in yeast and Drosophila (Stern et al., 2007). We have found evidence of a PPM-2 ortholog in the genome sequence of the protochordate *Ciona intestinalis* (XP_002127931.1).

Our proteomic analysis identified 5 unique peptides that covered 15% of the total PPM-2 protein sequence (data not shown). To confirm our proteomic result, we performed coimmunoprecipitation (coIP) from transgenic *C. elegans*. Animals were generated that expressed FLAG epitope tagged PPM-2 (FLAG::PPM-2) and RPM-1::GFP specifically in neurons using a pan-neuronal promoter (P*rgef-1*) and the *rpm-1* promoter, respectively. FLAG::PPM-2 was immunoprecipitated from whole worm lysates using an anti-FLAG antibody, and coprecipitating RPM-1::GFP was detected in immunoblots with an anti-GFP antibody (Figure 2-1A). This observation confirmed that PPM-2 is part of a neuronal protein complex that includes RPM-1.

2.2.2 *ppm-2* regulates axon termination in the mechanosensory neurons

Our promoter expression studies showed that the *ppm-2* promoter is active in many neurons including those of the nerve ring (Figure 2-1B), the motor neurons (Figure 2-1C), and the mechanosensory neurons (Figure 2-1D and E). *ppm-2* promoter activity was also detected in gut, muscle, and pharynx (data not shown). Because PPM-2 binds to RPM-1 and is expressed in a wide range of neurons, we hypothesized that PPM-2 might function in neuronal development, similar to RPM-1. To test this hypothesis, we analyzed two alleles of *ppm-2*, *ok2186* and *tm3480*. As shown in Figure 2-2A, *ok2186* is a deletion mutation that removes 1421 base pairs of sequence. *ok2186* deletes 5' intronic sequence as well as exonic sequence. This suggests that *ok2186* results in a truncated protein

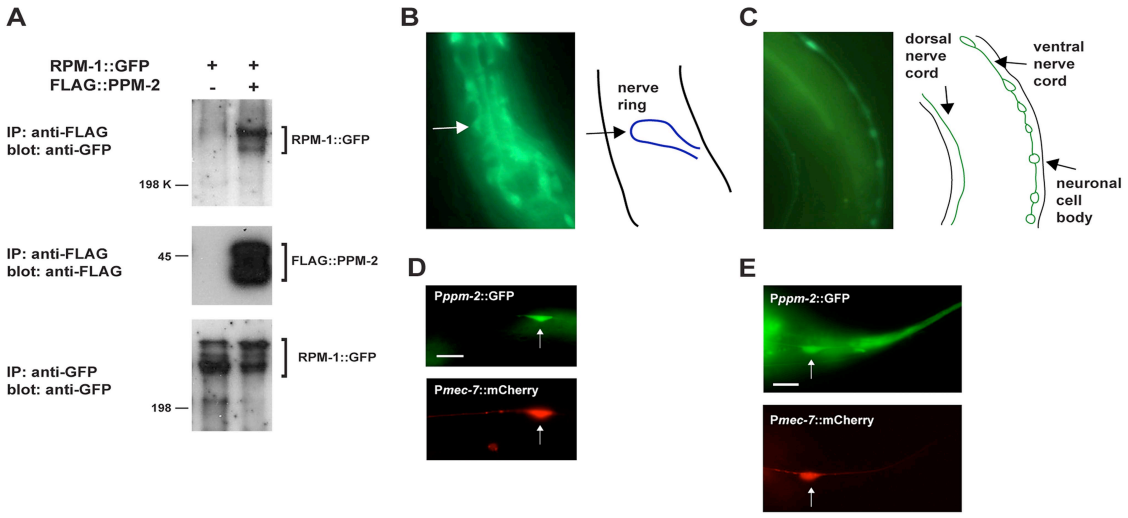

Figure 2-1. RPM-1 binds to the PP2C phosphatase PPM-2.
(A) RPM-1::GFP was transgenically expressed in the neurons of *C. elegans* alone or in combination with FLAG::PPM-2. Coprecipitating RPM-1::GFP was detected with FLAG::PPM-2 (upper panel). Levels of FLAG::PPM-2 (middle blot) and RPM-1::GFP (lower blot) were determined by immunoprecipitation (IP). *(B and C)* At left are epifluorescent images of transgenic animals expressing GFP from the native *ppm-2* promoter (P*ppm-2*::GFP). At right are schematic diagrams of the cells, nerve cords or regions of interest. *Pppm-2::GFP* expression was detected in *(B)* the nerve ring, and in *(C)* the dorsal and ventral nerve cords. *(D and E)* Shown are epifluorescent images of transgenic animals expressing both GFP from the native *ppm-2* promoter (P*ppm-2*::GFP) and mCherry from a cell-specific promoter for the mechanosensory neurons (P*mec-7*::mCherry). Expression of P*ppm-2*::GFP detected in *(D)* an ALM mechanosensory neuron (arrow) and *(E)* a PLM mechanosensory neuron (arrow). In all cases, multiple independently derived transgenic lines showed similar results, and images from a representative transgenic line are shown. Scale bars are 10mm.

at minimum and presumably causes a premature stop. Importantly, *ok2186* deletes three conserved residues (D59, H61 and R185, Figure 2-2B) that are required for the catalytic activity of PP2C phosphatases (Jackson et al., 2003; Takekawa et al., 1998). Thus, *ok2186* is likely to be a molecular null allele. *tm3480* is a deletion that removes 594 base pairs of *ppm-2* sequence, generates a frame-shift, and results in nonsense sequence encoding 7 amino acids prior to premature termination of the open reading frame (Figure 2-2A). The premature stop in *tm3480* leads to a predicted protein that is truncated and lacks two

conserved residues (R185 and D228) that are required for catalytic activity (Figure 2-2B) (Jackson et al., 2003; Takekawa et al., 1998). Therefore, *tm3480* is likely to be a molecular null allele. On gross examination, *ppm-2-/-* mutants had normal body size and shape, and moved normally.

Previous studies in *C. elegans* have shown that *rpm-1* regulates axon termination in the mechanosensory neurons (touch receptor neurons), which sense soft touch (Grill et al., 2007; Schaefer et al., 2000). These neurons are an excellent model to study axon termination for two reasons. First, *C. elegans* mechanosensory neurons terminate axon extension at precise anatomical locations (Chalfie and Thomson, 1979; Du and Chalfie, 2001), which are easily visualized using a transgene (*muIs32*) that expresses GFP in these cells (Ch'ng et al., 2003). Second, *C. elegans* and mammals share a similar but poorly understood mechanism that governs axon termination of sensory neurons. This is supported by the observation that loss-of-function mutations in *C. elegans rpm-1*, Drosophila *Highwire*, and murine Phr1 result in axon termination defects in sensory neurons (Kim et al., 2013; Lewcock et al., 2007; Schaefer et al., 2000).
C. elegans has two Posterior Lateral Microtubule (PLM) mechanosensory neurons. Each PLM neuron extends a single axon that terminates extension prior to the cell body of the Anterior Lateral Microtubule (ALM) mechanosensory neuron (Figure 2-2C, see schematic). In contrast, in *rpm-1*-/- animals the PLM axons fail to terminate extension properly, overgrow, and hook toward the ventral

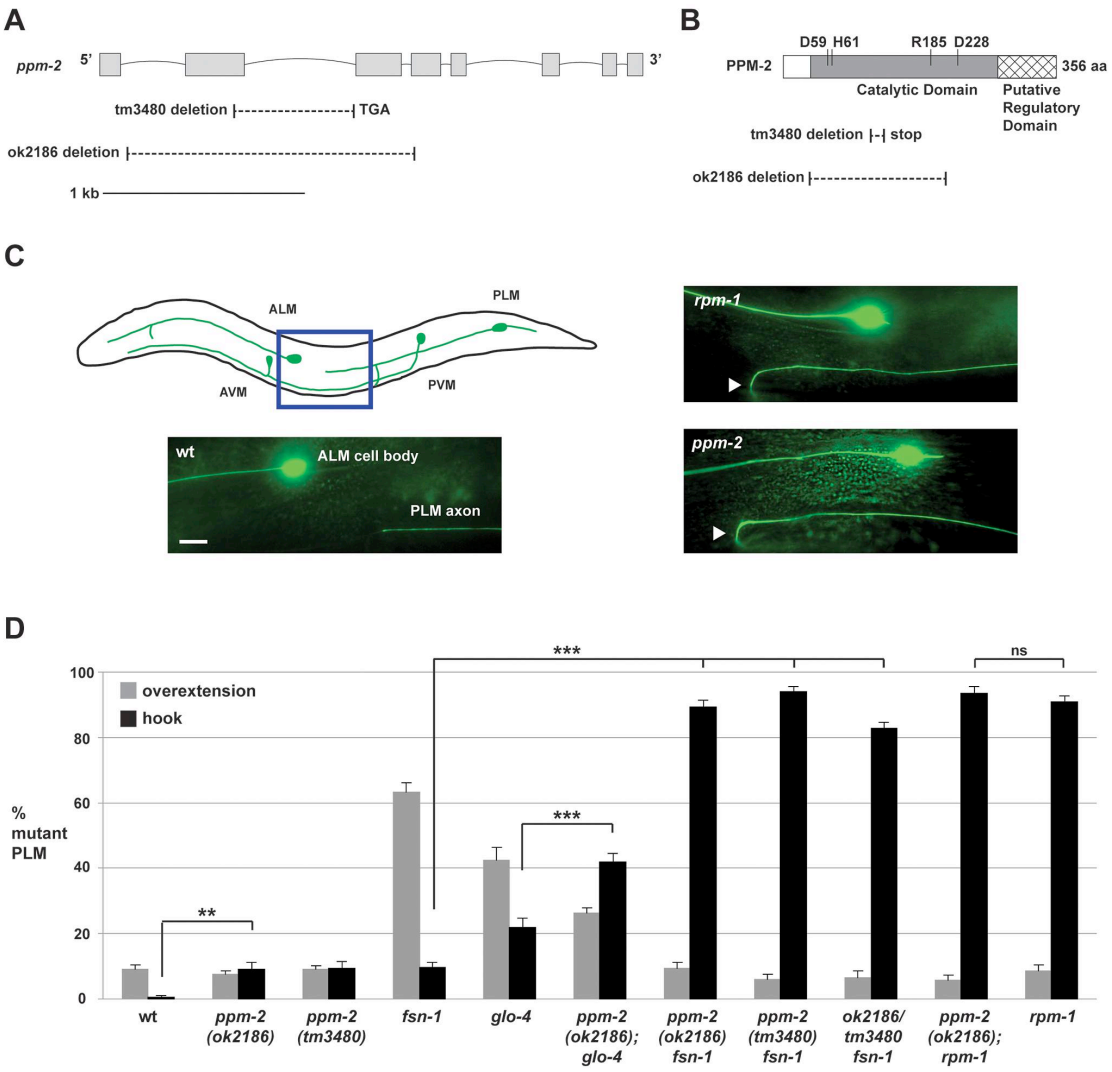

Figure 2-2. *ppm-2* regulates axon termination of PLM neurons.
(A) Schematic diagram of the *ppm-2* open reading frame. Exons are shown with boxes and introns as lines. Deletions generated by *ok2186* and *tm3480* are shown below. *(B)* Schematic diagram of the PPM-2 protein. Conserved residues that are required for catalytic activity are highlighted. Protein sequence deleted by *ok2186* and *tm3480* are shown below. *(C and D)* Defects in axon termination of the PLM mechanosensory neurons were visualized using *muIs32* ($P_{mec\text{-}7}$GFP). *(C)* Upper panel is a schematic diagram showing the mechanosensory neurons of *C. elegans* (modified from Worm Atlas). The box highlights the region shown below that was visualized using epifluorescent microscopy. An example of a PLM axon that overextends and hooks (hook) is shown for both *ppm-2(ok2186)-/-* and *rpm-1-/-* genotypes (arrowheads). Scale bar is 10 μm. *(D)* Quantitation of axon termination defects (hook represented in black, or overextension alone represented in grey) for the indicated genotypes. Averages are shown for data collected from 5-8 independent counts of 20-30 PLM neurons from young adult worms (16-20 hours post L4) grown at 23°C. Error bars represent the standard error of the mean, and significance was determined using an unpaired *t*-test. ** $p<0.01$, *** $p<0.001$ and ns = not significant.

side of the animal (Figure 2-2C). These overextension and hook defects, which will be referred to as “hook” defects for brevity of presentation, are highly penetrant in *rpm-1-/-* mutants (90.8 +/- 2.0% hook, Figure 2-2D). As noted in previous work, *rpm-1-/-* mutants also have a lower penetrance defect in which the PLM axon overextends, but does not hook (Figure 2-2D) (Grill et al., 2012; Tulgren et al., 2011). We refer to this phenotype simply as an “overextension” defect. *ppm-2(ok2186)-/-* and *ppm-2(tm3480)-/-* animals had hook defects that were of similar severity to *rpm-1-/-* mutants (Figure 2-2C), but the defects occurred with much lower penetrance (compare 9.0 +/- 2.2% for *ppm-2(ok2186)* and 9.3 +/- 2.2% for *ppm-2(tm3480)* to 90.8 +/- 2.0% for *rpm-1*, Figure 2-2D). *ppm-2-/-* mutants did not show significant overextension defects (Figure 2-2D).

In order to understand the genetic relationship between PPM-2 and other RPM-1 binding proteins, we made double mutants of *ppm-2* with *fsn-1* or *glo-4*. FSN-1 is an F-box protein that mediates the ubiquitin ligase activity of RPM-1 (Grill et al., 2007; Liao et al., 2004), and GLO-4 is a putative guanine nucleotide exchange factor (GEF) that is positively regulated by RPM-1 (Grill et al., 2007). Previous studies established that *fsn-1* and *glo-4* function in parallel genetic pathways (Grill et al., 2007; Tulgren et al., 2011). However, both *fsn-1* and *glo-4* function downstream of *rpm-1*, and in the same pathway as *rpm-1* to regulate axon termination and synapse formation (Grill et al., 2007; Liao et al., 2004). Consistent with prior work, *fsn-1-/-* and *glo-4-/-* single mutants displayed hook defects, but these defects occurred with less penetrance than in *rpm-1-/-* animals

(compare 22.0 +/- 2.7% for *glo-4* and 9.5 +/- 1.6% for *fsn-1* to 90.8 +/- 2.0% for *rpm-1*, Figure 2-2D). In contrast, *ppm-2-/- fsn-1-/-* double mutants had strongly enhanced penetrance of hook defects (compare 89.4 +/- 2.0% for *ppm-2(ok2186) fsn-1* and 94.0 +/- 1.5% for *ppm-2(tm3480) fsn-1* to 9.5 +/- 1.6% for *fsn-1*, Figure 2-2D). Hook defects were also mildly enhanced in *ppm-2-/-; glo-4-/-* double mutants (compare 41.8 +/- 2.8% for *ppm-2(ok2186); glo-4* to 22.0 +/- 2.7% for *glo-4*, Figure 2-2D).

Aside from defective axon termination in the PLM neurons, *rpm-1-/-* mutants also had other defects in the mechanosensory neurons, similar to what was described previously (Grill et al., 2007; Schaefer et al., 2000). In *rpm-1-/-* mutants, 85.6 +/- 1.6% of the PLM neurons that were analyzed lacked a synaptic branch (Figure 2-3). Notably, a previous study showed that the absence of the

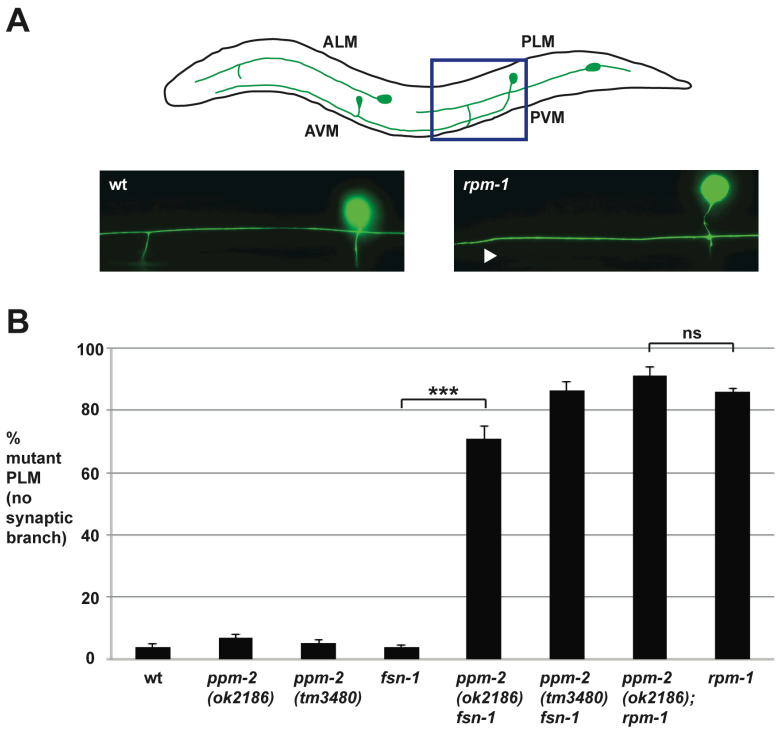

Figure 2-3. *ppm-2* regulates synaptogenesis, as assessed by synaptic branch extension, of the PLM neurons.
The synaptic branch of the PLM neurons was visualized using the transgene *muIs32* (P_{mec-7}GFP). *(A)* Epifluorescent microscopy was used to visualize the synaptic branch in wild-type or *rpm-1-/-* mutant animals. The images shown correspond to the boxed region of the diagram. Note the absence of the synaptic branch in *rpm-1-/-* mutants (arrow). Scale bar is 10 μm. *(B)* Quantitation of the defects in synaptic branch extension in the PLM neurons for the indicated genotypes. Averages are shown for data collected from 5-8 independent counts of 20-30 PLM neurons from adult worms grown at 23°C. Error bars represent the standard error of the mean, and significance was determined using an unpaired t-test. *** $p<0.001$ and ns = not significant.

PLM synaptic branch was due to a failure in synapse formation and/or maturation (Schaefer et al., 2000). *ppm-2-/- fsn-1-/-* double mutants had enhanced penetrance of defects in synaptic branch extension (70.5 +/- 4.3% for *ppm-2(ok2186) fsn-1*) compared to *ppm-2-/-* single mutants (6.6 +/- 1.3% for *ppm-2(ok2186)*) or *fsn-1-/-* single mutants (3.5 +/- 1.2%) (Figure 2-3). Thus, *ppm-2-/- fsn-1-/-* double mutants have enhanced defects in both axon termination and synaptogenesis in PLM neurons.

In *rpm-1-/-* animals, 66.1 +/- 2.1% of the ALM neurons had axon termination defects in which the ALM axon overgrew and extended towards the posterior of the animal, which we refer to as big hooks (Figure 2-4). *ppm-2-/- fsn-1-/-* double mutants had enhanced penetrance of defects in axon termination of the ALM neurons (37.6 +/- 4.1% big hook for *ppm-2(ok2186) fsn-1*) compared to either single mutant (0% for *ppm-2(ok2186)* and 12.5 +/- 2.0% for *fsn-1*, Figure 2-4).

While both alleles of *ppm-2* are likely to be molecular null alleles, we wanted to confirm this experimentally. To do so, we generated *ppm-2(ok2186/tm3480) fsn-1-/-* transheterozygous animals. The penetrance of hook

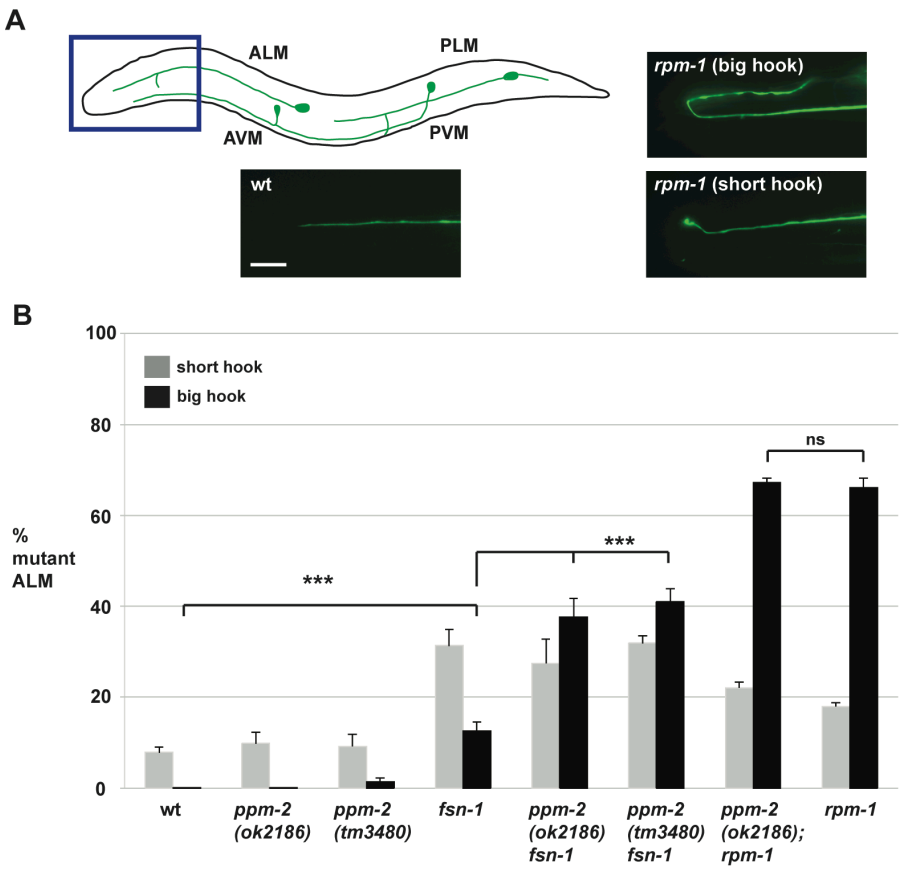

Figure 2-4. *ppm-2* regulates axon termination of the ALM neurons.
The axons of ALM mechanosensory neurons were visualized using the transgene *muIs32* (P_{mec-7}GFP). *(A)* Epifluorescent microscopy was used to visualize the ALM axon in wild-type or *rpm-1-/-* mutants. The images shown correspond to the boxed region of the diagram. Note that in *rpm-1-/-* mutants two types of axon termination defects are visible: 1) more severe big hooks in which the axon overextends and hooks to the posterior of animal (top panel), and 2) less severe short hooks in which the axon overextends more modestly, and does not extend towards the posterior (lower panel). *(B)* Quantitation of specific, short hook (grey) or big hook (black), axon termination defects in the ALM mechanosensory neurons of the indicated genotypes. Averages are shown for data collected from 5-8 independent counts of 20-30 ALM neurons from adult worms grown at 23°C. Error bars represent the standard error of the mean, and significance was determined using an unpaired t-test. *** p<0.001 and ns = not significant.

defects in the PLM neurons was enhanced in *ppm-2(ok2186/tm3480) fsn-1-/-* animals (82.8 +/- 2.0%) compared to *fsn-1-/-* single mutants (9.5 +/- 1.6%) and *ppm-2-/-* single mutants (9.0 +/- 2.2% for *ppm-2(ok2186)* and 9.3 +/- 2.2% for *ppm-2(tm3480)*, Figure 2-2D). These results are consistent with the interpretation

that both alleles of *ppm-2* are genetic nulls. Thus, our observation that null alleles of *ppm-2* enhance null alleles of *glo-4* or *fsn-1* is consistent with *ppm-2* functioning in a parallel genetic pathway to both *glo-4* and *fsn-1*.

Previous students have shown that *rpm-1-/-* mutant phenotypes are partially suppressed by loss-of-function (lf) mutations in *dlk-1*, because DLK-1 is targeted for ubiquitination and degradation by RPM-1 (Grill et al., 2007; Nakata et al., 2005). Given that PPM-2 is an RPM-1 binding protein, it was possible that RPM-1 might ubiquitinate and degrade PPM-2. To test this possibility, we constructed *ppm-2-/-; rpm-1-/-* double mutants. The PLM and ALM axon termination defects (Figure 2-2B and 2-4), and the defects in synaptic branch extension of the PLM neurons (Figure 2-3) were similar between *ppm-2-/-; rpm-1-/-* double mutants and *rpm-1-/-* single mutants. These observations suggest that PPM-2 is not targeted for ubiquitination and degradation by RPM-1. These results are also consistent with *ppm-2* functioning in the same genetic pathway as *rpm-1*.

It should be noted that although *rpm-1-/-* mutants have defects in axon termination and synapse formation in the mechanosensory neurons, previous studies have shown that *rpm-1-/-* mutants have normal locomotion, have normal soft touch sensation and are mildly dumpy (Schaefer et al., 2000; Zhen et al., 2000). We observed that *ppm-2-/-* mutants had normal body size, normal locomotion, and sensed soft touch normally (data not shown). Thus, defects in

axon termination associated with loss of function in the RPM-1 pathway do not lead to changes in the ability of the mechanosensory neurons to sense touch.

2.2.3 *ppm-2* functions cell autonomously, downstream of *rpm-1* to regulate axon termination

Having established that *ppm-2* regulates axon termination in the mechanosensory neurons, we next sought to determine if the genetic lesion in *ppm-2(ok2186)* was responsible for the observed axon termination defects. Given that RPM-1 and its known binding proteins function cell autonomously in the mechanosensory neurons (Grill et al., 2007; Grill et al., 2012; Schaefer et al., 2000), we also wanted to determine if PPM-2 functions cell autonomously. Using a transgenic approach, *ppm-2-/- fsn-1-/-* double mutants were engineered with an extrachromosomal array expressing PPM-2. We opted to analyze transgenic rescue using *ppm-2-/- fsn-1-/-* double mutants because axon termination defects were more penetrant in these animals than *ppm-2-/-* single mutants, thus facilitating ease of analysis. When PPM-2 was expressed in the mechanosensory neurons using a cell specific promoter (P*mec-7*), the axon termination defects in *ppm-2-/- fsn-1-/-* double mutants were significantly rescued (compare 89.4 +/- 2.0% for *ppm-2 fsn-1* with 32.0 +/- 2.5% for *ppm-2 fsn-1* + P*mec-7::*PPM-2, Figure 2-5A). In contrast, PPM-2 that was point mutated at a conserved residue (D59N) that is required for PP2C phosphatase activity, did not rescue the defects in *ppm-2-/- fsn-1-/-* double mutants (Figure 2-5A). These observations are

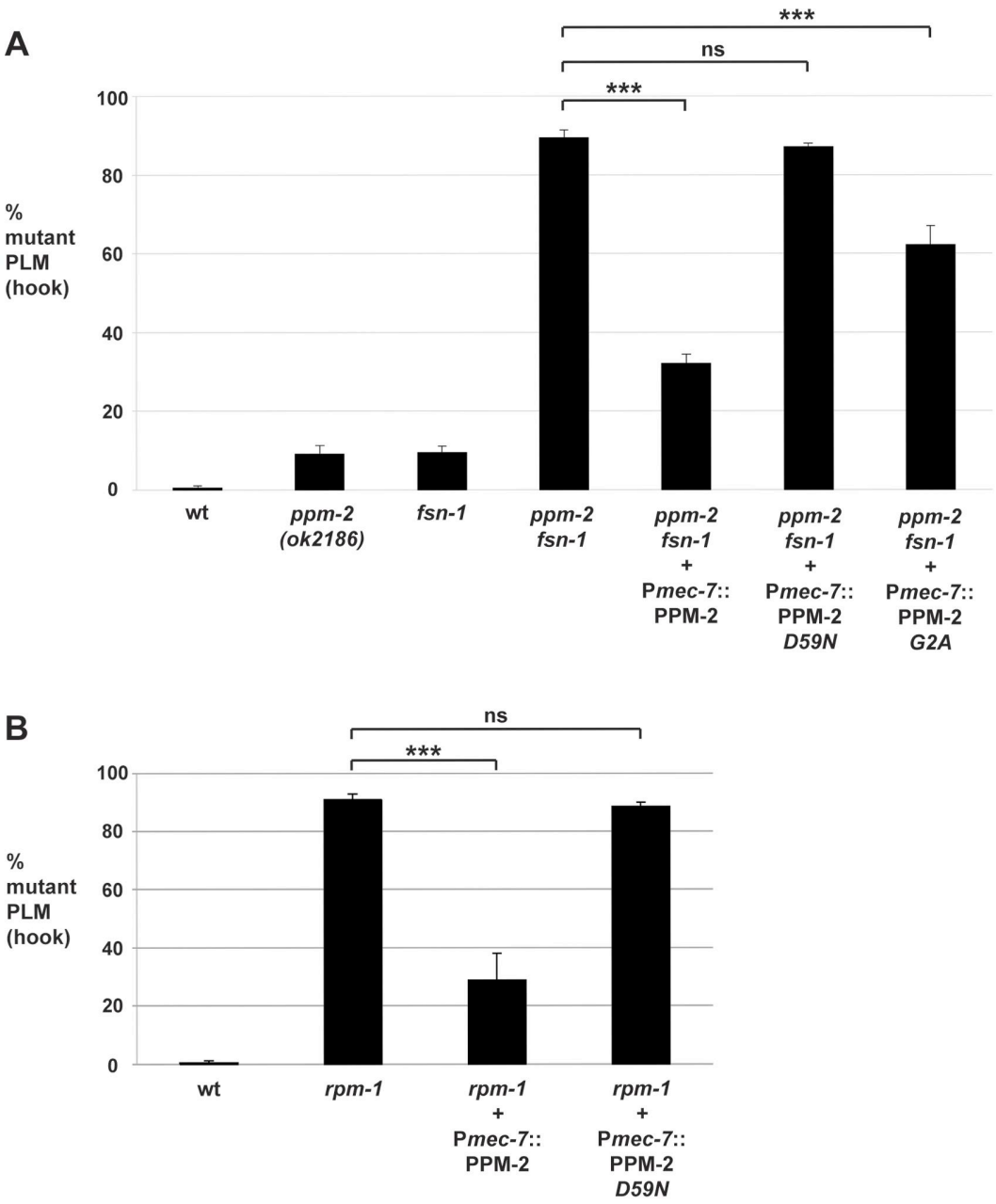

Figure 2-5. *ppm-2* functions cell autonomously downstream of *rpm-1*.
The PLM axon termination defects (hook) were quantified for all genotypes shown using the transgene *muIs32*. *(A)* A cell specific promoter (P*mec-7*) was used to transgenically express wild-type PPM-2, phosphatase-dead PPM-2 *D59N*, or PPM-2 *G2A* that was not N-myristoylated in the PLM neurons of *ppm-2-/- fsn-1-/-* double mutants. *(B)* A cell specific promoter (P*mec-7*) was used to transgenically express PPM-2 or phosphatase-dead PPM-2 *D59N* in *rpm-1-/-* single mutants. Averages are shown for data collected from 5 or more transgenic lines for each genotype. In all experiments, young adult worms (16-20 hours post L4) grown at 23^{o}C were analyzed. Error bars represent the standard error of the mean, and significance was determined using an unpaired *t*-test. *** p<0.001 and ns = not significant

consistent with *ppm-2* functioning cell autonomously through its phosphatase activity to regulate axon termination in the mechanosensory neurons.

Our genetic analysis showed that *ppm-2* functions in the same pathway as *rpm-1*, and we wanted to test if *ppm-2* functions up or downstream of *rpm-1*. To do so, we generated *rpm-1-/-* mutants that carried a transgenic extrachromosomal array that expressed PPM-2 specifically in the mechanosensory neurons. We observed that overexpression of PPM-2 partially rescued the axon termination defects in *rpm-1-/-* mutants (compare 90.8 +/- 2.0 % for *rpm-1* to 28.8 +/- 9.2% for *rpm-1* + P*mec-7*::PPM-2, Figure 2-5B). Defects were not rescued by overexpression of PPM-2 *D59N* (Figure 2-5B). These observations are consistent with *ppm-2* functioning downstream of *rpm-1*.

2.2.4 N-myristoylation is required for PPM-2 to be fully functional

During our mass spectrometry analysis, we detected N-myristoylation of a PPM-2 peptide (data not shown). Sequence analysis confirmed that the N-myristoylated glycine in PPM-2 is highly conserved with other PP2C family phosphatases (data not shown). To test if N-myristoylation was important for the function of PPM-2, we generated a point mutant of PPM-2, G2A, that cannot be myristoylated. We found that transgenic expression of PPM-2 *G2A* moderately rescued the axon termination defects in *ppm-2-/- fsn-1-/-* animals compared to wild-type PPM-2 (compare 89.4 +/- 2.0% for *ppm-2 fsn-1* to 32.0 +/- 2.5% for *ppm-2 fsn-1* + P*mec-7*::PPM-2 and 62.2 +/- 4.8% for *ppm-2 fsn-1* + P*mec-7*::PPM-2 *G2A*, Figure 2-

5A). This observation demonstrates that N-myristoylation is required for PPM-2 to function with full efficacy.

2.2.5 PPM-2 negatively regulates DLK-1

Previous studies in yeast, *Arabidopsis*, *C. elegans*, Drosophila, and cultured mammalian cells have shown that PP2C phosphatases can negatively regulate MAPK or MAP3K signaling (Baril et al., 2009; Hanada et al., 2001; Meskiene et al., 1998; Nguyen and Shiozaki, 1999; Takekawa et al., 1998; Tulgren et al., 2011). Given that RPM-1 negatively regulates a MAPK pathway that includes DLK-1, MKK-4 and PMK-3, we hypothesized that PPM-2 might also negatively regulate one or more of the kinases in this pathway. We began our analysis by studying the most upstream kinase in the pathway, the MAP3K DLK-1. Consistent with the interpretation that PPM-2 negatively regulates DLK-1, axon termination defects in the PLM neurons were suppressed in *ppm-2-/-; dlk-1-/-* double mutants (0% defect) compared to *ppm-2-/-* single mutants (9.0 +/- 2.2%, Figure 2-6A). Because PLM axon termination defects occur in *ppm-2-/-* mutants with low penetrance, we also performed our suppressor analysis using *glo-4-/-; ppm-2-/-* double mutants. Consistent with a previous study (Grill et al., 2007), we found that the hook defects in *glo-4-/-* single mutants were not suppressed by *dlk-1* (lf) (Figure 2-6A). In contrast, the enhanced penetrance of hook defects seen in *glo-4-/-; ppm-2-/-* double mutants (41.8 +/- 2.8%) was suppressed in *glo-4-/-; ppm-2-/-; dlk-1-/-* triple mutants (20.5 +/- 2.6%, Figure 2-6A).

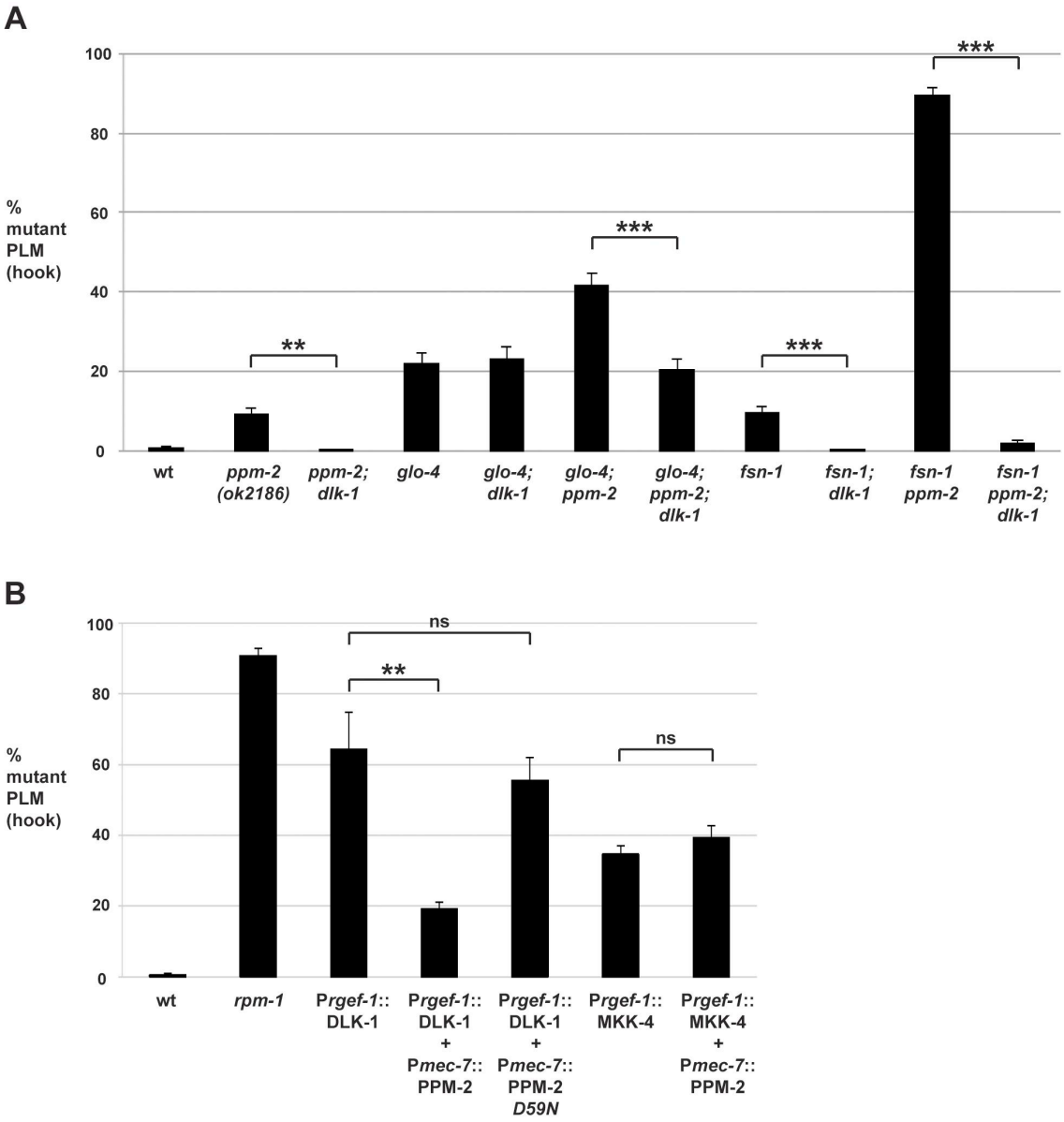

Figure 2-6. PPM-2 negatively regulates the MAP3K DLK-1.
PLM axon termination defects (hook) were quantified for the indicated genotypes using the transgene *muIs32*. *(A)* Loss of function in *dlk-1* suppresses the axon termination defects in *ppm-2-/-* single mutants and *glo-4-/-; ppm-2-/-* double mutants. Shown are averages for data collected from 5-8 independent counts of 20-30 PLM neurons from young adult worms (16-20 hours post L4) grown at 23°C for each genotype. *(B)* Transgenic overexpression of the MAP3K DLK-1, or the MAP2K MKK-4 results in PLM axon termination defects (hook). Coexpression of PPM-2 rescues defects caused by overexpression of DLK-1, but not MKK-4. Shown are averages for data pooled from 5 or more transgenic lines for the indicated genotypes; young adult worms grown at 23°C were analyzed. For A and B, error bars represent the standard error of the mean, and significance was determined using an unpaired *t*-test. ** $p < 0.005$, *** $p<0.001$ and ns = not significant

Previous studies in flies have shown that DLK/Wallenda functions downstream of DFsn (Wu et al., 2007). Consistent with these findings, we found that *fsn-1-/-; dlk-1-/-* double mutants were fully suppressed for hook defects compared to *fsn-1-/-* single mutants (compare 9.5 +/- 1.6% for *fsn-1* to 0% for *fsn-1; dlk-1*, Figure 2-6A). We also observed that enhanced hook defects in *fsn-1-/- ppm-2-/-* double mutants were fully suppressed in *fsn-1-/- ppm-2-/-; dlk-1-/-* triple mutants (compare 89.4 +/- 2.0% for *fsn-1 ppm-2* to 1.69 +/- 0.8% for *fsn-1 ppm-2; dlk-1*, Figure 2-6A). These results suggest that *ppm-2* and *fsn-1* function in a parallel genetic pathway that converges on the common target of *dlk-1*.

Having shown that PPM-2 negatively regulates the DLK-1 pathway, we next wanted to test if a specific kinase(s) in the pathway was regulated by PPM-2. To do so, we generated transgenic animals with extrachromosomal arrays that expressed a kinase in the DLK-1 pathway alone, or in combination with PPM-2. Similar to our previous observations (Tulgren et al., 2011), transgenic overexpression of DLK-1 or its downstream kinase MKK-4 using a pan-neuronal promoter (P*rgef-1*) resulted in axon termination defects in the PLM neurons (64.3 +/- 10.4% for P*rgef-1*::DLK-1 and 34.7 +/- 2.5% for P*rgef-1*::MKK-4, Figure 2-6B). Notably, MKK-4 overexpression did not cause as penetrant a phenotype as DLK-1 overexpression, presumably because the activity of MKK-4 is limited by the amount of endogenous upstream DLK-1 kinase activity. Coexpression of PPM-2 significantly rescued the defects caused by overexpression of DLK-1, but not the defects caused by overexpression of MKK-4 (compare 64.3 +/- 10.4% for P*rgef-*

1::DLK-1 to 19.2 +/- 2.0% for P*rgef-1*::DLK-1 + P*mec-7*::PPM-2, Figure 2-6B). It should be noted that we expressed DLK-1 and MKK-4 at moderate levels (2.5ng/μL PCR product injected for DLK-1 and 5ng/μL for MKK-4) in order to maximize the potential for rescue by coexpression of PPM-2. Importantly, incorporation of a second transgene into arrays did not rescue defects caused by DLK-1 overexpression, as inactive PPM-2 *D59N* did not show rescue (Figure 2-6B). Thus, PPM-2 acts through its phosphatase activity to negatively regulate DLK-1, but not MKK-4. Because PMK-3 functions downstream of MKK-4 (Nakata et al., 2005), our results are also consistent with the conclusion that PPM-2 does not regulate PMK-3. Overall, our results indicate that PPM-2 negatively regulates an upstream activator of DLK-1, acts on an inhibitor of DLK-1, or negatively regulates DLK-1 directly.

2.2.6 PPM-2 acts on DLK-1

Our genetic and transgenic experiments indicated that PPM-2 might directly dephosphorylate DLK-1. To test this hypothesis, we first determined if PPM-2 bound to DLK-1. To do so, we engineered transgenic *C. elegans* that used a pan-neuronal promoter (P*rgef-1*) to coexpress a GFP fusion protein of PPM-2 (PPM-2::GFP) with FLAG epitope tagged DLK-1 (FLAG::DLK-1). Because wild-type DLK-1 could not be expressed at sufficient levels for biochemistry (data not shown), we used a point mutant of DLK-1 *K162R* that has reduced kinase activity and can be expressed at higher levels to facilitate our analysis (Abrams et al.,

2008). Both wild-type PPM-2 and catalytically inactive PPM-2 *D59N* coprecipitated with DLK-1 (Figure 2-7A). Thus, PPM-2 is physically associated with DLK-1 or a protein complex that contains DLK-1.

A previous study identified a conserved point mutation in mammalian PP2Ca that results in increased binding to direct targets of dephosphorylation (Takekawa et al., 1998). This phosphatase trapping strategy has been used with other types of phosphatases as well (Furukawa et al., 1994; Sun et al., 1993). We observed that the corresponding point mutation in PPM-2, R185A, results in increased binding to DLK-1 *K162R* (Figure 2-7B). Quantitation of this interaction using multiple, independently-derived transgenic lines showed that PPM-2 *R185A* has significantly increased binding to DLK-1 (1.5 +/- 0.2), when compared to the level of binding between wild-type PPM-2 and DLK-1 (0.4 +/- 0.1, Figure 2-7C).

To further reinforce our model that DLK-1 is directly targeted for dephosphorylation by PPM-2, we used a combination of transgenics and biochemistry. During generation of animals with transgenic extrachromosomal arrays that used a pan-neuronal driver (P*rgef-1*) to express wild-type PPM-2::GFP or catalytically inactive PPM-2::GFP *D59N*, we noticed that the expression of PPM-2 *D59N* was elevated compared to wild-type PPM-2 (Figure 2-7D). This suggested that in neurons excess PPM-2 phosphatase activity is problematic, presumably due to dephosphorylation of endogenous targets. Thus, transgenic coexpression of PPM-2 with one of its direct dephosphorylation

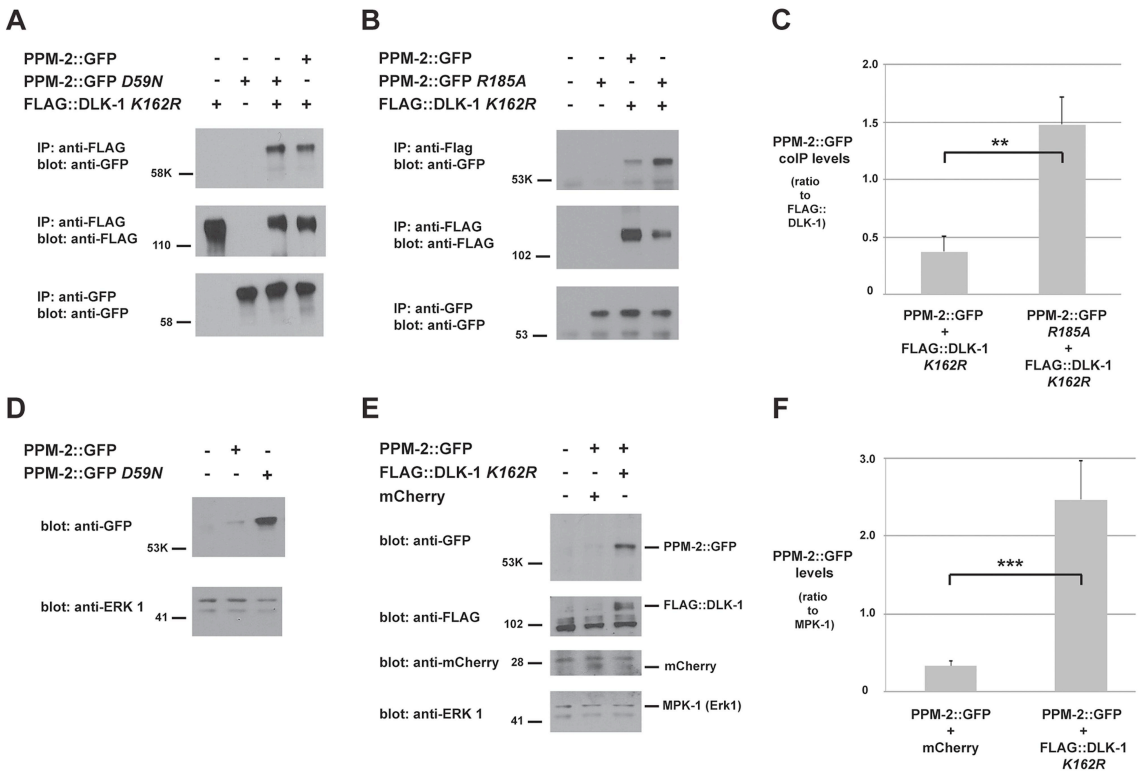

Figure 2-7. PPM-2 binds to DLK-1.
CoIP from transgenic whole worm lysates showing that *(A)* PPM-2::GFP and PPM-2::GFP *D59N* bind to FLAG::DLK-1 *K162R* (upper panel) *(B)* PPM-2::GFP *R185A* shows increased binding to FLAG::DLK-1 *K162R* compared to wild-type PPM-2::GFP (upper panel). *(C)* Quantitation of PPM-2::GFP coIP with FLAG::DLK-1 *K162R*. Note that data was acquired from 2 independently derived transgenic lines for each genotype, and histograms represent the ratio of the amount of PPM-2::GFP or PPM-2::GFP *R185A* in coIP to the amount of FLAG::DLK-1 *K162R* that was immunoprecipitated. *(D)* Immunoblots of whole worm lysates generated solely from transgenic worms. Catalytically inactive PPM-2::GFP *D59N* was consistently expressed at elevated levels compared to wild-type PPM-2::GFP (upper panel). *(E)* Immunoblots of whole worm lysates generated solely from transgenic worms. The level of wild-type PPM-2::GFP was elevated when coexpressed with FLAG::DLK-1 *K162R*, compared to when it was coexpressed with mCherry (upper panel). *(F)* Quantitation of PPM-2::GFP levels from lysates of the indicated transgenic genotypes. Shown are the average levels of PPM-2 acquired from 4 independently derived transgenic lines for each genotype normalized to MPK-1 (loading control). Error bars represent the standard error of the mean, and significance was determined using an unpaired *t*-test. ** p< 0.01, *** p<0.001, ns = not significant.

targets should result in elevated expression of PPM-2 due to titration of phosphatase activity. Consistent with this hypothesis, levels of wild-type PPM-2::GFP were increased when DLK-1 *K162R* was transgenically coexpressed,

compared to when PPM-2::GFP was coexpressed with a control protein, mCherry (Figure 2-7E). Because whole worm lysates used for these experiments were generated exclusively from transgenic animals, it was possible to use endogenous MPK-1 (the *C. elegans* Erk1 MAPK) as a loading control. As shown in Figure 2-7E, the levels of MPK-1 were similar between different transgenic samples. Quantitation of PPM-2::GFP levels using multiple, independently derived transgenic lines showed that coexpression of PPM-2::GFP with FLAG::DLK-1 *K162R* resulted in a significant increase in PPM-2::GFP expression levels (2.5 +/- 0.5) compared to coexpression with mCherry (0.3 +/- 0.1, Figure 2-7F). Collectively, these results support the conclusion that DLK-1 is likely to be a direct target of PPM-2 phosphatase activity.

2.2.7 PPM-2 acts on serine 874 in DLK-1L

A recent study showed that two conserved serine residues, S874 and S878, in the C-terminus of the long/full-length isoform of DLK-1 (DLK-1L) regulate its activity (Yan and Jin, 2012). When DLK-1L is phosphorylated, it homodimerizes and is active. When DLK-1L is dephosphorylated, it preferentially binds to a short isoform of DLK-1 (called DLK-1S) creating an inactive heterodimer. Given our observation that PPM-2 is a serine/threonine phosphatase that negatively regulates DLK-1, we tested if PPM-2 functions by dephosphorylating one or both of these C-terminal serine residues in DLK-1L. To test this hypothesis, we used a transgenic approach and analyzed axon termination in the PLM neuron. We

generated transgenic animals with extrachromosomal arrays that expressed either wild-type DLK-1L or a phosphomimetic point mutant of DLK-1L (*S874E S878E*) alone or in combination with PPM-2. Transgenic overexpression of DLK-1 or DLK-1 *S874E S878E* using a pan-neuronal promoter (P*rgef-1*) resulted in similar penetrance of hook defects in the PLM neurons (55.5 +/- 4.2% for DLK-1 and 56.8 +/- 5.4% for DLK-1 *S874E S878E*, Figure 2-8A). Coexpression of PPM-2 significantly rescued the defects caused by overexpression of DLK-1 (compare 55.5 +/- 4.2% for DLK-1 and 22.6 +/- 5.6% for DLK-1 + PPM-2), but did not rescue defects caused by overexpression of DLK-1 *S874E S878E* (compare 56.8 +/- 5.4% for DLK-1 *S874E S878E* and 46.1 +/- 2.3% for DLK-1 *S874E S878E* + PPM-2, Figure 2-8A). These results suggest that PPM-2 regulates phosphorylation of DLK-1L at S874, S878 or both serine residues.

We further mapped the target residue in DLK-1L that was regulated by PPM-2 by testing DLK-1L that was solely mutated at S874 or S878. As shown in Figure 2-8A, transgenic overexpression of DLK-1 *S874E* or DLK-1 *S878E* resulted in axon termination defects in the PLM neurons (59.1 +/- 6.8% for DLK-1 *S874E* and 56.1 +/- 7.2% for DLK-1 *S878E*). Coexpression of PPM-2 significantly rescued the defects caused by overexpression of DLK-1 *S878E* (compare 56.1 +/- 7.2% for DLK-1 *S878E* and 17.0 +/- 3.0% for DLK-1 *S878E* + PPM-2, Figure 2-8A). In contrast, PPM-2 did not rescue defects caused by overexpression of

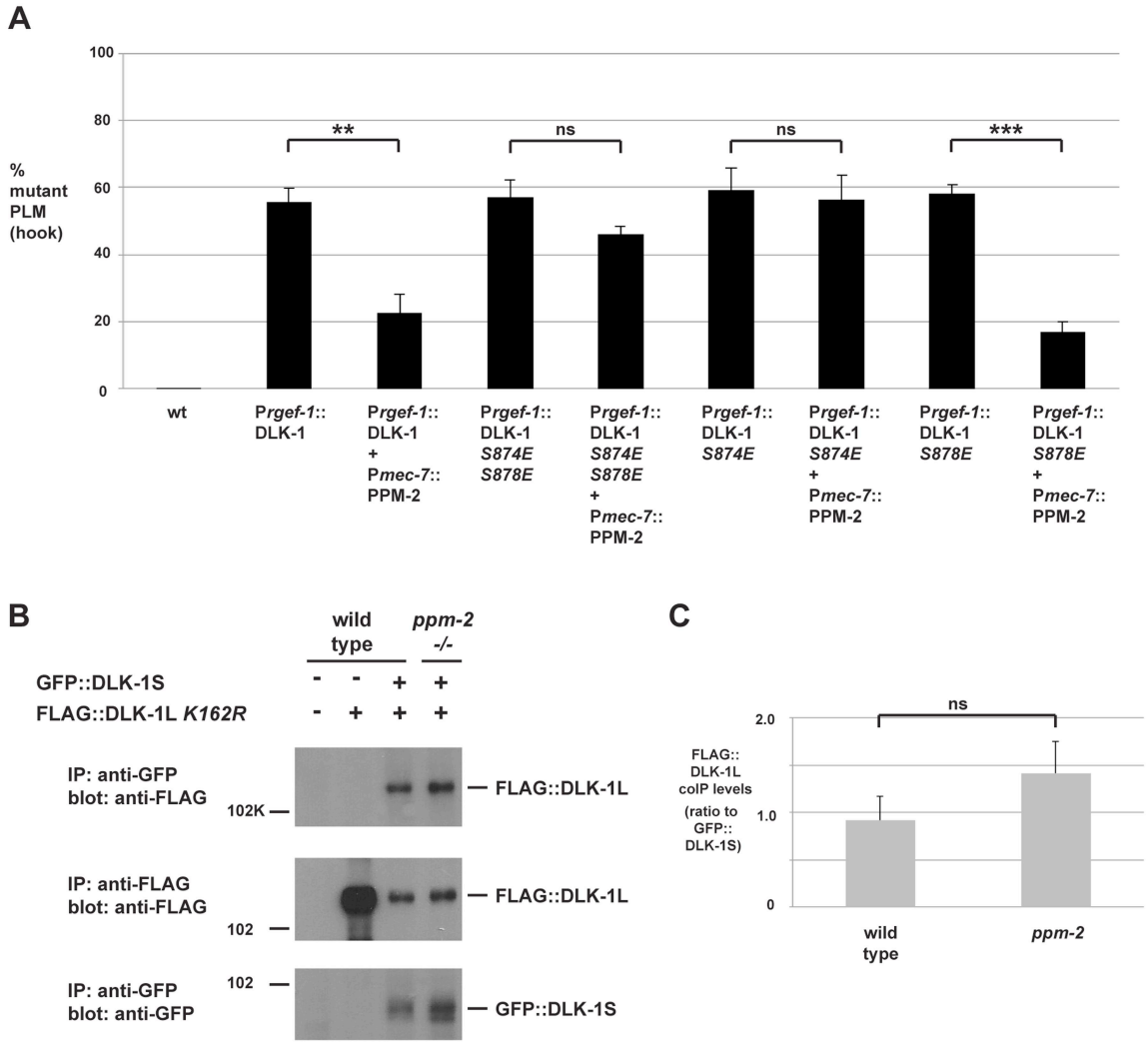

Figure 2-8. PPM-2 regulates DLK-1 by acting on S874.
(A) Quantitation of PLM axon termination defects (hook) caused by transgenic overexpression of DLK-1 and phosphomimetic DLK-1 point mutants. Note that coexpression of PPM-2 rescues defects caused by overexpression of DLK-1, but not defects caused by overexpression of DLK-1 *S874E S878E* and DLK-1 *S874E*. Shown are averages of data pooled from 5 or more transgenic lines for the indicated genotypes; young adult worms (16-20 hours post L4) grown at 23°C were analyzed. *(B)* CoIP from transgenic whole worm lysates showing that FLAG::DLK-1L *K162R* coprecipitates with GFP::DLK-1S, and binding of DLK-1L to DLK-1S is not altered in *ppm-2-/-* mutants (upper panel). *(C)* Quantitation of FLAG::DLK-1L *K162R* coIP with GFP::DLK-1S for the indicated genotypes normalized to amount of GFP::DLK-1S precipitated. Shown are the average levels of FLAG::DLK-1 *K162R* coprecipitating with GFP::DLK-1S acquired from 3 independently derived transgenic lines for each genotype. Error bars represent the standard error of the mean, and significance was determined using an unpaired *t*-test. ** p< 0.01, *** p<0.001, ns = not significant.

DLK-1 *S874E* (Figure 2-8A). Thus, PPM-2 regulates the activity of DLK-1L by acting on S874.

Given the results of our functional transgenic experiments, we next wanted to test if PPM-2 regulated the binding of DLK-1L to DLK-1S. We generated transgenic worms that used the pan-neuronal *rgef-1* promoter to coexpress FLAG::DLK-1L *K162R* with GFP::DLK-1S. As shown in Figure 2-8B, DLK-1L coprecipitates with DLK-1S, which is consistent with previous observations made using yeast two-hybrid analysis and a heterologous expression system (Yan and Jin, 2012). The interaction between DLK-1L and DLK-1S was unchanged in *ppm-2-/-* mutants (Figure 2-8B and C).

Thus, our functional genetic and biochemical experiments demonstrate that PPM-2 acts at S874 to regulate phosphorylation and activation of DLK-1. Our results are consistent with two possible signaling models: 1) S874 is an activating phosphorylation site on DLK-1L that is regulated by PPM-2, and does not regulate binding to DLK-1S. 2) DLK-1L must be phosphorylated at both S874 and S878 to prevent binding of DLK-1S and allow DLK-1L activation.

2.2.8 ppm-2 regulates synapse formation by GABAergic motor neurons

Previous studies in *C. elegans* have shown that *rpm-1* regulates synapse formation in motor neurons (Nakata et al., 2005; Zhen et al., 2000). In *C. elegans*, there are two sets of GABAergic, inhibitory motor neurons: the VD neurons that innervate the ventral muscles, and the DD neurons that innervate

the dorsal muscles (Figure 2-9A, see schematic). The presynaptic terminals of VD and DD motor neurons were visualized in living worms using *juIs1*, a transgene that uses a cell-specific promoter (P*unc-25*) to drive expression of a fusion protein of Synaptobrevin 1 (SNB-1) and GFP (SNB-1::GFP) (Hallam and Jin, 1998). In wild-type animals, SNB-1::GFP localized to presynaptic puncta that were uniform in size and evenly spaced along the dorsal nerve cord (Figure 2-9A). In *rpm-1-/-* mutants, the dorsal SNB-1::GFP puncta were abnormal in size and aggregated (Figure 2-9A, arrowheads), and there were sections of the dorsal cord with gaps in which no SNB-1::GFP puncta were present (Figure 2-9A, arrows). Previous studies using electron microscopy established that defects in the localization of SNB-1::GFP in *rpm-1-/-* mutants reflect defects in synapse formation, rather than simply defects in the formation of presynaptic terminals or the trafficking of synaptic vesicles (Nakata et al., 2005; Zhen et al., 2000). Quantitation of the number of SNB-1::GFP puncta showed that *rpm-1-/-* animals had fewer synapses than wild-type animals (compare 11.3 +/- 0.4 SNB-1::GFP puncta/100mm for *rpm-1* to 21.9 +/- 0.4 puncta/100mm for wild type, Figure 2-9B). This observation was consistent with previous studies (Nakata et al., 2005; Tulgren et al., 2011).

To test if *ppm-2* functions in synapse formation, we analyzed *ppm-2-/-* animals and a series of double mutants of *ppm-2* and members of the RPM-1 pathway. We found that *ppm-2(ok2186)-/-* and *ppm-2(tm3480)-/-* mutants had normal patterning and numbers of SNB-1::GFP puncta (Figure 2-9A and B). In

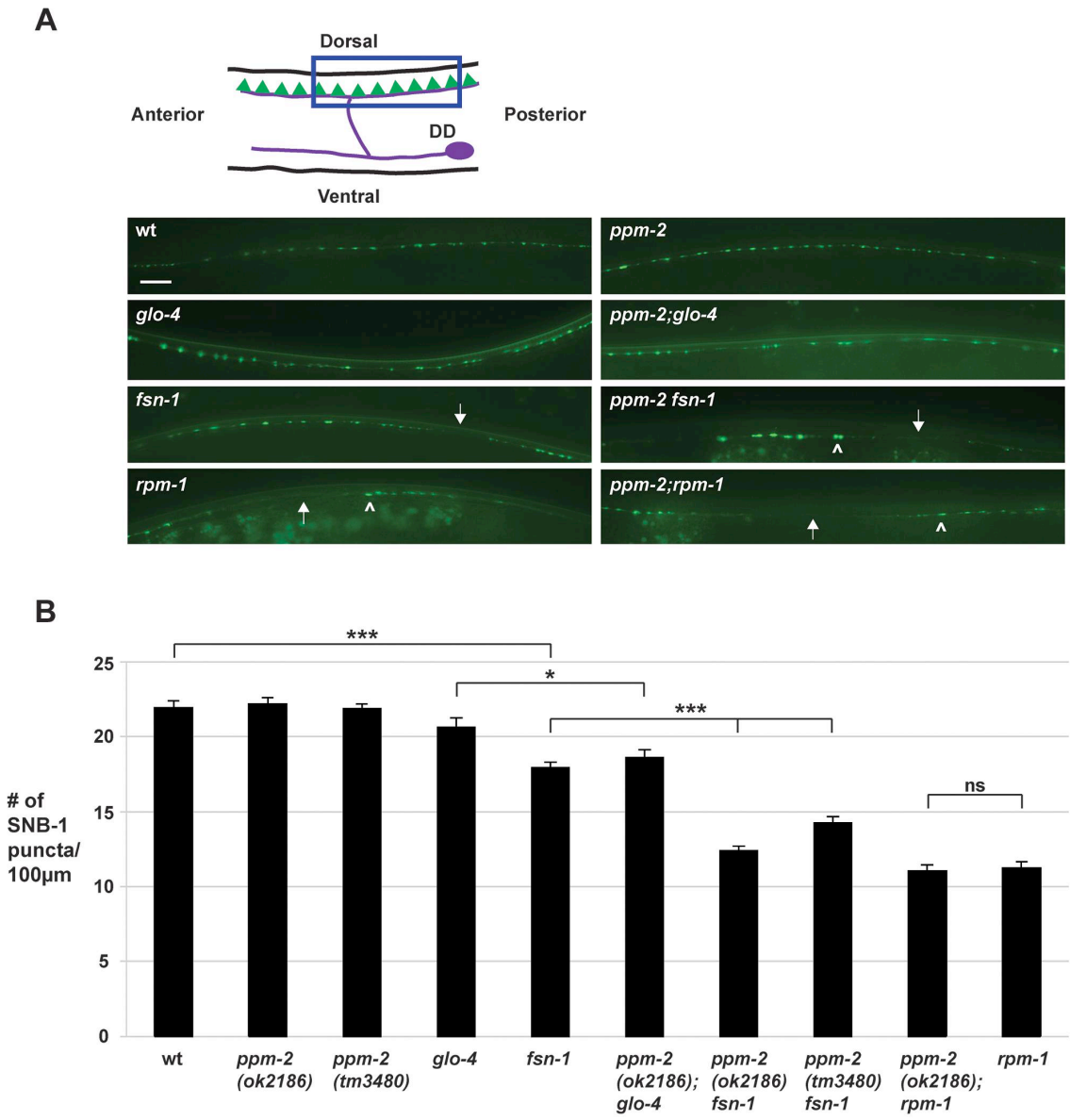

Figure 2-9. *ppm-2* regulates synapse formation by GABAergic motor neurons.
(A) Upper panel is a schematic diagram modified from Worm Atlas showing the GABAergic DD neurons that innervate the dorsal muscles (DD cell body and axon on the ventral side of the animal, and presynaptic terminals on the dorsal side of the animal). A transgene, *juIs1* (P_{unc-25}SNB-1::GFP), and epifluorescent microscopy was used to visualize the presynaptic terminals of the DD motor neurons for the indicated genotypes. Arrows note regions of the dorsal cord where presynaptic terminals are absent. Arrowheads highlight abnormal aggregation of presynaptic terminals. Scale bar is 10 µm. *(B)* Quantitation of synapse formation defects. Shown are averages for data collected from 3 or more independent experiments performed at 25°C in which 15-20 synchronized, young adult worms (16-20 hours post L4) were analyzed. Error bars represent the standard error of the mean, and significance was determined using an unpaired *t*-test. * $p<0.05$, *** $p<0.001$ and ns = not significant.

contrast, *ppm-2-/- fsn-1-/-* and *ppm-2-/-; glo-4-/-* double mutants had enhanced defects in synapse formation (Figure 2-9A) compared to single mutants (compare 14.2 +/- 0.5 puncta/100mm for *ppm-2(tm3480) fsn-1* and 12.4 +/-1.7 for *ppm-2(ok2186) fsn-1* to 17.9 +/- 0.4 for *fsn-1*, Figure 2-9B). We also analyzed *ppm-2-/-; rpm-1-/-* double mutants and found that they had similar defects in synapse formation to *rpm-1-/-* single mutants assessed qualitatively (Figure 2-9A) and quantitatively (Figure 2-9B). Our observations are consistent with two conclusions. First, *ppm-2* functions in a parallel genetic pathway to both *fsn-1* and *glo-4* to regulate synapse formation, since all the mutants used in our study are null alleles. Second, *ppm-2* functions in the same genetic pathway as *rpm-1* to regulate synapse formation, as synapse formation defects in *ppm-2-/-; rpm-1-/-* double mutants were not enhanced, and the synapse formation defects in *rpm-1-/-* mutants are not saturated (Liao et al., 2004).

2.2.9 PPM-2 is localized to presynaptic terminals

Having established the molecular mechanism of how PPM-2 functions in neuronal development, we wanted to determine if PPM-2 is localized to a particular subcellular compartment in neurons. To do so, we took a transgenic approach in which PPM-2 was expressed in the GABAergic motor neurons. The GABAergic motor neurons were analyzed to maintain consistency with prior cell biology studies on RPM-1 and its binding partners. A cell specific promoter (P*unc-25*) was used to express PPM-2 as a C-terminal fusion protein with GFP

(PPM-2::GFP), in order to ensure that GFP did not interfere with the myristoylation of PPM-2. PPM-2::GFP was localized broadly throughout the motor neuron axons and cell bodies with strong enrichment in puncta along the ventral and the dorsal nerve cord (Figure 2-10A). This localization pattern was similar to molecules that are localized to the presynaptic terminal, such as SNB-1. To test this possibility, transgenic animals were generated that expressed a fusion protein of SNB-1 and dsRED (SNB-1::dsRED) with PPM-2::GFP in the GABAergic motor neurons. As shown in Figure 2-10B, PPM-2::GFP and SNB-1::dsRED colocalized in puncta at the presynaptic terminals of the DD neurons on the dorsal side of the animal. Localization of PPM-2 to the presynaptic terminal is consistent with our finding that PPM-2 regulates synapse formation in the GABAergic motor neurons.

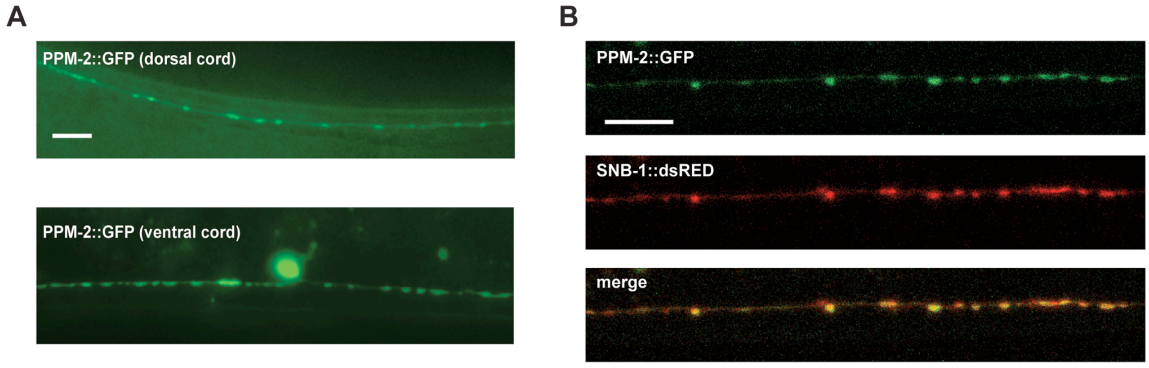

Figure 2-10. PPM-2 localizes to the presynaptic terminal.
(A) PPM-2::GFP was transgenically expressed in the GABAergic motor neurons using a cell specific promoter (P*unc-25*). Epifluorescent microscopy was used to visualize PPM-2::GFP puncta in the dorsal and ventral cords. *(B)* Transgenic worms expressing PPM-2::GFP and SNB-1::dsRED in the GABAergic motor neurons were analyzed by confocal microscopy. Shown are the presynaptic terminals of the DD neurons on the dorsal side of the animal. Scale bar is 10 μm.

2.3 Discussion

How axon outgrowth, synapse formation, and termination of axon outgrowth are molecularly coordinated during development remains poorly understood. The PHR proteins meet a growing list of criteria as molecules that integrate and coordinate these events during development. The PHR proteins function in synapse formation (Burgess et al., 2004; Schaefer et al., 2000; Wan et al., 2000; Zhen et al., 2000), axon guidance and outgrowth (D'Souza et al., 2005; Lewcock et al., 2007; Li et al., 2008), and axon termination (Kim et al., 2013; Lewcock et al., 2007; Schaefer et al., 2000), and importantly often do so in the same type of neuron. Studies using *C. elegans* and Drosophila have shown that PHR proteins are extremely large, intracellular signaling proteins that function cell autonomously. Thus, PHR proteins have the potential to integrate signals coming from different extracellular cues converging on a single neuron. There is evidence suggesting that the activity of the PHR proteins can be regulated (Pierre et al., 2004; Tian et al., 2011), although the extracellular signals that activate or inhibit PHR proteins remain unclear. Finally, the PHR proteins negatively and positively regulate multiple downstream signaling pathways that control gene transcription (Collins et al., 2006; Guo et al., 1998; Lewcock et al., 2007; Murthy et al., 2004; Nakata et al., 2005), signal transduction and local mRNA translation (Grill et al., 2007; Murthy et al., 2004; Pierre et al., 2008; Scholich et al., 2001; Yan et al., 2009), microtubule dynamics (Grill et al., 2012;

Hendricks and Jesuthasan, 2009; Lewcock et al., 2007), and vesicle trafficking/formation (Grill et al., 2007).

Studies in worms, flies, fish, and mice have shown that PHR proteins function as ubiquitin ligases to negatively regulate the MAP3K DLK, which represents a mechanism to control long-term signaling by the DLK pathway. We now show that *C. elegans* RPM-1 also utilizes a phosphatase, PPM-2, to negatively regulate DLK-1 (Figure 2-11). This suggests that RPM-1 has the potential to rapidly regulate signaling by DLK-1. Thus, our results suggest that RPM-1 has the potential to employ different regulatory mechanisms to spatially and/or temporally regulate DLK-1 signaling, which provides further support for the proposition that PHR proteins may coordinate different events during development. To our knowledge, RPM-1 also now represents the first example of

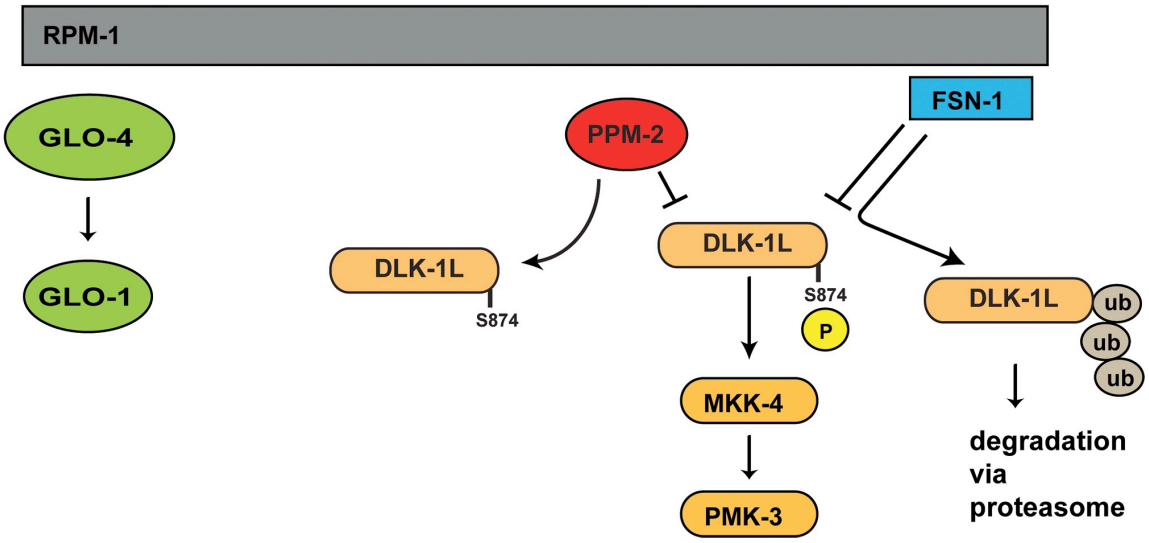

Figure 2-11. Summary of RPM-1 signaling.
RPM-1 is a positive regulator of the GLO-4 pathway, and acts as part of a complex with FSN-1 that ubiquitinates and negatively regulates DLK-1. PPM-2 is also part of an RPM-1 protein complex and negatively regulates DLK-1 via dephosphorylation at S874.

a single signaling protein that controls both ubiquitination and dephosphorylation of a MAP3K.

2.3.1 PPM-2 mediates RPM-1 function

Our proteomic screen for RPM-1 binding proteins identified the PP2C phosphatase PPM-2, which we confirmed using coIP from transgenic *C. elegans*. Genetic and transgenic experiments showed that *ppm-2* functions downstream of *rpm-1* to regulate axon termination and synapse formation. Importantly, our genetic analysis also demonstrated that *ppm-2* and *rpm-1* function in the same genetic pathway consistent with our observation that these molecules physically interact.

Axon termination and synapse formation defects were enhanced in *ppm-2-/- fsn-1-/-* double mutants and *ppm-2-/-;glo-4-/-* double mutants. Given that we analyzed null alleles of *ppm-2*, *glo-4*, and *fsn-1*, our results are consistent with these three molecules acting in parallel pathways that converge on a common molecular player or process in neurons. In the case of PPM-2 and FSN-1, we have identified this common player as DLK-1. It remains unclear which downstream molecule or process is commonly regulated by GLO-4 and PPM-2.

Our results support the conclusion that RPM-1 positively regulates PPM-2 for several reasons. First, *rpm-1* and *ppm-2* (lf) mutants both have axon termination defects. Second, defects in *ppm-2-/-; rpm-1-/-* double mutants were not suppressed. If PPM-2 were negatively regulated by RPM-1, we would expect

that loss of function in *ppm-2* would suppress the defects in *rpm-1* mutants. Such is the case for DLK-1, which is negatively regulated by RPM-1 (Nakata et al., 2005). Finally, none of the molecules we have identified in our proteomic screen for RPM-1 binding proteins (including: GLO-4, FSN-1, and RAE-1) have been genetic suppressors of *rpm-1* (lf) (Grill et al., 2007; Grill et al., 2012). Thus, our screen does not efficiently identify ubiquitination targets of RPM-1, presumably because such interactions are transient. Overall, our data are consistent with the conclusion that RPM-1 binds to and positively regulates PPM-2. Nonetheless, developing a more refined mechanistic understanding of how PPM-2 is regulated by RPM-1 remains an important goal.

RPM-1 is highly conserved with functional orthologs in Drosophila, zebrafish, and mice. The RPM-1 binding proteins we previously identified in our proteomic screen, including GLO-4, FSN-1 and RAE-1, are also evolutionarily conserved from worms to mammals (Grill et al., 2007; Grill et al., 2012). With regard to PPM-2, we identified clear orthologs in Drosophila and the protochordate *Ciona intestinalis*, which suggests that PPM-2 is likely to represent a conserved mechanism by which PHR proteins function. However, due to lack of sequence conservation we were unable to identify an orthologous phosphatase to PPM-2 in vertebrates. While PPM-2 may represent a unique mechanism of regulating neuronal development in invertebrates and protochordates, it is also possible that another PP2C phosphatase (or a member of a different phosphatase family) may perform the function of PPM-2 in

vertebrate neurons. It is notable that the PP2C phosphatase PPM-1, which is one of the closest homologs of PPM-2 in *C. elegans*, also regulates axon termination and synapse formation (Tulgren et al., 2011). In mammals, PPM-1 has three orthologs, PP2Ca, PP2Cb, and PP2Cb-like. Because the PPM-1 subfamily has undergone significant expansion in mammals, PP2Ca, PP2Cb, and PP2Cb-like are plausible candidates as the functional ortholog of PPM-2. Future experiments in *C. elegans* using mammalian PP2C phosphatases may be helpful in addressing this possibility.

2.3.2 A complex negative regulatory network controls the DLK-1 pathway

RPM-1 and the PHR proteins function in part by ubiquitinating and negatively regulating the MAP3K DLK-1 (Collins et al., 2006; Lewcock et al., 2007; Nakata et al., 2005). Transgenic overexpression of DLK-1 at higher levels than used in our study causes more severe defects than *rpm-1* (lf), such as uncoordinated locomotion and small body size (Abrams et al., 2008; Nakata et al., 2005). This observation suggested that negative regulatory mechanisms, aside from ubiquitination by RPM-1, restrain the activity of DLK-1 and/or its downstream kinases. Recent work in *C. elegans* has supported this hypothesis by showing that PPM-1 (a homolog of PPM-2) and VHP-1 (a dual specificity phosphatase) negatively regulate the DLK-1 pathway (Nix et al., 2011; Tulgren et al., 2011). Nonetheless, it remained uncertain if a specific phosphatase directly regulated

DLK-1. It also remained unclear if RPM-1 functions through mechanisms other than ubiquitination to control the activity of DLK-1.

We now address both these questions by showing that RPM-1 binds to the phosphatase PPM-2, and functions through this phosphatase-based mechanism to negatively regulate DLK-1 (Figure 2-11). Our biochemical and functional genetic analysis indicate that DLK-1 is negatively regulated by PPM-2. This is most likely the result of direct dephosphorylation as corroborated by several observations: 1) PPM-2 binds to DLK-1. 2) PPM-2 *R185A* acts as a trap for phosphorylation targets, and shows increased binding to DLK-1. 3) Transgenic expression of DLK-1 allows increased coexpression of PPM-2, presumably by titrating excess PPM-2 phosphatase activity that is otherwise problematic for neurons.

A previous study showed that phosphomimetic point mutation of DLK-1L at both S874 and S878 allowed DLK-1L to homodimerize and become active (Yan and Jin, 2012). Point mutations in DLK-1L that prevented phosphorylation at both S874 and S878 resulted in formation of an inactive heterodimer with DLK-1S (short, inhibitory isoform). This prior study did not determine if phosphorylation of DLK-1L at S874, S878 or both residues was required to regulate binding to DLK-1S. We have found that PPM-2 acts specifically on S874 to regulate DLK-1L activity (Figure 2-11). While PPM-2 activity is sufficient to inhibit transgenically overexpressed DLK-1 (Figure 2-8A), it was not sufficient to regulate binding of DLK-1L to DLK-1S (Figure 2-8B). This result is consistent with

two possible interpretations. 1) Phosphorylation of DLK-1 at S874 is required for activation of DLK-1, but this activation occurs through a mechanism that is independent of DLK-1S. 2) DLK-1L needs to be phosphorylated at both S874 and S878 to block binding to DLK-1S and become active. In this case, DLK-1L would display different levels of inactivation, with dephosphorylation at both residues presumably being the most inactive. Such a signaling model would allow sophisticated spatial and temporal control over how quickly DLK-1 is activated. A combination of future biochemical and genetic experiments will hopefully support one of these two signaling models.

C. elegans DLK-1 has two homologs in mammals, DLK (MAP3K12) and LZK (MAP3K13) both of which are highly expressed in brain (Holzman et al., 1994; Sakuma et al., 1997). While DLK plays an important role in neuronal development and axon regeneration, our knowledge regarding LZK remains relatively modest. Notably, the small segment of the *C. elegans* DLK-1L C-terminus that contains S874 and S878 is conserved with mammalian LZK, and not mammalian DLK (Yan and Jin, 2012). Thus, the mammalian functional ortholog of PPM-2 would be likely to regulate LZK rather than DLK.

Because RPM-1 binds to and positively regulates PPM-2, it is plausible that RPM-1 acts as a more sophisticated regulator of DLK-1 than originally thought by regulating long-term DLK-1 signaling (through ubiquitination) and short-term/local DLK-1 signaling (through the phosphatase activity of PPM-2). The idea that RPM-1 controls local/short-term signaling and long-term signaling

is supported by observations in flies and worms showing that the DLK-1 pathway regulates the activity of the transcription factors Fos and CEBP-1 (Collins et al., 2006; Yan et al., 2009), and the translation of CEBP-1 locally in axons (Yan et al., 2009). We note that our results cannot absolutely rule out the possibility that dephosphorylation of DLK-1 by PPM-2 is a prerequisite for ubiquitination and degradation of DLK-1 by an RPM-1/FSN-1 ligase complex. However, our finding that *ppm-2* and *fsn-1* function in parallel genetic pathways makes this extremely unlikely.

It remains important to address how RPM-1 determines whether to degrade DLK-1, or act through PPM-2 to dephosphorylate DLK-1. This may be based on developmental timing, the subcellular location of DLK-1, the activation state of DLK-1, post-translational modification of DLK-1, or a combination of these factors. Upstream signals may also instruct RPM-1 to degrade or dephosphorylate DLK-1. A better understanding of the mechanisms and molecules that activate RPM-1 and DLK-1 are likely to be helpful in addressing these possibilities.

Since both PPM-2 and PPM-1 negatively regulate the DLK-1 pathway, we attempted to analyze the genetic relationship between *ppm-2* and *ppm-1*. Unfortunately, *ppm-2-/-; ppm-1-/-* double mutants were embryonic lethal in the F2 generation (data not shown), which rendered our genetic analysis inconclusive. However, the synthetic lethality observed between *ppm-2* (lf) and *ppm-1* (lf) is consistent with these phosphatases acting on different targets. This agrees with

our prior study that suggested PPM-1 acts at the level of the p38 MAP kinase PMK-3 (Tulgren et al., 2011), and our work here demonstrating that PPM-2 acts on DLK-1. Several other pieces of evidence support the conclusion that PPM-2 and PPM-1 act on different targets in the DLK-1 pathway. The primary phenotype in *ppm-2-/-* animals was low penetrance hook defects in PLM neurons, while we previously showed that *ppm-1-/-* mutants primarily display low penetrance overextension defects in PLM neurons (Tulgren et al., 2011). Since the hook phenotype is more severe (Grill et al., 2007; Grill et al., 2012), our results are consistent with PPM-2 acting higher up in the kinase cascade than PPM-1. This model is further supported by our observation that *ppm-2-/- fsn-1-/-* double mutants show stronger enhancement of hook defects (Figure 2-2D) compared to *ppm-1-/-; fsn-1-/-* double mutants (Tulgren et al., 2011). Nonetheless, further biochemical and transgenic studies will be needed to definitively determine if PPM-2 and PPM-1 act at different points in the DLK-1 pathway.

2.3.3 N-myristoylation and PPM-2

Previous studies have shown that several types of phosphatases are myristoylated (Aitken et al., 1982; Alonso et al., 2004; Chida et al., 2013; Schwertassek et al., 2010). Our mass spectrometry and transgenic results indicated that N-myristoylation is also required for PPM-2 to be fully functional. Our findings are consistent with prior observations on PP2C phosphatases. First, other PP2C phosphatases have N-myristoylation consensus motifs (Feng et al.,

2010a). Second, a recent biochemical study showed that two PP2C phosphatases (PPM1A and PPM1B) are N-myristoylated, and myristoylation is required for substrate specificity, but not enzymatic activity (Chida et al., 2013). However, myristoylation is also known to regulate the membrane localization of signaling proteins. Thus, our findings coupled with these prior observations demonstrate that N-myristoylation is an important posttranslational modification that mediates the substrate specificity and/or membrane localization of PPM-2. We also show for the first time that myristoylation is important for the function of PP2C phosphatases in neurons.

Previous work showed that mammalian DLK is associated with the plasma membrane at synapses (Mata et al., 1996). While DLK in the cytosol is in both hyperphosphorylated and unphosphorylated forms, membrane bound DLK is phosphorylated to a lesser extent or unphosphorylated. Our observations that PPM-2 is N-myristoylated, that PPM-2 negatively regulates DLK-1, and that PPM-2 binds to DLK-1 suggest that PPM-2 may act at the plasma membrane of the presynaptic terminal to regulate the phosphorylation of DLK-1. This model is consistent with our observation that PPM-2 is localized to the presynaptic terminal (see Figure 8). Alternatively, N-myristoylation may regulate the target specificity of PPM-2 and, therefore, PPM-2 activity on DLK-1.

2.3.4 Conclusion

We now provide evidence that RPM-1 is potentially a more sophisticated regulator of DLK-1 than originally thought. While this is a significant step forward, important questions remain: 1) Does RPM-1 regulate molecules other than DLK-1 in a more precise and accurate manner, possibly through PPM-2 or other mechanisms? 2) How is RPM-1 activity regulated, and do upstream extracellular guidance cues, morphogens, or adhesion molecules instruct the activity of RPM-1 during neuronal development? 3) Is RPM-1 located in multiple subcellular compartments in a single neuron, which may explain the dual role of RPM-1 in axon termination and synapse formation? Addressing these questions will be essential to further support the previously proposed model that RPM-1 and the PHR proteins function to coordinate different events in neuronal development (Li et al., 2008; Po et al., 2010).

2.4 Materials and Methods

2.4.1 Genetics

The N2 isolate of *C. elegans* was propagated using standard procedures. The alleles used in this study included: *rpm-1(ju44)*, *fsn-1(gk429)*, *glo-4(ok623)*, *dlk-1(ju476)*, *ppm-2(ok2186)*, *ppm-2(tm3480)*, *unc-32(e189)*, *unc-103(e1597)*, *dpy-17(e164)*, and *lon-1(e1820)*. For generation of transheterozygous *ppm-2(ok2186)/ppm-2(tm3480) fsn-1* double mutants, *tm3480* was linked to *unc-32(e189)* and *ok2186* was linked to *lon-1(e1820)*. Transheterozygous animals were identified as non-lon, non-unc animals. *ppm-2(ok2186) fsn-1* and *ppm-*

2(tm3480) fsn-1 double mutants were constructed by recombination using *ok2186* and *tm3480* linked to *dpy-17(e164)* and *fsn-1* linked to *unc-103(e1597)*.

2.4.2 Transgenics

Transgenic animals were generated by standard microinjection procedures. All transgenes were constructed by injection of plasmid or DNA generated by PCR with P_{ttx-3}RFP (50 ng/μL) or P_{myo-2}mCherry (2.5 ng/μL) and pBluescript (50 ng/μL). Injection conditions and genotypes for all transgenes are provided upon request. For all transgenic and biochemical experiments, a cDNA encoding isoform B of DLK-1 was used. Point mutants of DLK-1 (S874E and S878E) were annotated based on isoform A for continuity of presentation with previous studies, but these residues correspond to S867 and S871 in isoform B.

2.4.3 Biochemistry and mass spectrometry

Purification of RPM-1::GFP from transgenic *C. elegans* and identification of associated RPM-1 binding proteins by mass spectrometry was described previously (Grill et al., 2007). In brief, transgenic mixed stage *C. elegans* were grown in liquid cultures using M9 buffer supplemented with cholesterol and HB101 *E. coli*. Worms were washed repeatedly in fresh M9 buffer, and pelleted by low speed centrifugation. Frozen worms were ground under liquid N_2 with a mortar and pestle, and extracted with 0.1% NP-40 lysis buffer (10mM Tris pH 7.4, 0.1% NP-40, 150mM NaCl, 1mM DTT, protease and phosphatase

inhibitors). GFP::RPM-1 was immunoprecipitated from worm extracts using an anti-GFP antibody (3E6 mouse monoclonal, Qbiogene), run on an SDS-PAGE gel, and proteins coprecipitating with GFP::RPM-1 were identified by LC-MS/MS.

For coIP of RPM-1 and PPM-2, worms were lysed in 0.1% NP-40 lysis buffer (50mM Tris pH 7.5, 0.1% NP-40, 150 mM NaCl, 10% glycerol, protease inhibitors, and phosphatase inhibitors: microcystin, NaVO4, NaF, NaMolybdate, and b-glycerophosphate). For coIP, transgenic proteins were immunoprecipitated with an anti-FLAG antibody (M2 mouse monoclonal, Sigma) or an anti-GFP antibody (3E6 mouse monoclonal, MP Biomedicals) and protein G agarose. Coprecipitating GFP fusion proteins or FLAG tagged proteins were detected by immunoblotting with an anti-GFP antibody (Roche, mouse monoclonal) or an anti-FLAG antibody (rabbit monoclonal, Cell Signaling), respectively. 3 mg of total worm lysate was used for coIP of FLAG::PPM-2 with RPM-1::GFP. 5mg of total worm lysate was used for coIP of wild-type or mutant PPM-2::GFP with FLAG::DLK-1 *K162R*. 10mg of total worm lysate was used for coIP of GFP::DLK-1S with FLAG:DLK-1L *K162R*.

For immunoblot analysis of whole *C. elegans* lysates, samples were prepared as described previously (Saha and Wolozin, 2011). Animals were age-synchronized by bleach treatment. Array positive young adults were selected using $P_{ttx\text{-}3}$RFP and cleaned by transferring to an NGM plate with no bacteria. 50 animals were picked for each genotype and placed into a tube with 20µL of water. Samples were mixed with 20µL of 2X Laemmli Sample Buffer (Biorad)

with 2-βmercaptoethanol. Animals were pelleted by centrifugation and samples were flash frozen in liquid nitrogen. Prior to immunoblotting, samples were incubated at 95^{o}C for 5 minutes, cooled for 5 minutes at room temperature, and loaded onto an SDS-PAGE gel. GFP fusion or FLAG tagged proteins were detected by immunoblotting with an anti-GFP antibody (Roche, mouse monoclonal) or an anti-FLAG antibody (rabbit monoclonal, Cell Signaling), respectively. MPK-1 (Erk1) was detected by immunoblotting with an anti-ERK1 antibody (K-23 rabbit polyclonal, Santa Cruz Biotechnology) and mCherry was detected by immunoblotting with an anti-mCherry antibody (mouse monoclonal, Clontech).

Immunoblots from coIP and whole cell lysates were visualized using secondary antibodies coupled to horseradish peroxidase, Supersignal FemtoWest chemiluminescent reagent (Pierce), and x-ray film. Western Lightning *Plus*-ECL (PerkinElmer) was used for anti-Erk immunoblotting of MPK-1. Quantitation of bands in immunoblots of whole worm lysates and coIP experiments was performed using image J software from NIH image (http://rsb.info.nih.gov/ij/).

2.4.4 Axon termination and synapse formation analysis

For analysis of GFP or SNB-1::GFP, live young adult animals (16-20 hours post L4) were anesthetized using 1% (v/v) 1-phenoxy-2-propanol in M9 buffer and visualized using a 40x magnification oil-immersion lens and an epifluorescent

microscope (Nikon Eclipse E40). Images were acquired using a CCD camera (Q-imaging Qicam 1394). Axon termination defects in the mechanosensory neurons were quantified by manually scoring *muIs32* (P_{mec-7}GFP). Synapse formation defects were quantified by collecting images of *juIs1* (P_{unc-25}SNB-1::GFP), and manually scoring puncta numbers in acquired images using Adobe Photoshop. The mechanosensory neurons were analyzed at 23^{o}C, as previous studies showed that axon termination defects in PLM neurons are maximally defective at 23^{o}C (Grill et al., 2007; Schaefer et al., 2000). While ALM axon termination and PLM synaptic branch extension are temperature sensitive processes, 23^{o}C is a sufficient temperature to achieve strong phenotypes. Synapse formation in GABAergic neurons was analyzed at 25^{o}C because a previous study showed that the *ju44* allele of *rpm-1* is temperature sensitive with regard to this process, and gives a maximal phenotype at 25^{o}C (Zhen et al., 2000).

2.4.5 Confocal microscopy

Colocalization of SNB-1::dsRED and PPM-2::GFP (*bggEx88*) was analyzed using a Zeiss 780 laser scanning confocal microscope at 63x magnification under immersion oil. Images were acquired using Zeiss Zen software, and analyzed using Image J. Young adult animals were analyzed in all cases.

2.5 Acknowledgements

We would like to thank Drs. Brian Ackley and Samuel Young Jr. for manuscript review and discussions. We are also grateful to Drs. Kirill Martemyanov and Yishi Jin for helpful discussions. Allison Gurney provided technical assistance. We also wish to thank the *C. elegans* knockout consortium for generating the deletion alleles used in this study, and the *C. elegans* Genetics Center for providing strains.

2.6 Author Contributions

Conceived and designed the experiments: STB WB BG. Performed the experiments: STB EDT KJO SMT WB. Analyzed the data: STB EDT WB BG. Wrote the paper: STB and BG.

3 Neuronal Development in *Caenorhabditis elegans* is Regulated by Inhibition of an MLK MAP Kinase Pathway

Content adapted from published article: **Baker ST**, Turgeon SM, Tulgren ED, Wigant J, Rahimi O, Opperman KJ, Grill B (2015) Neuronal development in *C. elegans* is regulated by inhibition of an MLK MAP kinase pathway. Genetics 199:151-156

3.1 Introduction

In *C. elegans*, the ubiquitin ligase Regulator of Presynaptic Morphology 1 (RPM-1) regulates neuronal development by inhibiting the DLK-1 pathway (composed of DLK-1, MKK-4, and PMK-3) (Nakata et al., 2005). RPM-1 and the DLK-1 pathway regulate axon regeneration post-developmentally (Hammarlund et al., 2009; Yan et al., 2009). The MLK-1 pathway, which includes the kinases MLK-1, MEK-1, and KGB-1/JNK, also regulates axon regeneration (Nix et al., 2011). It remains unclear if RPM-1 functions through the MLK-1 pathway to regulate development.

Protein Phosphatase Mg/Mn2+ dependent 1 (PPM-1) and PPM-2 negatively regulate the DLK-1 pathway (Baker et al., 2014; Tulgren et al., 2011). PPM-2 is regulated by RPM-1 and dephosphorylates full-length DLK-1 (DLK-1L). PPM-1 is likely to function lower in the DLK-1 pathway. It remains unclear whether PPM-1 and PPM-2 regulate other signaling pathways in the neurons of *C. elegans*.

Here, we show that mutations in *mlk-1*, *mek-1*, and *kgb-1/jnk* suppress defects in synapse formation and axon termination caused by *rpm-1* loss of function (lf). These results suggest that RPM-1 might negatively regulate the MLK-1 pathway, which is consistent with our observation that transgenic overexpression of MLK-1 or KGB-1 caused axon termination defects. Further, our results are consistent with PPM-1 negatively regulating the MLK-1 pathway,

in addition to inhibiting the DLK-1 pathway. In contrast, our findings suggested that PPM-2 only acts on DLK-1L.

3.2 Results

3.2.1 Loss-of-function mutations in kinases of the MLK-1 pathway suppress defects in synapse formation caused by *rpm-1* (lf)

The fly ortholog of RPM-1, called Highwire, functions through JNK to regulate synapse formation (Collins et al., 2006). It is unclear if RPM-1 functions through JNK to regulate synapse formation in worms, but studies on axon regeneration suggested that this might be a possibility (Nix et al., 2011). Hence, we assessed the genetic relationship between kinases of the MLK-1 pathway, including *kgb-1/jnk*, and *rpm-1* in the context of synapse formation.

Consistent with previous studies, the GABAergic motor neurons of *rpm-1-/-* mutants had synapse formation defects that were strongly, but incompletely, suppressed in *rpm-1-/-; dlk-1-/-* double mutants (Figure 3-1A and B) (Nakata et al., 2005). In double mutants of *rpm-1* with *mlk-1*, *mek-1* or *kgb-1*, significant but modest suppression occurred (Figure 3-1A and B). *rpm-1-/- mlk-1-/-; kgb-1-/-* triple mutants did not show increased suppression, demonstrating that *mlk-1* and *kgb-1* function in the same genetic pathway (Figure 3-1B). *rpm-1-/- mlk-1-/-; dlk-1* triple mutants showed a small, but significant increase in suppression, consistent with *mlk-1* and *dlk-1* functioning in partially redundant pathways (Figure 3-1B).

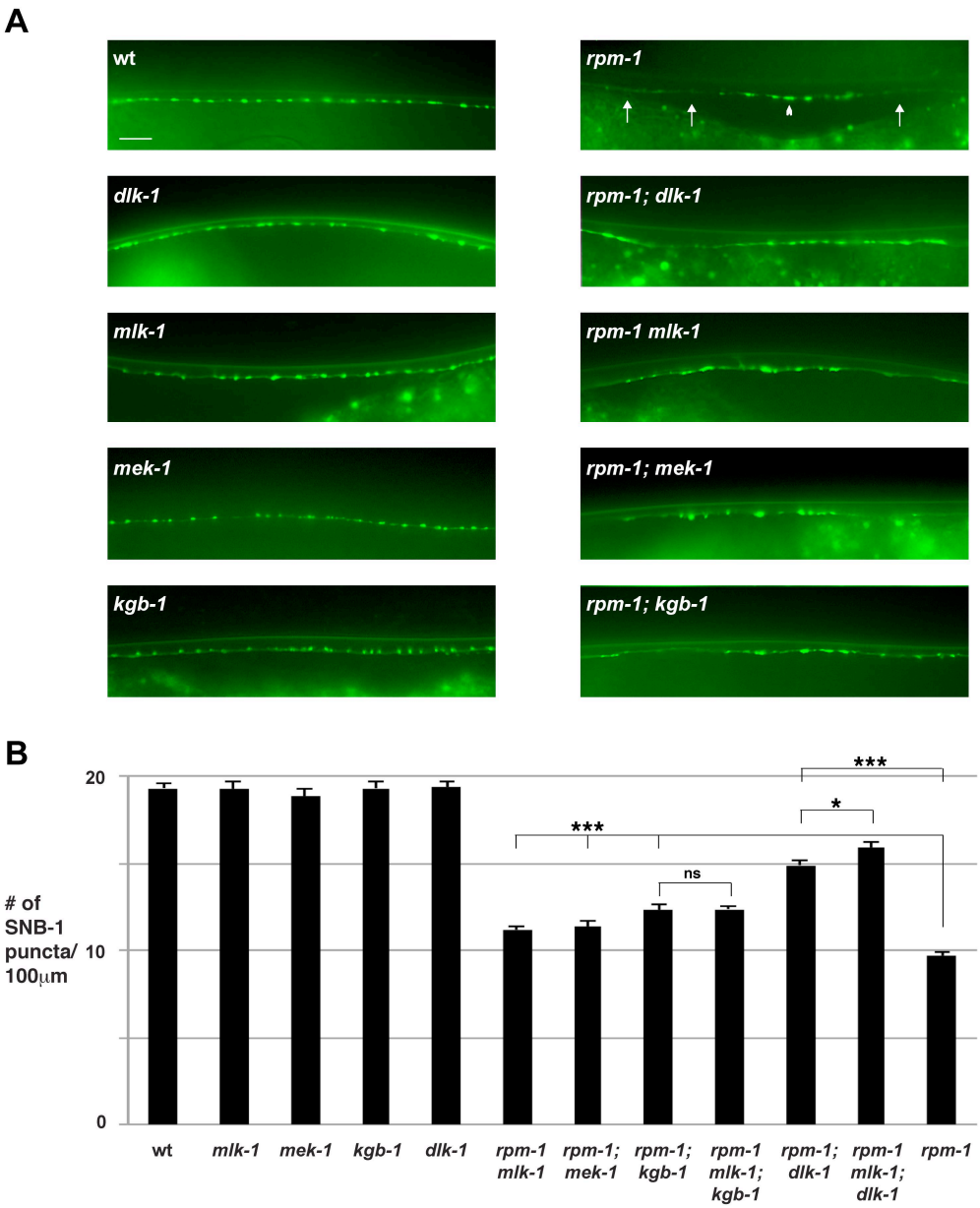

Figure 3-1. **Loss-of-function mutations in kinases of the MLK-1 pathway suppress synapse formation defects in *rpm-1* mutants**.
(A) Defects in synapse formation in the GABAergic motor neurons were analyzed using a transgene, *juIs1* (P_{unc-25}SNB-1::GFP), and epifluorescent microscopy under 40x magnification. *rpm-1* mutants had abnormal synapse formation with aggregated synapses (arrowheads) and gaps in the dorsal cord (arrows). Defects caused by *rpm-1* (lf) were partially suppressed by loss of function in *mlk-1*, *mek-1*, or *kgb-1*. Scale bar is 10μm. (B) Quantitation of synapse formation defects in GABAergic motor neurons for the indicated genotypes. Alleles used included: *rpm-1 (ju44)*, *dlk-1 (ju476)*, *mlk-1 (ok2471)*, *mek-1 (ks54)*, and *kgb-1 (um3)*. Shown are averages for data collected from 3 or more independent experiments performed at 25°C in which 15-20 synchronized, young adult worms were analyzed. Error bars represent the standard error of the mean, and significance was determined using an unpaired Student's *t*-test. ****P*<0.001, **P*<0.05, and ns = not significant

These results are consistent with RPM-1 regulating synapse formation by inhibiting both the DLK-1 and MLK-1 pathways. Notably, these findings do not rule out the possibility that kinases in the MLK-1 pathway function in a parallel genetic pathway to *rpm-1*.

3.2.2 Mutations in kinases of the MLK-1 pathway suppress axon termination defects caused by *rpm-1* (lf)

Two types of axon termination defects are present in the PLM mechanosensory neurons of *rpm-1-/-* mutants (Grill et al., 2007; Schaefer et al., 2000; Tulgren et al., 2011). 1) Severe, highly penetrant defects in which an axon overextends and hooks towards the ventral cord, referred to as hook defects (Figure 3-2A and B). 2) Rarely observed, milder defects in which an axon overextends but fails to hook ventrally, referred to as overextension defects. Hook defects were strongly suppressed in *rpm-1-/-; dlk-1-/-* double mutants (Figure 3-2B). In double mutants of *rpm-1* with *mlk-1, mek-1*, or *kgb-1* the frequency of hook defects was moderately suppressed, while the expressivity of less severe overextension defects was increased (Figure 3-2A and B). These effects were not increased in *rpm-1-/- mlk-1-/-; kgb-1-/-* triple mutants (Figure 3-2B). Transgenic expression of MLK-1 specifically in the mechanosensory neurons rescued the suppression in *rpm-1-/- mlk-1-/-* double mutants (Figure 3-2C).

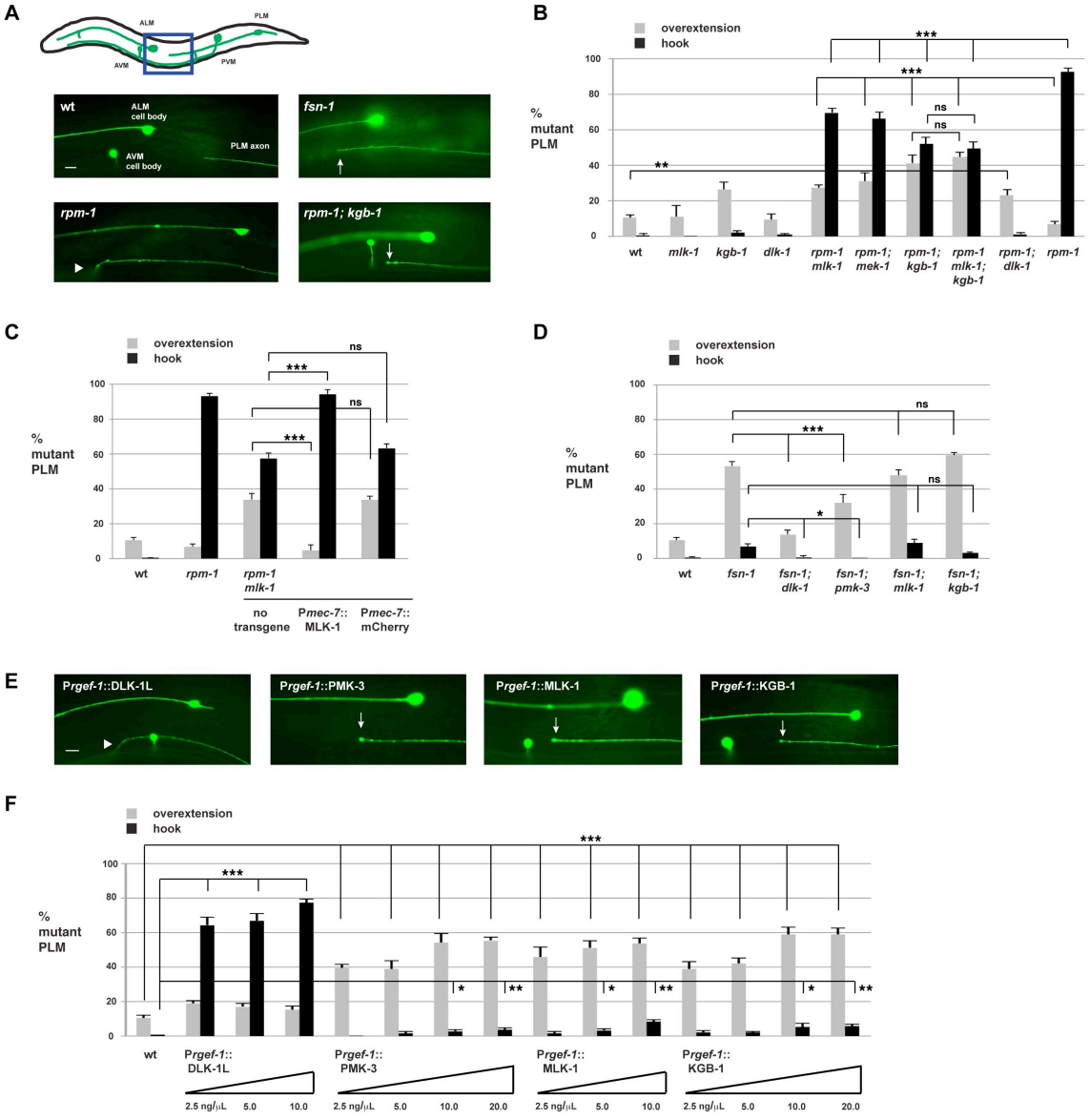

Figure 3-2. Axon termination defects in *rpm-1* mutants are suppressed by loss of function in *mlk-1*, *mek-1*, or *kgb-1*.
(A) Shown is a schematic of the mechanosensory neurons of *C. elegans* (adapted from Baker *et al.*, 2014). Axon termination of the PLM mechanosensory neurons was analyzed using a transgene, *muIs32* ($P_{mec\text{-}7}$GFP), and epifluorescent microscopy under 40x magnification. Shown are representative images of a more severe axon termination defect in a *rpm-1* mutant in which the PLM neuron overextends beyond the ALM cell body and hooks towards the ventral cord (hook, arrowhead), and a less severe axon termination defect in a *fsn-1* mutant and in a *rpm-1; kgb-1* double mutant in which the PLM axon only overextends beyond the ALM cell body (overextension, arrow). Note that the AVM cell body is only present on one side of the animal and is not always shown. Scale bar is 10µm.

(B) Quantitation of PLM axon termination defects (hook in black, overextension in grey) for the indicated genotypes. Note that double mutants of *rpm-1* and kinases in the MLK-1 pathway result in a reduction in hook defects and increased expressivity of less severe overextension defects. (C) Transgenic expression of MLK-1 using a promoter that is specifically expressed in mechanosensory neurons (P*mec-7*) rescues suppression of severe hook defects and rescues increased expressivity of less severe overextension defects in *rpm-1 mlk-1* double mutants. Rescue does not occur with transgenic expression of a control protein, mCherry. (D) Quantitation of PLM axon termination defects for the indicated genotypes. Note that *fsn-1* (lf) is not suppressed by *mlk-1* or *kgb-1* (lf). (E) Representative images are shown for a PLM neuron from transgenic animals overexpressing the indicated kinases using a pan-neuronal promoter (P*rgef-1*). A more severe hook defect is highlighted with an arrowhead, and less severe overextension defects are highlighted with arrows. (F) Quantitation of the PLM axon termination defects caused by transgenic overexpression of the indicated kinases. Shown are different concentrations of the indicated PCR products that were injected to generate extrachromosomal arrays. Notably, the molar ratios of constructs were similar with the exception of *mlk-1*, which was 1.6 times larger than other constructs. Transgenic animals were generated by microinjecting a mixture of PCR product encoding the indicated construct, 50ng/µL of P*ttx-3*::RFP (coinjection marker), and 50ng/µL of pBluescript. Injection conditions and genotypes for all transgenes are available upon request 1. Averages are shown for data collected from 5-8 independent counts of 20-30 PLM neurons from young adult worms grown at 23^{o}C. For transgenic genotypes, averages shown are data pooled from 4 or more independent lines. Alleles used included: *rpm-1 (ju44)*, *fsn-1 (gk429*), *dlk-1 (ju476)*, *pmk-3 (ok169*), *mlk-1 (ok2471)*, *mek-1 (ks54)*, and *kgb-1 (um3)*. Error bars represent the standard error of the mean, and significance was determined using an unpaired Student's *t*-test. ***P<0.001, **P<0.01, *P<0.05, and ns = not significant

These results show that *mlk-1*, *mek-1*, and *kgb-1* function cell autonomously in the same genetic pathway to suppress *rpm-1* (lf). These findings are also consistent with RPM-1 negatively regulating the MLK-1 pathway.

3.2.3 *fsn-1* (lf) is suppressed by mutations in kinases of the DLK-1 pathway, but not in kinases of the MLK-1 pathway

RPM-1 functions as a complex with the F-box protein FSN-1 to regulate PLM axon termination (Grill et al., 2007; Liao et al., 2004). Axon termination defects in *fsn-1-/-* mutants were suppressed in *fsn-1-/-; dlk-1-/-* and *fsn-1-/-; pmk-3-/-* double mutants (Figure 3-2D) (Baker et al., 2014). In contrast, the frequency of

axon termination defects remained unchanged in *fsn-1-/-; mlk-1-/-* or *fsn-1-/-; kgb-1-/-* double mutants (Figure 3-2D). These findings are consistent with FSN-1 inhibiting the DLK-1 pathway, but not the MLK-1 pathway.

3.2.4 Excess MLK-1 pathway function impairs axon termination

One explanation for why *rpm-1* (lf) is suppressed by mutations in the MLK-1 pathway is that *rpm-1* mutants have excess, unchecked MLK-1 pathway function. To test this hypothesis, we generated transgenic animals with extrachromsomal arrays that expressed different kinases in the DLK-1 and MLK-1 pathways. To assess the range of defects that might be caused by kinase overexpression, we generated arrays with varying levels of DNA encoding different kinases. For MLK-1 and KGB-1, we observed primarily less severe overextension defects, and very low, but significant, levels of hook defects at higher concentrations (Figure 3-2E and F). Similar results were observed with overexpression of PMK-3 (Figure 3-2E and F). In contrast, overexpression of DLK-1L caused more severe hook defects, which occurred with increasing frequency as the concentration of DLK-1L increased (Figure 3-2E and F) (Baker et al., 2014; Tulgren et al., 2011). We did not analyze MKK-4, but previous work showed that MKK-4 overexpression causes an intermediate frequency of hooks (Baker et al., 2014). These results provide further support for the model that RPM-1 negatively regulates the MLK-1 pathway.

3.2.5 Analysis of PPM-1 and PPM-2 function on the MLK-1 pathway

The phosphatases PPM-1 and PPM-2 negatively regulate the DLK-1 pathway (Baker et al., 2014; Tulgren et al., 2011). Using a combination of suppressor genetics and transgenics, we tested whether PPM-1 and/or PPM-2 affect the function of the MLK-1 pathway.

Previously, we found that *ppm-2-/-* mutants had very low penetrance hook defects, which were completely suppressed in *ppm-2-/-; dlk-1-/-* double mutants (Baker et al., 2014). In contrast, hook defects were not suppressed in *ppm-2-/-; mlk-1-/-* or *ppm-2-/-; kgb-1-/-* double mutants (Figure 3-3A). In the case of *ppm-1-/-* mutants which lack hooks defects, we utilized a *glo-4* (lf) sensitizing background which is enhanced by *ppm-1* (lf) (Figure 3-4A) (Tulgren et al., 2011).

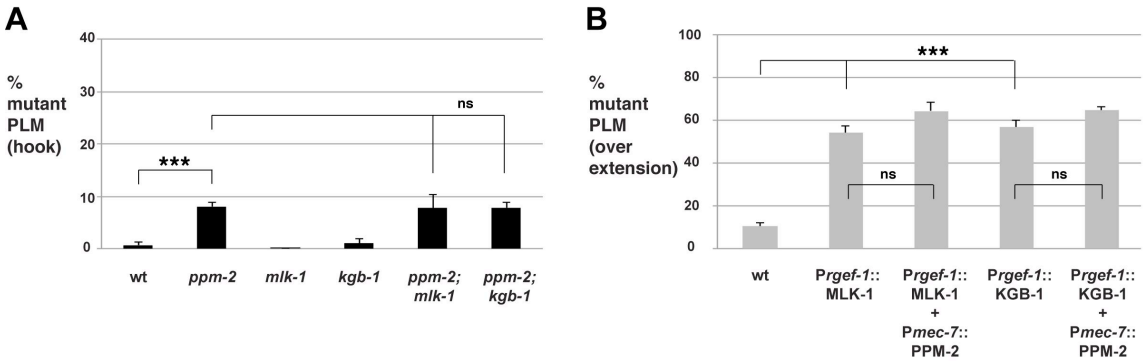

Figure 3-3. **PPM-2 does not regulate the MLK-1 pathway.**
(A) Quantitation of PLM axon termination defects (hook) for the indicated genotypes. Alleles used included: *mlk-1 (ok2471)*, *kgb-1 (um3)*, and *ppm-2 (ok2186)*. Shown are averages for data collected from 5-8 independent counts of 20-30 PLM neurons. (B) Quantitation of the PLM axon termination defects (overextension) caused by transgenic overexpression of MLK-1 (5ng/µL PCR product) or KGB-1 (10ng/µL PCR product) using the pan-neuronal *rgef-1* promoter. Note that transgenic coexpression of PPM-2 (5ng/µL plasmid) using the *mec-7* promoter, which is specifically expressed in mechanosensory neurons, fails to rescue defects caused by expression of MLK-1 or KGB-1. Shown are averages for data pooled from 4 or more transgenic lines for the indicated genotypes. In all cases, young adult worms grown at 23^{o}C were analyzed. Error bars represent the standard error of the mean, and significance was determined using an unpaired Student's *t*-test. ****P*<0.001 and ns = not significant

The enhanced frequency of hooks present in *ppm-1-/- glo-4-/-* double mutants was suppressed in *ppm-1-/- glo-4-/- mlk-1-/-* and *ppm-1-/- glo-4-/-; kgb-1-/-* triple mutants (Figure 3-4A). In contrast, hook defects in *glo-4-/-* mutants were not suppressed in *glo-4-/- mlk-1-/-* and *glo-4-/-; kgb-1-/-* double mutants.

Next, we analyzed whether PPM-1 and PPM-2 regulate the MLK-1 pathway in the context of transgenic overexpression experiments. As shown in Figure 3-3B, transgenic overexpression of MLK-1 or KGB-1 resulted in axon termination defects, and coexpression of PPM-2 in the same transgenic arrays did not affect MLK-1 or KGB-1 functional efficacy. In contrast, transgenic coexpression of PPM-1 significantly reduced the defects caused by overexpression of MLK-1 and KGB-1 (Figure 3-4B). Consistent with the previous findings on DLK-1L (Tulgren et al., 2011), defects caused by transgenic overexpression of PMK-3 were reduced by transgenic coexpression of PPM-1 (Figure 3-4B). Importantly, catalytically inactive PPM-1 *D246N* did not reduce defects caused by overexpression of MLK-1 or KGB-1. Thus, PPM-1 phosphatase activity regulates excess MLK-1 pathway function, and the reduction caused by coexpression of PPM-1 was not an indirect consequence of incorporating a second gene into extrachromosomal arrays (Figure 3-4B).

Collectively, these results are consistent with PPM-1 phosphatase activity inhibiting both the DLK-1 and the MLK-1 pathways. In contrast, these results suggest that PPM-2 is more specific for DLK-1L, and not capable of regulating the MLK-1 pathway.

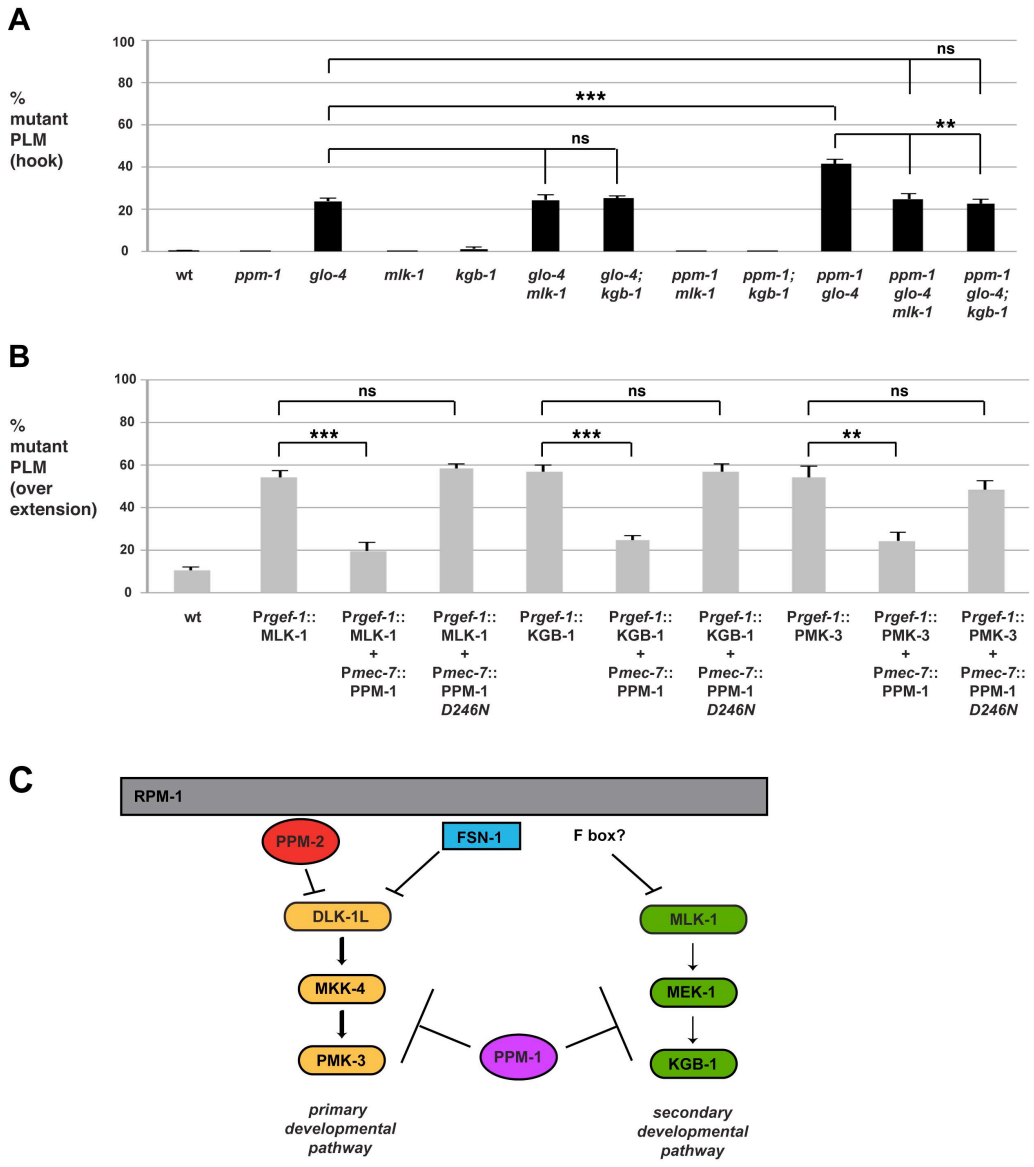

Figure 3-4. **PPM-1 functions to inhibit the MLK-1 and DLK-1 pathways.**
(A) Quantitation of PLM axon termination defects (hook) for the indicated genotypes. Alleles used included: *mlk-1 (ok2471)*, *kgb-1 (um3)*, *ppm-1 (ok578)*, *glo-4 (ok623)*. Shown are averages for data collected from 5-8 independent counts of 20-30 PLM neurons. (B) Quantitation of the PLM axon termination defects (overextension) caused by transgenic overexpression of MLK-1 (5ng/µL PCR product), KGB-1 (10ng/µL PCR product), or PMK-3 (10ng/µL PCR product) using the pan-neuronal *rgef-1* promoter. Note that transgenic coexpression of PPM-1 (2ng/µL plasmid) using the *mec-7* promoter rescues defects caused by expression of all kinases. (C) Signaling model of the DLK-1 and MLK-1 pathways with regulatory mechanisms that function during neuronal development. Because *rpm-1* (lf), but not *fsn-1* (lf), is suppressed by kinases in the MLK-1 pathway, we speculate that should RPM-1 ubiquitinate and inhibit MLK-1, it would be likely to do so through a presently unknown F box protein. ***P<0.001, **P<0.01, and ns = not significant

3.3 Discussion

RPM-1 is an important signaling molecule that regulates neuronal development through multiple mechanisms (Baker et al., 2014; Grill et al., 2007; Grill et al., 2012; Tulgren et al., 2014), including ubiquitination and inhibition of DLK-1L (Nakata et al., 2005). Our genetic suppressor analysis and transgenic results suggest that RPM-1 also negatively regulates the MLK-1 pathway during development. Our findings are consistent with a previous study, which showed that MLK-1 levels are increased in the neurons of *rpm-1* (lf) mutants (Nix et al., 2011). One simple explanation for these findings is that RPM-1 ubiquitinates MLK-1, which results in MLK-1 degradation and inhibition of the MLK-1 pathway (Figure 3-4C). However, an alternative explanation for our results is that the MLK-1 pathway functions in parallel to RPM-1. Because mutations in kinases of the DLK-1 pathway are stronger suppressors of *rpm-1* (lf) than mutations in kinases of the MLK-1 pathway, it is likely that RPM-1 functions primarily through the DLK-1 pathway, and secondarily through the MLK-1 pathway (Figure 1 and 2) (Nakata et al., 2005).

Our results are consistent with the PPM-1 phosphatase representing a further, conserved negative regulatory mechanism imposed on the DLK-1 and MLK-1 pathways (Figure 3-4C). In contrast, we found no evidence that PPM-2 regulates the MLK-1 pathway. Therefore, taking prior work into account, PPM-2 is likely to be a relatively specific mechanism for restraining DLK-1L activity (Baker et al., 2014).

During neuronal development, JNK and p38 MAP kinases mediate the function of Drosophila Highwire and mammalian Phr1 (Collins et al., 2006; Huntwork-Rodriguez et al., 2013; Klinedinst et al., 2013; Lewcock et al., 2007). Given prior work and our findings here, it is increasingly likely that the Pam/Highwire/RPM-1 (PHR) protein family generally regulates two MAP kinase pathways exemplified by the DLK-1 and MLK-1 pathways in *C. elegans*.

3.4 Acknowledgements

We thank Drs. Michael Bastiani and Paola Nix for providing *C. elegans* strains, and helpful discussions. Strains were also provided by the *C. elegans* Genetics Center. BG was funded by NIH R01 NS072129 and NSF IOS-1121095.

3.5 Author Contributions

Conceived and designed the experiments: STB BG. Performed the experiments: STB SMT EDT JW OR KJO. Analyzed the data: STB EDT BG. Wrote the paper: STB and BG.

4 Identification of a Peptide Inhibitor of the RPM-1/FSN-1 Ubiquitin Ligase Complex

This research was originally published in The Journal of Biological Chemistry. Sharma J*, **Baker ST***, Opperman KJ, Turgeon SM, Gurney AM, Opperman KJ, Grill B. Identification of a Peptide Inhibitor of the RPM-1/FSN-1 Ubiquitin Ligase Complex. *The Journal of Biological Chemistry.* 2014; Vol 289: 34654-34666.

*Both authors contributed equally. Figure by figure contributions listed in author contributions section at end of chapter.

4.1 Introduction

C. elegans Regulator of Presynaptic Morphology 1 (RPM-1) along with Drosophila Highwire, murine Phr1, and human Pam (MCYBP2) are part of a conserved family of E3 ubiquitin ligases referred to as Pam/Highwire/RPM-1 (PHR) proteins (Po et al., 2010). Studies in worms, flies, fish, and mice have identified roles for the PHR proteins in synapse formation (Burgess et al., 2004; Schaefer et al., 2000; Wan et al., 2000; Zhen et al., 2000), axon guidance and extension (Bloom et al., 2007; Culican et al., 2009; D'Souza et al., 2005; Lewcock et al., 2007; Li et al., 2005; Shin and DiAntonio, 2011), and axon termination (Grill et al., 2007; Kim et al., 2013; Refai et al., 2013; Schaefer et al., 2000).

The PHR proteins function through multiple signaling mechanisms to control neuronal development, one of which is ubiquitination, and negative regulation of the MAP3K Dlk (DLK-1 in worms and Wallenda in flies) (Collins et al., 2006; Huntwork-Rodriguez et al., 2013; Lewcock et al., 2007; Nakata et al., 2005). In *C. elegans*, RPM-1 functions as part of an ubiquitin ligase complex that includes F-box Synaptic protein 1 (FSN-1) (Liao et al., 2004). The functional relationship between RPM-1 and FSN-1 is conserved in flies and mammals (Saiga et al., 2009; Wu et al., 2007).

Despite significant and important progress with genetic approaches, our knowledge of the structure-function relationship between PHR proteins and F-box proteins, such as FSN-1, remains limited. Nonetheless, knowledge gained

from structure-function analysis is likely to be valuable for developing specific inhibitors of PHR ubiquitin ligase complexes. Studies in worms and flies have shown that inhibiting PHR protein function results in improved axon regeneration (Hammarlund et al., 2009; Nix et al., 2011; Xiong et al., 2010), and reduced axon degeneration following trauma (Babetto et al., 2013; Xiong et al., 2012). Thus, an inhibitor that specifically blocks the PHR ubiquitin ligase complex might prove valuable for improving axon regeneration, and reducing axon degeneration in the context of trauma and disease.

Here, we detail our discovery of a 97 amino acid (aa) region of RPM-1 that is sufficient for binding to FSN-1. The conservation of key residues in RPM-1 that mediate binding to FSN-1 suggests that this could be a conserved mechanism of interaction. The results of transgenic and genetic analysis are consistent with this peptide inhibiting the RPM-1/FSN-1 complex *in vivo*. Hence, we have termed it the RPM-1/FSN-1 complex inhibitory peptide (RIP). To our knowledge, RIP represents the first inhibitor of a PHR ubiquitin ligase complex.

4.2 Results

4.2.1 A single domain in RPM-1 is sufficient for binding to FSN-1

Previous genetic and biochemical experiments have shown that *C. elegans* RPM-1 and Drosophila Hiw are part of a complex that includes the F-box protein FSN-1 (Liao et al., 2004; Wu et al., 2007). In mammals, the Myc binding domain of Pam binds to Fbxo45, the ortholog of FSN-1 (Saiga et al., 2009). Despite

significant progress in understanding the function of the PHR ubiquitin ligase complex, the biochemical mechanisms underlying the formation of this complex remain minimally explored.

Because the interaction between RPM-1 and FSN-1 is evolutionarily conserved, we hypothesized that FSN-1 would bind to a region in RPM-1 that corresponded with a conserved portion of the Myc binding domain of Pam. ClustalW2 analysis of the PHR proteins showed that the Myc binding domain of Pam (aa 2413-2712) was composed of a C-terminal region that was not present in Hiw or RPM-1 (Figure 4-1A, MBD), and an N-terminal region that was well conserved (22.4% identical and 52.3% conservation between Pam and RPM-1) (Figure 4-1A). This N-terminal region contained several conserved motifs that might mediate binding between RPM-1 and FSN-1 (Figure 4-3A). To test this possibility, we cloned cDNAs encoding 9 individual protein domains (D1-9) that represented the entire RPM-1 coding sequence (Figure 4-1A). The boundaries of each domain were engineered at locations where conservation was strongly decreased. We transiently transfected HEK 293 cells with plasmids that express a GFP fusion protein for each of the 9 RPM-1 domains, and FLAG epitope tagged FSN-1. Coimmunoprecipitation (coIP) was used to determine if FSN-1 binds to a specific RPM-1 domain. As predicted by our bioinformatic analysis, FSN-1 coprecipitated with RPM-1 domain 5 (D5), which shared homology with the N-terminal portion of the Pam Myc binding domain (Figure 4-1B, top panel). We previously showed that D5 is sufficient for binding to RAE-1, so we also refer

to this domain as the RAE-1 binding domain (Figure 4-1A and B) (Grill et al., 2012). We noted that coexpression of D5 with FSN-1 consistently resulted in increased expression of FSN-1 (Figure 4-1B and 2B, bottom panels). This result is consistent with prior work, which showed that the Myc binding domain of Pam stabilizes Fbxo45 protein levels, presumably by sequestering it from degradation by an endogenous E3 ligase (Saiga et al., 2009).

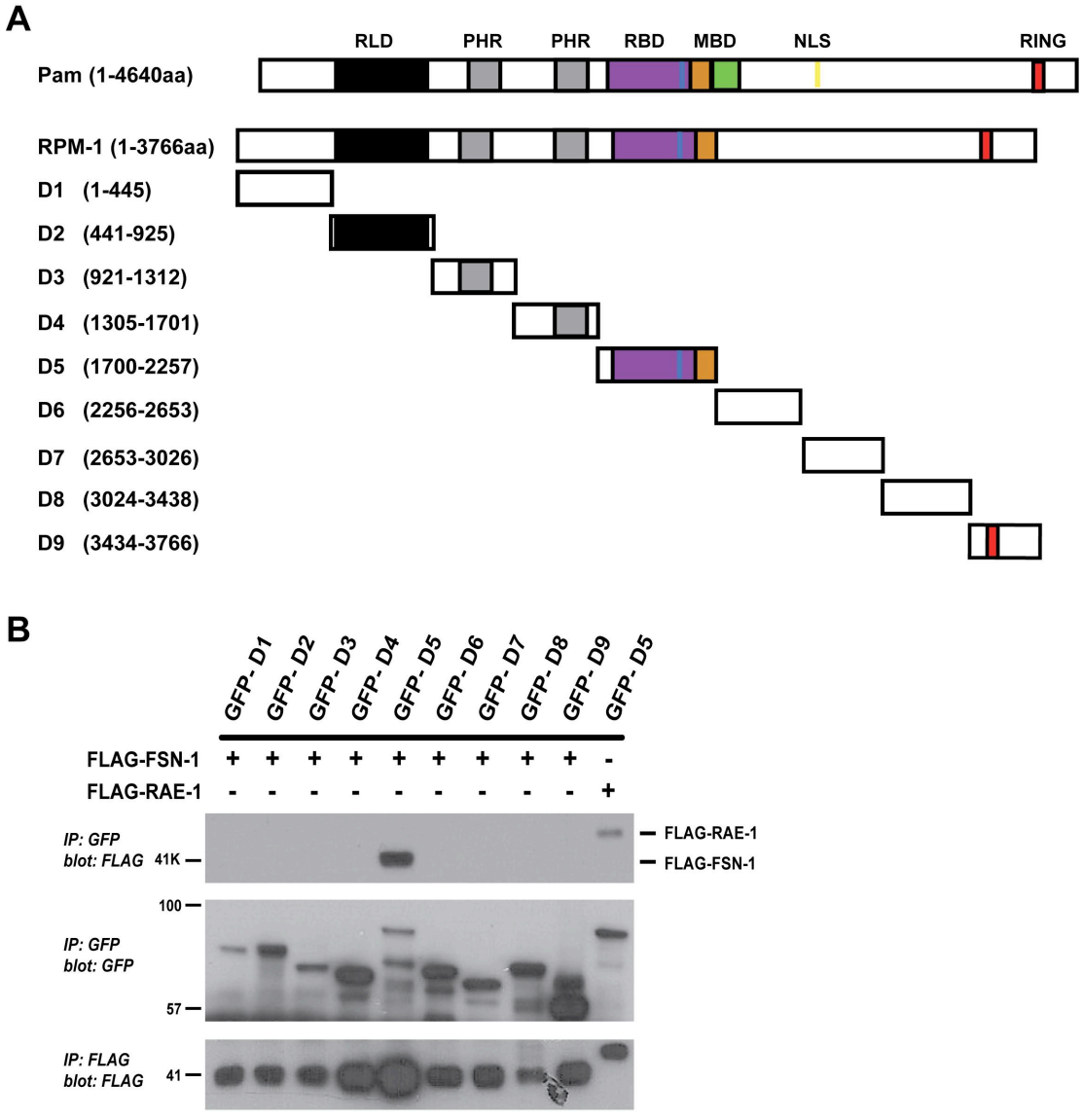

Figure 4-1: Identification of a domain in RPM-1 that is sufficient for binding to FSN-1.
A) Shown is a schematic of human Pam and *C. elegans* RPM-1. Annotated protein domains include: the RCC-1 like domain (RLD), two PHR family specific domains (PHR), the RAE-1 binding domain (RBD), the Myc binding domain (MBD), nuclear localization signal (NLS), and the RING-H2 ubiquitin ligase domain (RING). Highlighted is a motif in the RBD that is essential for binding to RAE-1. The portion of the MBD in Pam next to RBD is well conserved with RPM-1, and the portion highlighted to the right is not conserved. Also shown are 9 cDNA constructs encompassing the entire length of RPM-1, each of which corresponds to an individual, conserved domain of RPM-1 (D1-9). Domain 5 (D5) (also called the RBD) was further dissected into smaller subdomains (D5a-c). B) CoIP was performed from lysates of transfected HEK 293 cells that expressed FLAG tagged FSN-1 (FLAG-FSN-1) or FLAG tagged RAE-1 (FLAG-RAE-1), and fusion proteins of GFP and RPM-1 D1-D9. Note that FLAG-FSN-1 coprecipitated exclusively with domain 5 of RPM-1 (GFP-D5) (top panel). Consistent with a previous study, FLAG-RAE-1 also coprecipitated with GFP-RPM-1 domain 5 (GFP-D5) (top panel, last lane) (Grill et al., 2012). Shown are representatives of experiments that were independently performed at least three times

To further map the interaction between FSN-1 and RPM-1, we generated smaller fragments of RPM-1 D5 (Figure 4-2A). As shown in Figure 4-2B, the N-terminal half of D5 (D5a) did not bind to FSN-1, while the C-terminal half (D5b) was sufficient for binding. We then generated a smaller, 97 aa portion of D5b (D5c) that contained only sequence conserved with the Myc binding domain of human Pam. GFP-D5c coprecipitated with FLAG-FSN-1 with similar efficiency to GFP-D5 and GFP-D5b (Figure 4-2B).

To test whether this interaction occurs *in vivo* in neurons, we generated transgenic *C. elegans* that used a pan-neuronal promoter (P*rgef-1*) to simultaneously express both GFP::D5c and FLAG::FSN-1. As shown in Figure 4-2C, when GFP::D5c was precipitated with an anti-GFP antibody, robust coprecipitation of FLAG::FSN-1 was detected. In contrast, when FLAG::FSN-1 was expressed alone in transgenic worms, no coprecipitation occurred (Figure 4-2C). These results demonstrate that D5c, a conserved 97 aa region of RPM-1, is

sufficient for binding to FSN-1 in a heterologous expression system and in the neurons of *C. elegans*.

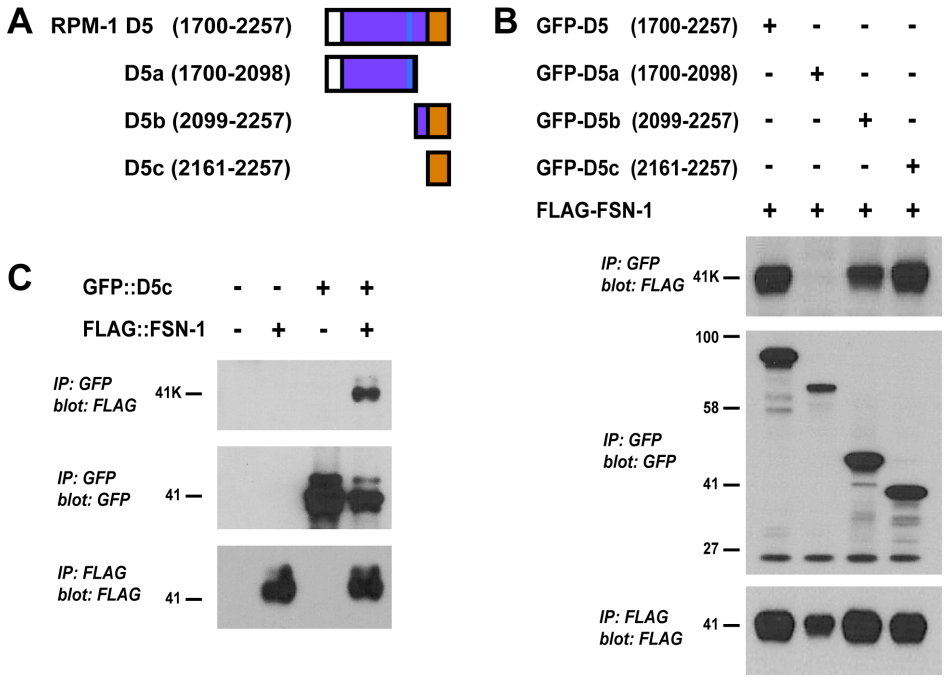

Figure 4-2: RPM-1 D5 contains a 97 aa region that is sufficient for binding to FSN-1.
A) Shown is a schematic of RPM-1 domain 5 (RPM-1 D5) and three smaller fragments of D5 (D5a-c). B) CoIP performed from lysates of transfected HEK293 cells that expressed FLAG-FSN-1 and fragments of RPM-1 domain 5 fused with GFP (GFP-D5a-c). Note that GFP-D5b and GFP-D5c coprecipitated with FLAG-FSN-1 with similar efficiency to full length GFP-D5 (top panel). C) CoIP performed from lysates of transgenic *C. elegans*. FLAG::FSN-1 coprecipitates efficiently only when coexpressed with GFP::D5c. Shown are representatives of experiments that were independently performed at least three times.

4.2.2 Residues in RPM-1 D5 required for binding to FSN-1

We next wanted to identify the motifs and residues in D5c that are required for binding to FSN-1. Sequence alignment using ClustalW2 identified 5 motifs in RPM-1 D5c that were highly conserved with Drosophila Hiw and human Pam (Figure 4-3A, underlined). As an initial mapping strategy, we generated GFP-D5

that was simultaneously point mutated at multiple residues in one of the 5 conserved motifs. Point mutants included: *WCL 2239, 2240, 2241 AAA*; *RL 2220, 2221 AA*; *DD 2214, 2215 AA*; *FI 2207, 2208 AA*; and *G2182A, R2184A, R2186A*. Binding of FLAG-FSN-1 to D5 point mutants was analyzed using coIP from lysates of transiently transfected HEK 293. GFP-D5 fusion proteins were precipitated from transfected cell lysates using an anti-GFP antibody. While FLAG-FSN-1 coprecipitated well with wild-type GFP-D5, binding was strongly reduced for all GFP-D5 point mutants (Figure 4-3B, top panel). Thus, all 5 conserved motifs in RPM-1 D5 that we tested were required for binding to FSN-1.

To further map where FSN-1 binds to RPM-1 and to minimize structural impacts caused by mutation of multiple residues simultaneously, we generated point mutants of RPM-1 D5 in which only a single amino acid was mutated to alanine (Figure 4-3A, boxes). This was done for three of the five motifs in D5 that were required for binding to FSN-1. As shown in Figure 4-3C, coprecipitation of FSN-1 was strongly reduced for three individual point mutants of RPM-1 D5: *W2239A*, *D2214A*, and *F2207A*. Coprecipitation of FSN-1 was more mildly reduced for D5 *I2208A* (Figure 4-3C).

Having used a heterologous expression system to identify specific residues in RPM-1 that mediate binding to FSN-1, we wanted to test if the corresponding point mutations in full length RPM-1 would inhibit binding to FSN-1 in the neurons of *C. elegans*. To address this, we generated transgenic worms that coexpressed a GFP fusion protein with full length RPM-1 (RPM-1::GFP), and

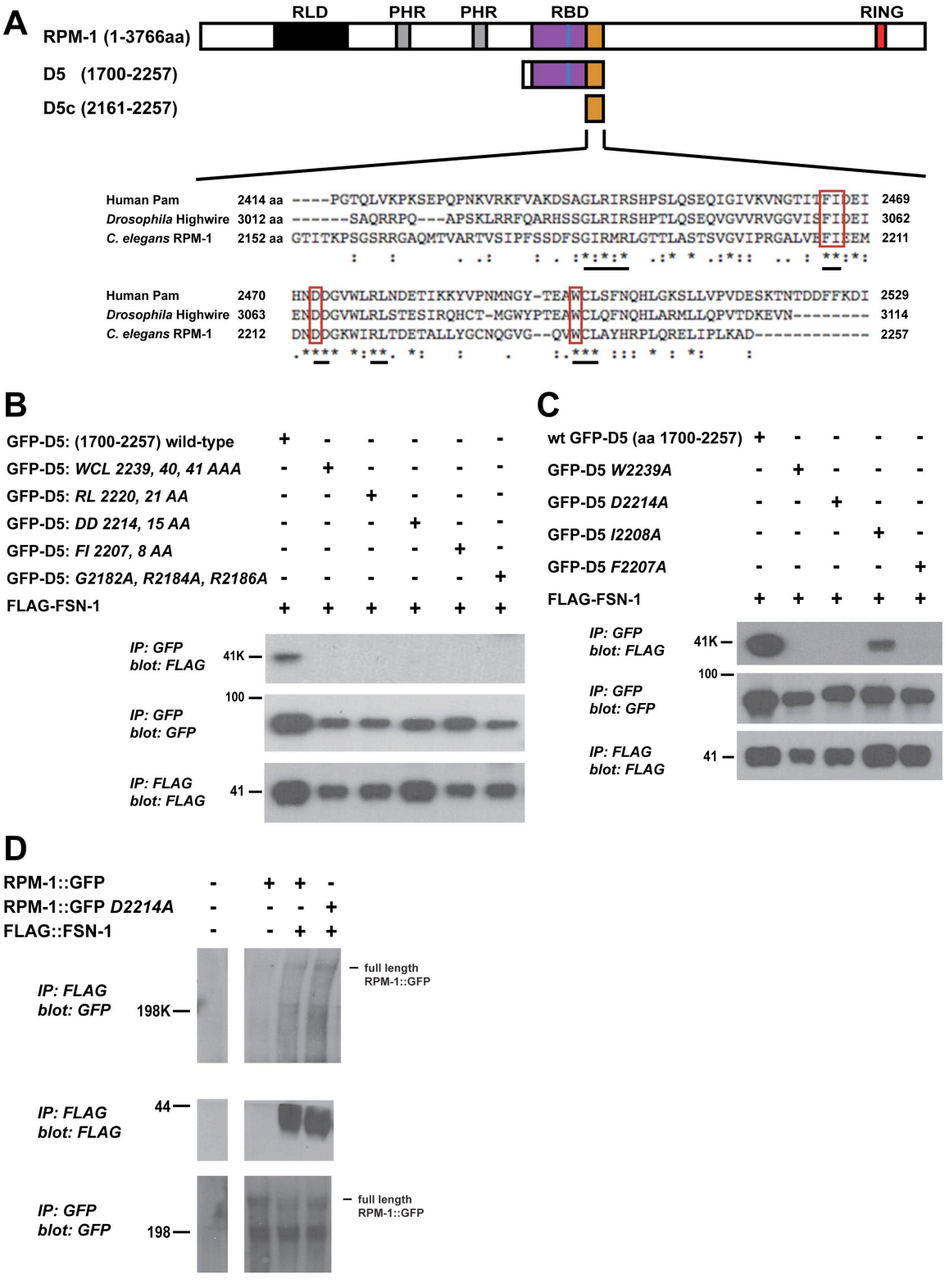
A
RPM-1 (1-3766aa)
RLD
PHR
PHR
RBD
RING
D5 (1700-2257)
D5c (2161-2257)
Human Pam 2414 aa ----PGTQLVKPKSEPQPNKVRKFVAKDSAGLRIRSHPSLQSEQIGIVKVNGTITFIDEI 2469
Drosophila Highwire 3012 aa ------SAQRRPQ---APSKLRRFQARHSSGLRIRSHPTLQSEQVGVVRVGGVISFIDEI 3062
C. elegans RPM-1 2152 aa GTITKPSGSRRGAQMTVARTVSIPFSSDFSGIRMRLGTTLASTSVGVIPRGALVEFIEEM 2211
Human Pam 2470 HNDDGVWLRLNDETIKKYVPNMNGY-TEAWCLSFNQHLGKSLLVPVDESKTNTDDFFKDI 2529
Drosophila Highwire 3063 ENDDGVWLRLSTESIRQHCT-MGWYPTEAWCLQFNQHLARMLLQPVTDKEVN-------- 3114
C. elegans RPM-1 2212 DNDDGKWIRLTDETALLYGCNQGVG--QVWCLAYHRPLQRELIPLKAD---------- 2257
B
GFP-D5: (1700-2257) wild-type
GFP-D5: WCL 2239, 40, 41 AAA
GFP-D5: RL 2220, 21 AA
GFP-D5: DD 2214, 15 AA
GFP-D5: FI 2207, 8 AA
GFP-D5: G2182A, R2184A, R2186A
FLAG-FSN-1
IP: GFP blot: FLAG
41K
IP: GFP blot: GFP
100
IP: FLAG blot: FLAG
41
C
wt GFP-D5 (aa 1700-2257)
GFP-D5 W2239A
GFP-D5 D2214A
GFP-D5 I2208A
GFP-D5 F2207A
FLAG-FSN-1
IP: GFP blot: FLAG
41K
100
IP: GFP blot: GFP
IP: FLAG blot: FLAG
41
D
RPM-1::GFP
RPM-1::GFP D2214A
FLAG::FSN-1
IP: FLAG blot: GFP
198K
full length RPM-1::GFP
IP: FLAG blot: FLAG
44
IP: GFP blot: GFP
198
full length RPM-1::GFP

Figure 4-3: Identification of conserved residues in RPM-1 D5 required for binding to FSN-1.
A) Schematic of full length RPM, RPM-1 domain 5 (D5), and a portion of RPM-1 domain 5 that is sufficient for binding to FSN-1 (D5c). Shown below is a sequence alignment of the D5c region of RPM-1 with its orthologs Pam (also called MYCBP-2) and Highwire that was generated using ClustalW2. Underlined are portions of motifs that were mutated and analyzed in B. Highlighted in boxes are amino acid residues that were individually point mutated and analyzed in C and D. B) and C) CoIP using lysates from transfected HEK 293 cells expressing FLAG-FSN-1 and a fusion protein of GFP and domain 5 of RPM-1 (GFP-D5). Wild-type GFP-D5 or the indicated point mutants were analyzed for coprecipitation with FLAG-FSN-1. Note in C that the point mutants of GFP-D5 *W2239A*, *D2214A*, and *F2207A* strongly reduced coprecipitation with FLAG-FSN-1 compared to wild-type GFP-D5 (top panel). The interaction between GFP-D5 *(I2208A)* and FLAG-FSN-1 was more modestly reduced. D) CoIP was performed from whole worm lysates of transgenic *C. elegans* expressing FLAG::FSN-1 and wild-type RPM-1::GFP or RPM-1::GFP point mutated to inhibit binding to FSN-1 (RPM-1 *D2214A*). Note that wild-type RPM-1::GFP and RPM-1::GFP *D2214A* coprecipitate with FLAG::FSN-1 equally. Shown are representatives of experiments that were independently performed at least three times

FLAG epitope tagged FSN-1 (FLAG::FSN-1). RPM-1::GFP was expressed using the native *rpm-1* promoter that is expressed exclusively, but broadly in neurons (Zhen et al., 2000). FLAG::FSN-1 was expressed using a pan-neuronal promoter (P*rgef-1*). Coprecipitating RPM-1::GFP was detected when FLAG::FSN-1 was immunoprecipitated from whole worm lysates (Figure 4-3D). This result is consistent with a prior study that used anti-FSN-1 antibodies to show that RPM-1 binds to FSN-1 (Liao et al., 2004). RPM-1::GFP *D2214A* also coprecipitated with FLAG::FSN-1, and did not show reduced binding compared to wild-type RPM-1::GFP (Figure 4-3D). These results suggest that FSN-1 might bind to multiple sites in RPM-1. We did not find another portion of RPM-1 sequence with strong homology to RPM-1 D5c, which suggests that the second FSN-1 binding site in RPM-1 utilizes a different structural mechanism.

Nonetheless, our biochemical results indicate that FSN-1 binds either directly, or through an adaptor such as a Skp, to a very precise region in RPM-1:

the D5c fragment, which we refer to as the FSN-1 binding domain 1 (FBD1) in the context of full length RPM-1. Moreover, our findings suggest that the D5c peptide might block the interaction between endogenous RPM-1 and FSN-1 *in vivo* potentially making it a highly specific inhibitor of the RPM-1/FSN-1 ubiquitin ligase complex. Therefore, when D5c is expressed recombinantly, we refer to it as RIP or the RPM-1/FSN-1 complex inhibitory peptide.

4.2.3 Transgenic expression of RIP inhibits axon termination and synapse formation

Previous studies have shown that *rpm-1*, *fsn-1*, and *glo-4* loss-of-function (lf) mutants have defects in axon termination and synapse formation in the mechanosensory neurons of *C. elegans* (Grill et al., 2007; Schaefer et al., 2000). Further, *fsn-1* and *glo-4* function in parallel genetic pathways to mediate the function of *rpm-1* (Grill et al., 2007). The genetic relationship between *fsn-1* and *glo-4*, and our biochemical results showing that RIP (D5c) binds to FSN-1, provided a basis for determining whether exogenous expression of RIP would inhibit the function of the endogenous RPM-1/FSN-1 ubiquitin ligase complex. To test this hypothesis, we analyzed how transgenic overexpression of RIP affects axon termination in the mechanosensory neurons that sense soft touch in *C. elegans*.

In *C. elegans*, there are two Posterior Lateral Microtubule (PLM) mechanosensory neurons each of which extends a single axon that terminates

extension well before the cell body of the Anterior Lateral Microtubule (ALM) mechanosensory neurons (Figure 4-4A). The morphology of the PLM neurons can be rapidly and accurately analyzed using a transgene, *muIs32* (P_{mec-7}GFP), which expresses GFP specifically in the mechanosensory neurons (Ch'ng et al., 2003). In *fsn-1-/-* or *glo-4-/-* single mutants, two axon termination phenotypes were observed in the PLM neurons consistent with prior studies. The primary, most frequent phenotype was a less severe defect in which the PLM axon failed to terminate extension and grew past the ALM cell body, a defect we refer to as overextension (Figure 4-4A and B) (Grill et al., 2007; Tulgren et al., 2011). A second, more severe phenotype in which the PLM axon overextended and then hooked towards the ventral cord, which we refer to as a hook defect, was also observed but at very low expressivity (Figure 4-4B). Similar to prior work, we observed that *fsn-1-/-; glo-4-/-* double mutants had strongly enhanced expressivity of hook defects, which was the primary phenotype in these animals (Figure 4-4A and B) (Grill et al., 2007; Tulgren et al., 2011). The frequency of hook defects in *fsn-1-/-; glo-4-/-* double mutants is similar to *rpm-1-/-* mutants (Grill et al., 2007; Schaefer et al., 2000; Tulgren et al., 2011).

To determine whether RIP inhibits the function of the endogenous RPM-1/FSN-1 complex, we used a transgenic approach in which the *rgef-1* promoter (a strong, pan-neuronal promoter) was used to overexpress RIP. If RIP inhibits the RPM-1/FSN-1 complex, we expected transgenic overexpression of RIP to yield phenotypes that were similar to *fsn-1* (lf) mutations. Notably, we did not

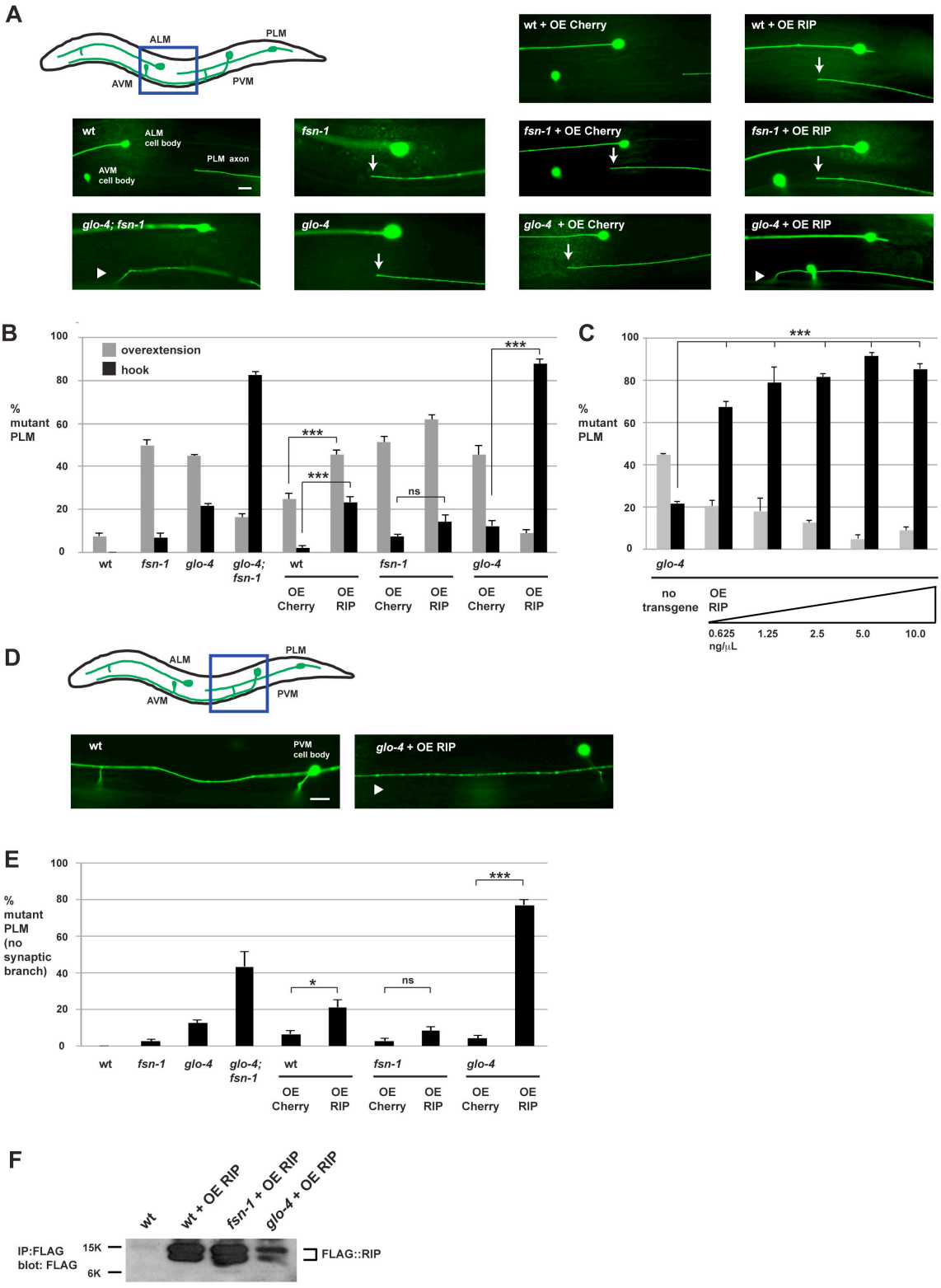
A
ALM
PLM
AVM
PVM
wt + OE Cherry
wt + OE RIP
wt
ALM cell body
PLM axon
AVM cell body
fsn-1
fsn-1 + OE Cherry
fsn-1 + OE RIP
glo-4; fsn-1
glo-4
glo-4 + OE Cherry
glo-4 + OE RIP
B
overextension
hook
% mutant PLM
wt
fsn-1
glo-4
glo-4; fsn-1
OE Cherry
OE RIP
***
ns
C
glo-4
no transgene
OE RIP
0.625 ng/µL
1.25
2.5
5.0
10.0
D
wt
PVM cell body
glo-4 + OE RIP
E
% mutant PLM (no synaptic branch)
*
F
wt
wt + OE RIP
fsn-1 + OE RIP
glo-4 + OE RIP
IP:FLAG
blot: FLAG
15K
6K
FLAG::RIP

Figure 4-4: Transgenic overexpression of RIP (RPM-1 D5c) inhibits axon termination in the PLM neurons of *C. elegans*.
A) A schematic (adapted from Baker *et al.*, 2014) showing the mechanosensory neurons of *C. elegans* (anterior left, dorsal top). The box highlights the region of the animal shown below, which was visualized using *muIs32* (P_{mec-7}GFP) and epifluorescent microscopy. Note that the AVM cell body is only present on one side of the animal and is not always shown. Images are shown for the most prevalent phenotype observed for each genotype. Shown are two different types of PLM axon termination defects: overextension (arrow), and more severe hook defects (arrowhead). Note that transgenic overexpression (OE) of RIP on a wild-type background primarily resulted in overextension, where as overexpression of RIP on a *glo-4* mutant background primarily resulted in a more severe hook defect. B) Quantitation of PLM axon termination defects for the indicated genotypes (overextension in grey, hook in black). C) Analysis of PLM axon termination defects in *glo-4* mutants carrying transgenic extrachromosomal arrays that were generated by injecting DNA encoding RIP at a range of concentrations as indicated. D) The box in the schematic highlights the region shown below that was visualized using *muIs32* and epifluorescent microscopy. In wild-type animals, the PLM neuron extends its synaptic branch ventrally. Also shown is an example of a *glo-4* mutant that transgenically overexpressed RIP, in which the PLM synaptic branch is absent (arrowhead). E) Quantitation of synaptic branch defects for the indicated genotypes. F) IP with an anti-FLAG antibody was used to detect FLAG::RIP in whole worm lysates of representative transgenic lines for the indicated genotypes. B, C, E) Shown are the averages of 5 or more independent counts (20-30 neurons/count) for each genotype. For transgenes, averages are shown for data pooled from 4 or more transgenic lines. Unless noted otherwise, transgenic animals were generated by injecting PCR product at 10ng/µL. Error bars represent the standard error of the mean, and significance was determined using an unpaired Student's *t* test. ***P<0.001, *P<0.05, ns = not significant. Scale bars are 10µm.

expect RIP overexpression to yield phenotypes that occurred with the same expressivity as *rpm-1* (lf) because RPM-1 functions through several FSN-1 independent mechanisms including: the GLO Rab pathway, the microtubule binding protein RAE-1, the phosphatase PPM-2, and the ANC-1/β-catenin pathway (Baker et al., 2014; Grill et al., 2007; Grill et al., 2012; Tulgren et al., 2014). We generated transgenic animals that overexpressed FLAG epitope tagged RIP by injecting PCR product at relatively high concentrations (10ng/µL). As a control for promoter effects, we also generated transgenes that overexpressed mCherry. The primary phenotype observed when RIP was transgenically overexpressed in wild-type animals was overextension of the PLM

axon (Figure 4-4A). Quantitation showed that overextension occurred with increased frequency when RIP was overexpressed (45.4 +/- 2.2%), but not mCherry (24.7 +/- 2.8%, Figure 4-4B). Transgenic overexpression of RIP in wild-type animals also resulted in significant, but lower frequency hook defects (Figure 4-4B). Notably, defects caused by overexpression of RIP in wild-type animals resulted in a similar frequency of defects as observed in *fsn-1* (lf) mutants (Figure 4-4B). When we overexpressed RIP or mCherry in *fsn-1-/-* mutants, we observed no differences between the two transgenes with regard to the hook phenotype and an extremely small increase in the overextension phenotype (Figure 4-4A and B). Next, we tested the effect of RIP overexpression in *glo-4-/-* animals. *glo-4-/-* mutants that overexpress mCherry were similar to non-transgenic *glo-4-/-* mutants, and primarily showed overextension defects, with lower expressivity of the more severe hook defects (Figure 4-4A and B). In contrast, transgenic overexpression of RIP in *glo-4-/-* mutants resulted in enhanced frequency of hook defects, while the expressivity of less severe overextension defects was decreased (compare 87.9 +/- 2.1% hook for *glo-4* + OE RIP with 12.4 +/- 2.4% for *glo-4* + OE Cherry, Figure 4-4A and B). To test the potency of transgenic RIP, we engineered *glo-4-/-* animals with transgenic arrays that were generated by injecting DNA encoding RIP at a range of concentrations. In all cases, including when arrays were constructed at relatively low concentrations (0.625ng/μL), we observed strong enhancer effects in the expressivity of PLM hook defects (Figure 4-4C). Notably, the enhancer effects

caused by overexpression of RIP in *glo-4-/-* animals were comparable to levels of enhancement observed in *fsn-1-/-; glo-4-/-* double mutants (Figure 4-4B). Collectively, these results demonstrate that overexpression of RIP behaves genetically like *fsn-1* (lf).

In wild-type animals, each PLM neuron also extends a single synaptic branch that innervates interneurons of the ventral nerve cord (Figure 4-4D). It was previously shown that *rpm-1-/-* mutants lack a PLM synaptic branch at high frequency (Grill et al., 2007; Schaefer et al., 2000). Likewise, *fsn-1-/-; glo-4-/-* double mutants have enhanced frequency of PLM synaptic branch defects (Figure 4-4E) (Grill et al., 2007; Tulgren et al., 2011). It was previously noted that the absence of the PLM synaptic branch in *rpm-1-/-* mutants was likely due to a failure to form or stabilize PLM synaptic connections, as opposed to defects in synaptic branch extension (Schaefer et al., 2000). Thus, this phenotype is likely to reflect a defect in synapse formation.

Transgenic overexpression of RIP in *glo-4-/-* mutants primarily resulted in the absence of the PLM synaptic branch (Figure 4-4D). Quantitation showed an enhanced frequency of PLM synaptic branch defects when RIP was overexpressed compared to when mCherry was overexpressed in *glo-4-/-* mutants (compare 77.1 +/- 2.7% for *glo-4* + OE RIP with 4.1 +/- 1.7% for *glo-4* + OE Cherry, Figure 4-4E). When RIP was overexpressed in wild-type animals, the frequency of synaptic branch defects was mildly, but significantly, increased (compare 21.2 +/- 4.0% for wild-type + OE RIP with 6.6 +/- 1.8% for wild-type +

OE Cherry, Figure 4-4E). In contrast, RIP overexpression in *fsn-1-/-* mutants did not significantly change the frequency of synaptic branch defects compared to overexpression of mCherry (Figure 4-4E).

The two ALM neurons sense anterior soft touch, and terminate extension at a precise location in the head of the animal (Figure 4-5A). In wild-type animals, the ALM axon terminates well before the anterior tip of the animal's nose (Figure 4-5A). Consistent with previous work, we observed ALM axon termination defects in *glo-4-/-* or *fsn-1-/-* single mutants (Figure 4-5B) (Grill et al., 2007). Categorizing ALM axon termination defects into less severe short hooks and more severe big hooks facilitated identification of genetic enhancer effects in *fsn-1-/-; glo-4-/-* double mutants (Figure 4-5B) (Tulgren et al., 2011). Previous studies showed that ALM axon termination defects in *fsn-1-/-; glo-4-/-* double mutants occur at similar frequency and severity as *rpm-1-/-* mutants (Grill et al., 2007; Schaefer et al., 2000; Tulgren et al., 2011).

When RIP was transgenically overexpressed in *glo-4-/-* mutants, we primarily observed big hooks in ALM neurons (Figure 4-5A). The frequency of these defects was enhanced compared to *glo-4-/-* mutants that overexpressed mCherry (compare 86.3 +/- 2.1% big hook for *glo-4* + OE RIP with 34.0 +/- 3.6% for *glo-4* + OE Cherry, Figure 4-5B). Overexpression of RIP on a wild-type background gave both short hook and big hook phenotypes that were relatively low in frequency, but significant (compare 7.0% +/- 1.5% short hook for wild-type + OE RIP with 1.6 +/- 0.8% short hook for wild-type + OE Cherry, Figure 4-5B).

Transgenic overexpression of RIP in *fsn-1-/-* mutants did not alter the frequency of ALM axon termination defects compared to overexpression of mCherry (Figure 4-5B).

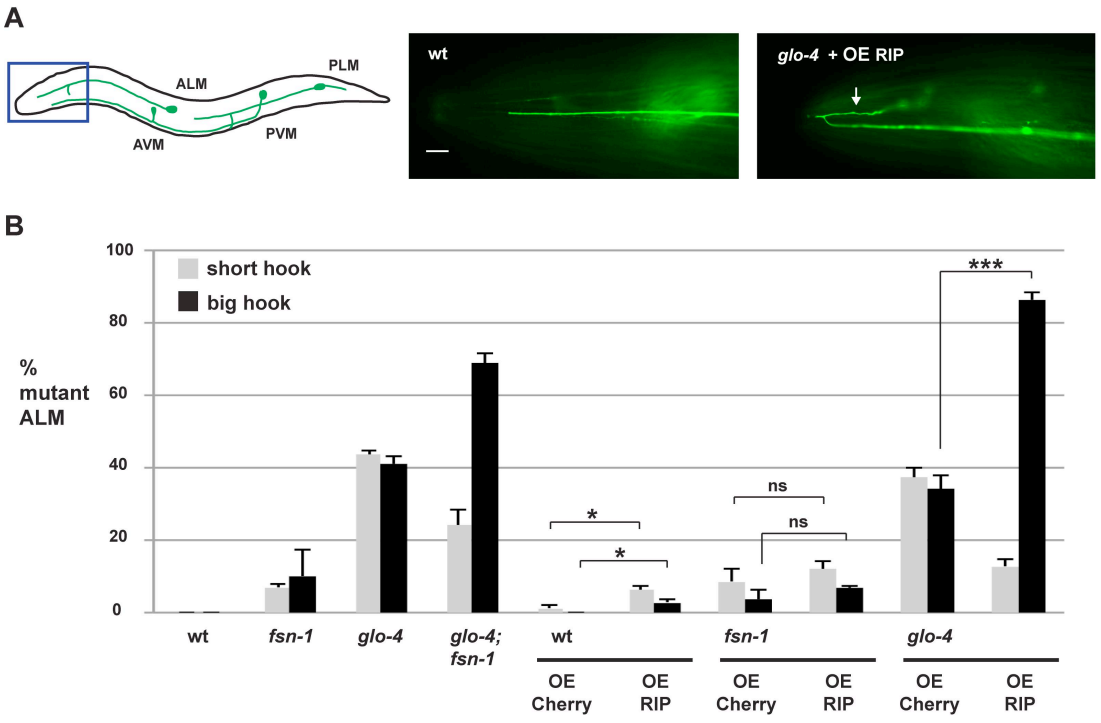

Figure 4-5: Transgenic overexpression of RIP (RPM-1 D5c) inhibits axon termination in the ALM neurons of *C. elegans*.
A) A schematic shows the mechanosensory neurons of *C. elegans* (anterior left, dorsal top), which were analyzed using the transgene *muIs32* (P_{mec-7}GFP). The box highlights the region of the animal shown below that was visualized using epifluorescent microscopy. Shown is an example of normal ALM axon termination in a wild-type animal. Also shown is a *glo-4* animal that is overexpressing RIP where the ALM axon fails to terminate properly, overextends and hooks towards the posterior of the animal (big hook, arrow). The scale bar is 10µm. B) Quantitation of ALM axon termination defects for the indicated genotypes (short hook in grey, big hook in black). A, B) Shown are the averages of 5 or more independent counts (20-30 neurons/count) for each genotype. For transgenes, averages are shown for data pooled from 4 or more transgenic lines. Transgenic animals were generated by injecting PCR products at 10ng/µL. Error bars represent the standard error of the mean, and significance was determined using an unpaired Student's *t* test. ***P<0.001, *P<0.05, ns = not significant

Transgenic overexpression of FLAG::RIP in PLM and ALM neurons had strong functional effects, but we wanted to ensure that changes in transgenic RIP expression in different genetic backgrounds did not account for these findings. Therefore, we biochemically assessed expression of FLAG::RIP in a representative transgenic line for each genotype. As shown in Figure 4-4F, we detected expression of transgenic FLAG::RIP in whole worm lysates of all RIP transgenic genotypes assessed in our functional analysis. Importantly, we did not observe lower expression of FLAG::RIP in genotypes with lower expressivity of axon termination defects, such as *fsn-1-/-* mutants that overexpress RIP. Thus, our functional transgenic results are not simply due to variation in expression of FLAG::RIP on different genetic backgrounds. We note that FLAG::RIP migrated at the expected size of 13.5 kDa, but was detected as a doublet. This was most likely the result of protein degradation that occurred during preparation of protein extracts from whole animals. Alternatively, the doublet might reflect post-translational modification of RIP that only occurs in the neurons of *C. elegans*.

In summary, several of our findings are consistent with overexpression of RIP acting similar to *fsn-1* (lf). 1) Transgenic overexpression of RIP on a wild-type background resulted in defects that occurred with similar frequency to non-transgenic *fsn-1-/-* mutants. 2) We observed no enhancer effects when RIP was overexpressed on an *fsn-1-/-* mutant background. 3) Strong enhancer effects occurred when RIP was overexpressed on a *glo-4-/-* mutant background, and enhancer effects occurred with similar frequency to *fsn-1-/-; glo-4-/-* double

mutants. Taken together, these results are consistent with RIP binding to FSN-1 and inhibiting formation of a functional RPM-1/FSN-1 ubiquitin ligase complex.

4.2.4 Transgenic RIP functions through DLK-1

Previous studies have shown that the RPM-1/FSN-1 complex functions through ubiquitination and inhibition of the MAP3K DLK-1 (Baker et al., 2014; Nakata et al., 2005; Wu et al., 2007). To provide further evidence that RIP was functioning by inhibiting endogenous FSN-1, we tested if the effects of overexpression of RIP were altered by *dlk-1* (lf). As shown in Figure 4-6, transgenic overexpression of RIP in *glo-4-/-* mutants resulted in an enhanced frequency of the more severe ALM and PLM axon termination defects, as well as PLM synaptic branch defects. Enhancer effects caused by RIP overexpression were completely suppressed in *glo-4-/-; dlk-1-/-* double mutants (Figure 4-6). This result was not due to suppression of *glo-4* by *dlk-1*, as similar levels of defects were observed in *glo-4-/-* single mutants and *glo-4-/-; dlk-1-/-* double mutants (Figure 4-6). These results are consistent with RIP impairing endogenous FSN-1, which functions through ubiquitination and inhibition of DLK-1.

4.2.5 RIP function is inhibited by point mutations that block binding to FSN-1

We wanted to test whether point mutations in RIP (D5c), which reduce binding to FSN-1 in HEK 293 cells (Figure 4-3C), affected the function of

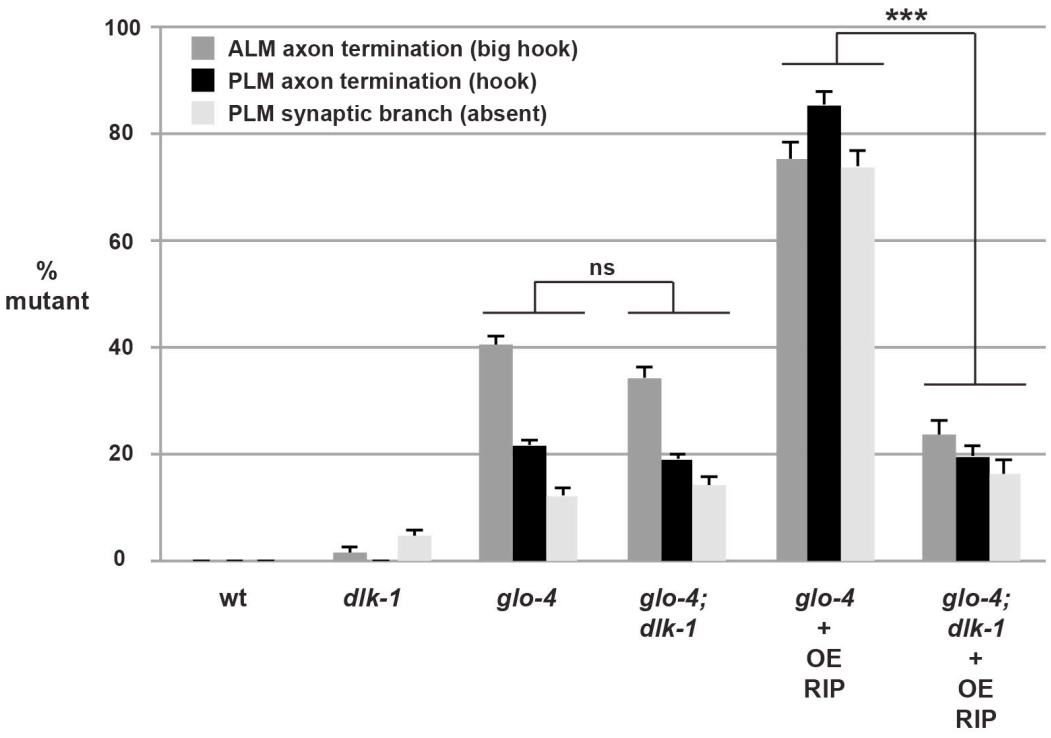

Figure 4-6: Effects of transgenic overexpression of RIP (RPM-1 D5c) on axon termination are mediated by DLK-1.
Quantitation of ALM axon termination defects (dark grey, left bar), PLM axon termination defects (black, middle bar), and PLM synaptic branch defects (light grey, right bar) for the indicated genotypes. Note that defects caused by transgenic overexpression of RIP in *glo-4* mutants are completely suppressed when RIP is overexpressed in *glo-4; dlk-1* double mutants. Averages are shown for data pooled from 6 or more transgenic lines. Transgenic animals were generated by injecting PCR products at 10ng/µL. Error bars represent the standard error of the mean, and significance was determined using an unpaired Student's *t* test. ****P*<0.001, ns = not significant

transgenic RIP in worms. To do so, we analyzed PLM axon termination in *glo-4-/-* mutants that carried transgenic extra-chromosomal arrays that overexpressed wild-type RIP or RIP point mutants. In order to maximize our ability to detect changes in RIP efficacy, transgenic arrays were generated with 2.5ng/µL of PCR product encoding RIP, a lower concentration at which maximal effects from RIP overexpression were still observed (Figure 4-4C). As shown in Figure 4-7A,

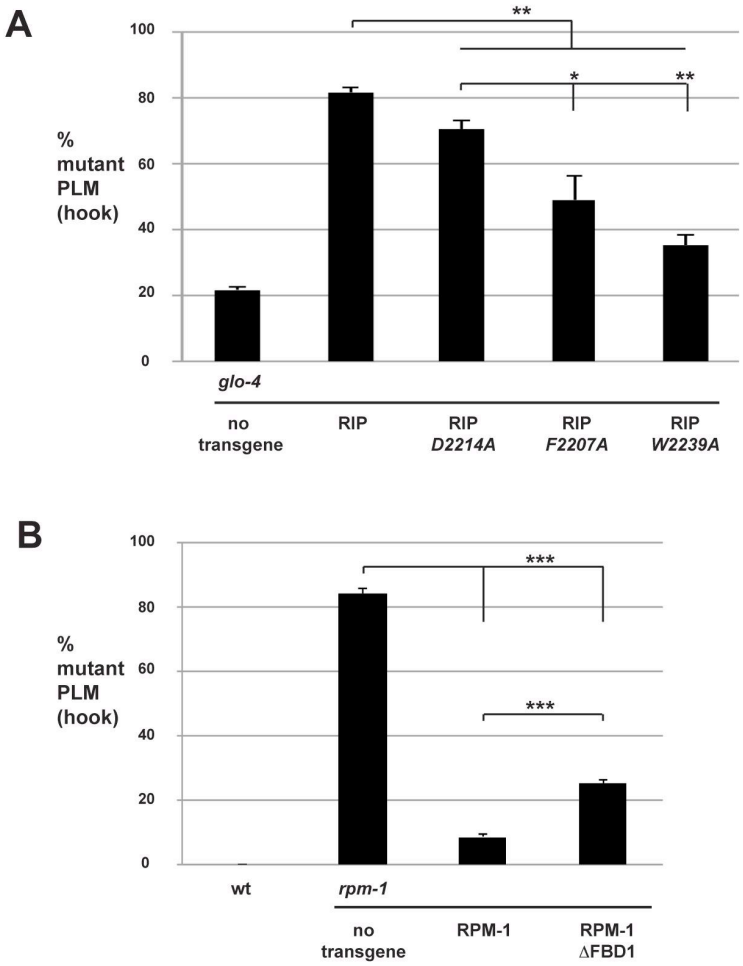

Figure 4-7: Mutations in RIP that reduce binding to FSN-1 impair the efficacy of transgenic RIP. Quantitation of PLM axon termination defects (hook) for the indicated genotypes. A) Mutations in RIP that impair binding to FSN-1 reduce the level of RIP enhancer effects in *glo-4* mutants. Transgenic animals were generated by injecting PCR products at 2.5ng/µL. B) RPM-1 ΔFBD1 rescues defects in PLM axon termination caused by *rpm-1* (lf) less efficiently than wild-type RPM-1. Transgenic animals were generated by injecting plasmid at 25ng/µL. A, B) Averages are shown for data pooled from 5 or more transgenic lines. Significance was determined using an unpaired Student's *t* test. **P*<0.05 ***P*<0.01 ****P*<0.001

overexpression of wild-type RIP resulted in enhanced PLM axon termination defects compared to non-transgenic *glo-4-/-* animals. In contrast, enhancer effects were significantly lower in *glo-4-/-* mutants that overexpressed RIP point mutants (Figure 4-7A). RIP *W2239A* had the weakest enhancer effect compared to wild-type RIP, which suggested that this point mutant was the most functionally impaired (Figure 4-7A). RIP *D2214A* was the point mutant with the highest level of enhancement (Figure 4-7A). Thus, RIP *D2214A* was the least functionally impaired point mutant. While CoIP from HEK 293 cells showed that point mutation of *D2214*, *F2207*, or *W2239* strongly impaired binding to FSN-1

(Figure 4-3), analysis of axon termination in PLM neurons highlighted the functional importance of individual residues in RIP. Presumably this is because the neurons of *C. elegans* are a more physiologically relevant setting, and therefore more sensitive to changes in the efficiency of RIP binding to FSN-1. Nonetheless, functional analysis of RIP point mutants provided further evidence that is consistent with exogenous RIP binding to FSN-1, and inhibiting formation of a functional RPM-1/FSN-1 complex.

4.2.6 RPM-1 lacking FBD1 is functionally impaired

RPM-1 functions though several downstream signaling molecules and pathways, one of which is FSN-1 (Baker et al., 2014; Grill et al., 2007; Grill et al., 2012; Liao et al., 2004; Nakata et al., 2005; Tulgren et al., 2014). A previous study showed that mutating RPM-1 to reduce binding with a single RPM-1 binding protein, RAE-1, resulted in a partial loss of RPM-1 function (Grill et al., 2012). This prompted us to test whether RPM-1 that lacked FBD1 would be fully functional. To do so, we generated transgenic *rpm-1-/-* mutants that carried extrachromosomal arrays and used the native *rpm-1* promoter to express wild-type RPM-1 or RPM-1 lacking FBD1 (RPM-1 ΔFBD1). Consistent with prior studies, we observed that transgenic expression of RPM-1 strongly rescued the PLM hook defects in *rpm-1-/-* mutants (Figure 4-7B). In contrast, RPM-1 ΔFBD1 significantly, but partially, rescued the hook defects in *rpm-1-/-* mutants (Figure 4-7B). Thus, RPM-1 ΔFBD1 is only partially functional.

4.3 Discussion

4.3.1 RIP: an *in vivo* inhibitor of the RPM-1/FSN-1 ubiquitin ligase complex

Previous studies highlighted the functional relationship between the PHR proteins and FSN-1, but the biochemical mechanism of how PHR proteins bind to FSN-1 has remained poorly understood (Liao et al., 2004; Saiga et al., 2009; Wu et al., 2007). Here, we describe the identification of one mechanism by which FSN-1 binds to RPM-1. We show that this interaction is mediated by several key motifs in the D5c fragment of RPM-1, which we refer to as RIP when expressed recombinantly and as FBD1 (FSN-1 binding domain 1) within the context of the overall RPM-1 protein (Figure 4-8). Importantly, the residues in RPM-1 that mediate binding to FSN-1 are highly conserved, which suggests that this mechanism is likely to be relevant to all PHR proteins.

Several of our results suggest that RIP functions as an inhibitor of the RPM-1/FSN-1 ubiquitin ligase complex *in vivo*. 1) Transgenic overexpression of RIP caused defects in axon termination that occurred with similar frequency to defects caused by *fsn-1* (lf) (Figures 4-4 and 4-5). 2) Transgenic overexpression of RIP in *glo-4* (lf) mutants, but not *fsn-1* (lf) mutants, caused enhanced defects in axon termination. This is consistent with previous work showing that *glo-4* and *fsn-1* function in parallel pathways to regulate axon termination (Grill et al., 2007). 3) Enhanced axon termination defects caused by overexpression of RIP in a *glo-4-/-* mutant background are suppressed by *dlk-1* (lf) (Figure 4-6). This result is consistent with previous studies that showed FSN-1 regulates axon termination

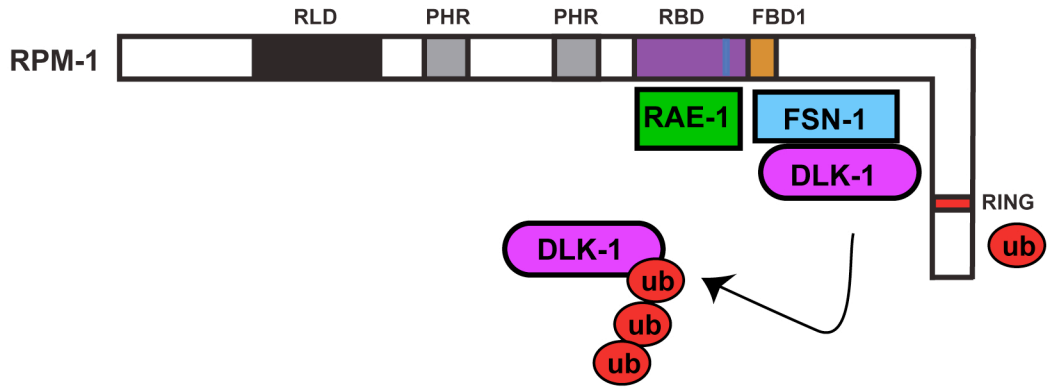

Figure 4-8: Summary of structure-function analysis of RPM-1 and FSN-1.
Schematic shows the annotated and known functional domains of RPM-1: the RAE-1 binding domain (RBD), the RAE-1 binding motif boxed within the RBD, and the FSN-1 binding domain 1 (FBD1). Note that RIP corresponds to the FBD1 region of RPM-1. Our structure-function analysis coupled with previous work (Grill et al., 2012) demonstrates that RAE-1 and FSN-1 bind at very close, but different locations on RPM-1. Our data support a model whereby FSN-1 scaffolds DLK-1 at FBD1 in the center of RPM-1, while the E3 ligase domain (RING) of RPM-1 acts independently to ubiquitinate DLK-1.

by inhibiting DLK-1 (Baker et al., 2014; Wu et al., 2007). 4) Point mutations that reduce binding of RIP to FSN-1 impair the function of transgenic RIP *in vivo* (Figure 4-7A). 5) Finally, RPM-1 that lacks FBD1 is only partially functional (Figure 4-7B). These results provide a body of consistent evidence to support the conclusion that transgenically expressed RIP binds to endogenous FSN-1, and prevents it from forming a functional complex with RPM-1. RIP now represents the first reagent to our knowledge that specifically inhibits the function of a PHR ubiquitin ligase complex.

A version of RIP that targets mammalian PHR proteins might be a useful reagent on several levels. First, viral delivery of RIP or an inducible system for RIP expression might be used to study the post-developmental function of the ubiquitin ligase activity of PHR proteins. Second, previous work has shown that

loss of function in *rpm-1* or *Hiw* results in improved axon regeneration (Hammarlund et al., 2009; Nix et al., 2011; Xiong et al., 2010). This suggests that transgenic overexpression of RIP might improve regeneration. Finally, loss of function in PHR proteins in flies and mice dramatically blocks axon degeneration, and this is likely to be mediated by Fbxo45 (Babetto et al., 2013; Xiong et al., 2012). Thus, specifically inhibiting the Phr1/Fbxo45 complex with RIP could have potential therapeutic implications for blocking or slowing the progression of axon damage following trauma, and possibly in the context of neurodegenerative diseases.

4.3.2 Implications for Myc binding to PHR proteins

We used HEK 293 cells as a heterologous expression system for biochemistry with *C. elegans* proteins, and identified a 97 aa region of RPM-1, annotated as FBD1, that is sufficient for binding to FSN-1 (Figure 4-8). We found that 5 highly conserved motifs within FBD1 are required for binding to FSN-1. FBD1 is contained within a larger domain we previously showed binds to RAE-1 (Grill et al., 2012). Our results here show that FSN-1 relies upon a different binding site in RPM-1 than RAE-1 (Figure 4-1 and 4-3) (Grill et al., 2012). Thus, while RAE-1 and FSN-1 are likely to be in close physical proximity, FSN-1 is unlikely to act as an adaptor for recruitment of RAE-1 into RPM-1 protein complexes, and vice versa. Our biochemical results are consistent with prior genetic and proteomic

results, which showed that RAE-1 is not a target of RPM-1 ubiquitin ligase activity (Grill et al., 2012; Tian et al., 2011).

Our findings also have important implications for the relationship between PHR proteins and Myc. Myc was originally found to bind to a region of Pam referred to as the Myc binding domain (Guo et al., 1998); more recently this domain was shown to also bind the F-box protein Fbxo45 (Saiga et al., 2009). The N-terminal half of the Pam Myc binding domain is conserved with Hiw and RPM-1, and the C-terminal half of this domain is not conserved. Our results show that FBD1, which corresponds with the conserved N-terminal portion of the Myc binding domain of Pam, is sufficient for binding to FSN-1. Further, all the conserved motifs we identified in FBD1 are required for binding to FSN-1. Thus, a likely structural model is that Myc binds to the C-terminal portion of the Myc binding domain of Pam, which is not conserved in Hiw and RPM-1. In this scenario, Myc would only bind to vertebrate PHR proteins, which is consistent with the absence of Myc in proteomic screens for Hiw and RPM-1 binding proteins (B. Grill, unpublished observation, and C. Wu, personal communication).

An alternative possibility is that FSN-1 might mediate binding of Myc to PHR proteins, in which case Myc would be ubiquitinated by the PHR proteins. In this scenario, we would have expected mutations in orthologs of Myc to be identified in previous suppressor screens with *rpm-1* or *Hiw* (lf), which has not occurred to our knowledge. Further, we would not have expected full length Pam to bind to Myc in the absence of proteasome inhibitors, which has been observed

(Guo et al., 1998). Thus, it is unlikely that FSN-1/Fbxo45 mediates binding of Myc to mammalian PHR proteins.

4.3.3 The FSN-1 binding domain of RPM-1 and formation of ubiquitin ligase complexes

Based on our analysis it is unclear whether we have mapped a direct interaction site between RPM-1 and FSN-1, or a region of RPM-1 that binds to an adaptor protein to recruit FSN-1. Previous work showed that PHR proteins form complexes that include FSN-1 and Skp proteins, such as SKR-1 in *C. elegans* (Brace et al., 2014; Liao et al., 2004; Saiga et al., 2009). A Cullin, CUL-1, has also been implicated in the RPM-1/FSN-1 ubiquitin ligase complex. However, Cullins are absent in the non-canonical Hiw/DFsn and Pam/Fbxo45 ubiquitin ligase complexes. Given the structural nature of Skp/Cullin/F-box complexes (Zheng et al., 2002), we would expect CUL-1 to bind directly to RPM-1 and act as an adaptor for SKR-1, which would then recruit FSN-1. In PHR ubiquitin ligase complexes that lack a Cullin, such as Pam/Fbxo45, we would expect Skp1 to mediate binding of Fbxo45 to Pam. Interestingly, our biochemical results using transgenic *C. elegans* showed that mutation of a residue, *D2214,* that is required for FBD1 to bind to FSN-1 does not impair binding of full length RPM-1 to FSN-1. Thus, while FBD1 is sufficient for binding to FSN-1, it is unlikely to be the only site that mediates binding of FSN-1 to RPM-1. There are two molecular models that explain this observation. First, CUL-1/SKR-1 might mediate binding of FSN-1

to RPM-1 at multiple interaction sites. Alternatively, FSN-1 might bind directly to RPM-1 at one location, and CUL-1/SKR-1 could mediate binding of FSN-1 to RPM-1 at another location(s).

There are several caveats to our experiments in HEK 293 cells that could explain why we only identified a single domain that bound to FSN-1. First, because we generated 9 individual domains that compose RPM-1, it is possible that another FSN-1 interaction site might span a junction between two domains. Second, we used a non-native expression system for biochemical mapping. Hence, we might fail to detect a second FSN-1 binding site because post-translational modifications required for the interaction did not occur in 293 cells. Alternatively, adaptor proteins (such as Skp or Cul proteins) required for interaction between FSN-1 and a second site in RPM-1 might not be expressed in these cells or might be unable to bind to *C. elegans* RPM-1 or FSN-1.

The RING-H2 domain of RPM-1 is the catalytic domain that mediates ubiquitin conjugation to target proteins (Nakata et al., 2005). FSN-1 did not bind to domain 9 of RPM-1, which contains the RING motif. This suggests that FSN-1 binds to FBD1 of RPM-1 to recruit DLK-1, while the RING-H2 domain at the C-terminus of RPM-1 is available for ubiquitin conjugation to DLK-1 (Figure 4-8). This model is consistent with previous work using HEK 293 cells, which showed that a C-terminal fragment of RPM-1 (aa 2970-3766) lacking FBD1 binds to DLK-1 in the presence of proteasome inhibitors (Nakata et al., 2005). While FBD1 and the RING domain are a large distance from one another in the primary protein

sequence of RPM-1, it is plausible that these two domains could be in close proximity within the tertiary structure of RPM-1. Our findings on RPM-1 and FSN-1 are consistent with prior work, which showed that other RING-H2 E3 ligases bind F-box proteins and ubiquitination targets at locations that are structurally distinct from the catalytic RING-H2 domain (Duda et al., 2011; Zheng et al., 2002).

Our results also have implications for the non-canonical ubiquitin ligase complexes formed by Hiw and Pam that lack Cullins (Brace et al., 2014; Saiga et al., 2009). The Rbx/Cul1/Skp1/Skp2 crystal structure shows that Rbx1, a relatively small E3 ligase, is bound by a relatively large Cullin (Zheng et al., 2002). This results in an arch-like structure that brings the F-box protein Skp2 and the ubiquitination target into close proximity with Rbx1. Given the large size of RPM-1 compared to Rbx1 and the extensive amount of protein sequence between the RPM-1 RING domain and FBD1, it is plausible that PHR proteins might not require a Cullin to generate a protein complex structure that is conducive to target recruitment and ubiquitination.

4.3.4 RIP as a potential therapeutic reagent

To date, designing specific inhibitors of PHR ubiquitin ligase activity has been challenging, due to the large size and complex biochemistry of these proteins. While many regions of Hiw have dominant negative effects on synapse formation at the neuromuscular junction (Wu et al., 2005), a region in Hiw that specifically

regulates FSN-1 function has remained elusive. We now show that RIP specifically inhibits the RPM-1/FSN-1 complex *in vivo*. The conservation of the motifs and residues that mediate the interaction between RIP and FSN-1 suggest that a mammalian version of RIP might be used to block the function of the Pam/Fbxo45 ubiquitin ligase complex *in vivo*. Previous studies showed that loss of PHR protein function mediated by Fbxo45 prevented axon degeneration following injury, and in some types of neurons improved axon regeneration (Babetto et al., 2013; Hammarlund et al., 2009; Nix et al., 2011; Xiong et al., 2012; Xiong et al., 2010). Given the role of PHR proteins in axon degeneration and regeneration, a reagent such as RIP might have potential as a broad-spectrum treatment for neurodegenerative diseases.

4.4 Experimental Procedures

4.4.1 Genetics and axon morphology analysis

Genetic analysis was performed using the N2 isolate of *C. elegans* and standard procedures (Brenner, 1974). The alleles used in this study included: *fsn-1(gk429*), *rpm-1(ju44)*, *glo-4(ok623)*, and *dlk-1(ju476)*. The transgene *muIs32* ($P_{mec\text{-}7}$GFP) was used for analyzing axon and synaptic branch morphology in ALM and PLM neurons. Live, young adult animals were anesthetized using 1% (v/v) 1-phenoxy-2-propanol in M9 buffer, and mounted on glass slides with 2% agarose. Animals were visualized using a 40x magnification oil-immersion lens

and an epifluorescent microscope (Leica CRF 5000). Images were acquired using a CCD camera (Leica DFC345 FX).

4.4.2 Cloning

The 9 domains (D1-9), and subdomains (D5a, b and c) of RPM-1 were amplified by RT-PCR from *C. elegans* total RNA using Superscript III reverse transcriptase (Invitrogen). cDNAs were inserted into pCR8 Topo GY, and sequenced to ensure they were mutation free. Clones in pCR8 Topo GY were recombined using LR recombinase with pBG-GY14 to create pBG-GY189 (GFP-D1), pBG-GY190 (GFP-D2), pBG-GY191 (GFP-D3), pBG-GY192 (GFP-D4), pBG-GY193 (GFP-D5), pBG-GY194 (GFP-D6), pBG-GY195 (GFP-D7), pBG-GY196 (GFP-D8), pBG-GY197 (GFP-D9), pBG-GY389 (GFP-D5a), pBG-GY412 (GFP-D5b), and pBG-GY384 (GFP-D5c). For transgenic expression of RIP (D5c) in *C. elegans*, pBG-GY152 (P_{rgef-1}FLAG GY) was recombined with pBG-GY349 (pCR8 Topo GY RIP (D5c)) to generate pBG-GY440 (P_{rgef-1}FLAG::RIP (D5c)). pCZ161 encoding full length RPM-1::GFP driven by its native promoter was engineered to contain a point mutation *D2214A* (pBG-190). For point mutagenesis, an HpaI-SpeI fragment of RPM-1 was amplified by PCR using pCZ161 as a template and inserted into pCR2.1. The HpaI-SpeI fragment was point mutated using oligonucleotides with the desired changes and a QuikChange II XL Site-Directed Mutagenesis Kit (Agilent Technologies). After mutations were confirmed by sequencing the mutated HpaI-SpeI fragment was subcloned back into pCZ161 to

create pBG-190. Similar mutagenesis procedures were performed on pBG-GY440 (P_{rgef-1}FLAG::RIP (D5c)) to generate RIP point mutants. These point mutations were also sequenced to confirm the accuracy of mutagenesis.

4.4.3 Transgenics

Transgenic animals were generated by standard microinjection procedures (Mello et al., 1991). Transgenic animals were constructed by injecting plasmid of interest or PCR product with plasmid encoding P_{ttx-3}RFP (50ng/μL). For dominant negative experiments PCR products were amplified by a long PCR kit (Roche) and injected at 0.625-10ng/μL as specified. The following plasmids were used as templates for long PCR: P_{rgef-1}FLAG::RIP (pBG-GY440) or point mutants, and P_{rgef-1}FLAG::mCherry (pBG-GY371). Transgenic animals used for biochemistry were generated by injecting plasmids: P_{rgef-1}FLAG::FSN-1 (pBG-GY422) at 25ng/μL and P_{rpm-1}RPM-1::GFP (pCZ161) or P_{rpm-1}RPM-1::GFP *D2214A* (pBG-190) at 25ng/μL into *rpm-1; fsn-1* mutants. For coIP of GFP::D5c with FLAG::FSN-1 transgenic animals were generated by injecting plasmids: P_{rgef-1}FLAG::FSN-1 and P_{rgef-1}GFP::D5c (RIP) at 25ng/μL into wild-type animals. Notably, expression of FLAG::FSN-1 was higher on a wild-type background than an *fsn-1* mutant background.

4.4.4 Biochemistry

For biochemistry in HEK 293 cells or from transgenic *C. elegans*, FLAG proteins were immunoprecipitated (IP) with a mouse monoclonal anti-FLAG antibody (M2, Sigma), and immunoblotted with a rabbit polyclonal anti-FLAG antibody (Cell Signaling). GFP fusion proteins were precipitated with a mouse monoclonal anti-GFP antibody (3E6, MP Biomedicals), and immunoblotted with a mixture of mouse monoclonal anti-GFP antibodies (Roche). Precipitates were boiled in SDS Laemmli Sample Buffer (Biorad), and run on a 3-8% Tris acetate gel (Invitrogen) for RPM-1::GFP coIP, or a 4-12% Bis Tris gel (Invitrogen) for coIP of RPM-1 domains. Gels were transferred to PVDF membranes in Tris-Acetate transfer buffer (16-20 hours at 30 Volts for full length RPM-1::GFP), and immuno-blotted. Blots were visualized with HRP conjugated anti-mouse or anti-rabbit secondary antibodies, enhanced chemiluminescent reagent (ECL), and x-ray film. When necessary due to the size of target proteins, light chain reactive secondary antibodies were used (Millipore). Western Lightning Plus ECL was used for HEK 293 experiments, and Supersignal FemtoWest ECL (Pierce) was used for transgenic *C. elegans* experiments.

For experiments with HEK 293 cells, 6cm dishes of cells were transfected with a mixture of lipofectamine 2000 (Invitrogen) and a total of 9-11µg of DNA that included: plasmid encoding FLAG-FSN-1 (5.2µg DNA), plasmid encoding a GFP-RPM-1 domain (3-6µg DNA), and varying amounts of pBluescript (amount required to reach total of 9-11µg DNA). A variable amount of DNA was

transfected for particular constructs to ensure similar levels of expression. 36-48 hours after transfection, cells were lysed with 1.0% NP-40 buffer (50mM Tris pH 7.5, 150mM NaCl, 10% glycerol, 1mM DTT, EDTA-free protease inhibitor pellets (Roche), pepstatin, microcystin, NaVO4, NaF, NaMolybdate, and β-glycerophosphate). 1000 µg of total protein from transfected 293 cells was used for individual coIP experiments. Lysates were incubated with primary antibody for 30 minutes, and precipitated for 4 hours with 10µL of protein G agarose (Roche) at 4^{o}C.

For biochemistry using transgenic worms, animals containing extrachromosomal arrays were propagated using *E. coli* (strain HB101) on 10cm NGM agar plates. Worms were harvested directly off 10cm plates, or moved to liquid culture for 1-2 days if larger amounts of material were needed. Animals were harvested by centrifugation and washed 3x in M9 buffer. Animals were ground using a mortar and pestle, and lysed using sonication and 0.1% NP-40 lysis buffer (50mM Tris pH 7.5, 0.1% NP-40, 150 mM NaCl, 10% glycerol, 1mM DTT, and EDTA-free protease inhibitor pellets). For coIP of RPM-1::GFP with FLAG::FSN-1, 20-120mg of total protein from transgenic worm lysates was used. For coIP of FLAG::FSN-1 with GFP::D5c from transgenic worm lysates, 25mg of total lysate was used. Lysates were incubated with 3µL of M2 (anti-Flag) antibody or 3µL of 3E6 (anti-GFP) antibody for 30 minutes, and precipitated for 4 hours at 4^{o}C with 10µL of protein G agarose.

4.4 Acknowledgments

We thank the *C. elegans* knock-out consortium for generating deletion alleles and the *C. elegans* Genetics Center for providing strains.

4.5 Author Contributions

Conceived and designed the experiments: JP STB BG. Performed the experiments: JP STB SMT AMG KJO. Analyzed the data: JP STB BG. Wrote the paper: JP STB BG. Figure 1: JP performed most of the experiments with help from STB and AMG. Figure 2: JP and SB performed the experiments. Figure 3: JP performed most of the experiments with help from STB and SMT. Figure 4: STB performed most the experiments with help from JP and SMT. Figure 5: STB performed most of the experiments with help from JP and SMT. Figure 6: STB performed the experiments with help from KJO. Figure 7: STB performed the experiments with help from KJO.

5 Conclusion

5.1 Summary

The formation of the nervous system is an intricate process that is controlled by a complex network of signaling pathways that allow neurons to extend an axonal projection that forms synapses with the correct target. Dynamic interactions between the pre- and post-synaptic terminals then provide a way for neurons to communicate, propagate information, and engage in plasticity. Understanding where and how synapses form is crucial if we are to unravel how the nervous system is accurately constructed. The organization of synaptic circuits is remarkably well controlled, which suggests inherent mechanisms exist to create the identity and connectivity of each neuron in the brain. A limited number of conserved molecules and pathways have been shown to both guide axons towards their targets, and build functional synapses. While it's clear that a number of events must be coordinated and regulated to form functional synapses, the underlying molecular mechanisms remain unknown. The PHR proteins, a conserved family of large signaling proteins with ubiquitin ligase activity, function in numerous events during neuronal development including: axon guidance, axon termination, and synapse formation. Previous findings and our own presented here have provided growing evidence that the PHR proteins are likely to coordinate and integrate multiple events during neuronal development.

The first insight into the physiological function of the PHR proteins came from the identification of the invertebrate PHRs, RPM-1 and Hiw, in genetic screens looking for abnormal axon and/or synapse morphology. Later studies on *C. elegans* RPM-1 revealed several downstream effectors and signaling pathways critical to PHR function (Figure 1-2). In this dissertation, our studies provide new insight into the role of the phosphatase PPM-2, and the MLK-1 pathway in mediating RPM-1 signaling and subsequent effects on axon termination and synapse formation (Figure 5-1). Our structure-function analysis helped define the biochemical relationship between RPM-1 and FSN-1, and further advanced our understanding of how PHR ubiquitin ligase complexes form.

In Chapter 2, we show that PHR proteins are more accurate and sensitive regulators of DLK that originally thought by demonstrating that they function through both phosphatase and ubiquitin ligase mechanisms to inhibit DLK. Using mass spectrometry, we identified the PP2C phosphatase PPM-2 as a novel RPM-1 binding protein that regulates axon termination and synapse formation. Our genetic, transgenic, and biochemical studies indicated that PPM-2 functions coordinately with the ubiquitin ligase activity of RPM-1 and the F-box protein FSN-1 to negatively regulate DLK-1. We also showed that PPM-2 specifically acts on a serine residue of DLK-1 (S874) that has been implicated in regulation of full length DLK-1 (DLK-1L) binding to its short inhibitory isoform (DLK-1S).

In Chapter 3, we show that a loss of function mutation in kinases of the MLK-1 pathway function cell-autonomously in neurons to suppress defects in

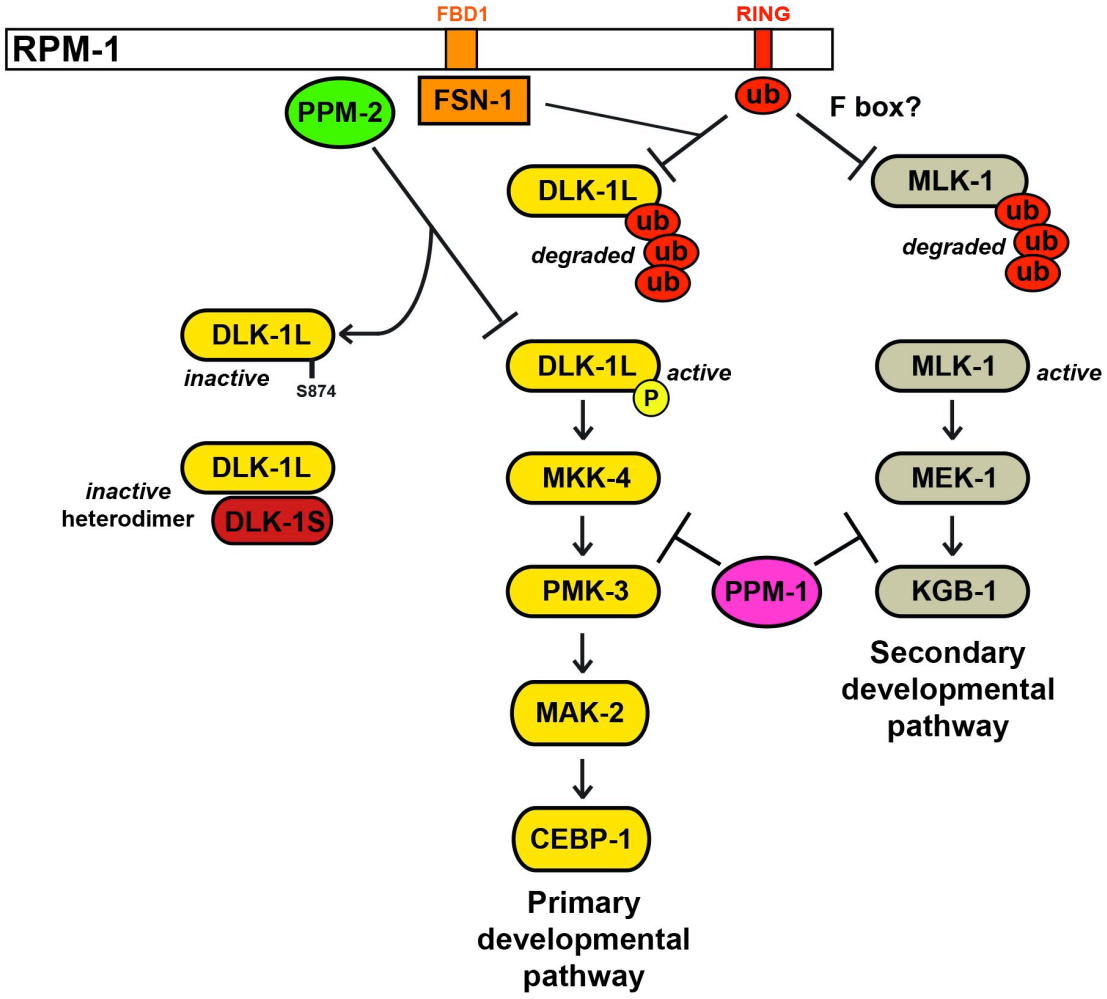

Figure 5-1. Summary of new signaling in the RPM-1 pathway.
The PP2C phosphatase PPM-2 binds to RPM-1, and negatively regulates signaling through the DLK-1 pathway by dephosphorylating a serine residue on DLK-1L (S874). This residue is involved in regulation of DLK-1L binding to its short inhibitory isoform DLK-1S. RPM-1 primarily functions through the DLK-1 pathway and secondarily through the MLK-1 pathway to regulate neuronal development. PPM-1 broadly inhibits both the DLK-1 and MLK-1 pathways. While FSN-1 mediates DLK-1 ubiquitination, it does not function as the F-box protein to negatively regulate the MLK-1 pathway. A conserved 97-amino acid region of RPM-1 (FBD1) is sufficient for binding to FSN-1.

synapse formation and axon termination caused by *rpm-1* loss of function. This suppression is much weaker than what is observed with mutations in kinases of the DLK-1 pathway, suggesting that RPM-1 functions primarily through the DLK-1 pathway and secondarily through the MLK-1 pathway to regulate neuronal

development. Our genetic and transgenic analysis also show that the phosphatase PPM-1 is a potential inhibitor of kinases in the MLK-1 pathway, while PPM-2 seems to be more specific and only inhibits DLK-1.

Finally in Chapter 4, we have demonstrated that RPM-1 uses a conserved mechanism to bind FSN-1 that is independent of the domain in RPM-1 that has catalytic ubiquitin ligase activity. We found a single domain centrally located in RPM-1 that is sufficient for binding to FSN-1, and further refined this to a conserved 97-amino acid region of RPM-1. Mutagenesis identified several conserved motifs and individual amino acids that mediate this interaction. Transgenic overexpression of this small fragment of RPM-1 causes defects in axon termination and synapse formation similar to loss of function in *fsn-1*. These defects were suppressed by loss of function in *dlk-1* and were alleviated by point mutations that reduce binding to FSN-1. Together, our biochemical and genetic analysis has led to the identification of the first *in vivo* inhibitor of the RPM-1/FSN-1 ubiquitin ligase complex.

5.2 Future directions

5.2.1 Regulation of DLK-1 activation

Our study on the PP2C phosphatase PPM-2 has provided the first evidence that PHR proteins are able to regulate a single target through multiple independent mechanisms. We proposed a model whereby RPM-1 inhibits local activation of the MAP3K DLK-1 through PPM-2 and long-term regulation of DLK-1 through

ubiquitination (Figure 5-1). In worms, two isoforms of DLK-1 exist, and a single hexapeptide motif in full length DLK-1 (DLK-1L) regulates binding to a short inhibitory isoform (DLK-1S) (Yan and Jin, 2012). This conserved hexapeptide contains two serine residues (S874 and S878), and phosphomimetic manipulations suggest that the charge state of this hexapeptide tightly regulates the balance between inactive DLK-1L/S heteromeric complexes and active DLK-1L homomeric complexes (Yan and Jin, 2012). Our study shows that this motif is the site of PPM-2 inhibitory activity, but with PPM-2 specifically dephosphorylating the S874 residue of DLK-1L (Figure 5-1). However, we still do not understand the complete mechanism by which dephosphorylation of this motif affects binding of DLK-1S to DLK-1L. While binding of these two isoforms was not altered in *ppm-2* mutants, DLK-1S shows greatly reduced binding to a phosphomimetic DLK-1L when both serine residues of the hexapeptide are mutated to mimic a phosphorylated state (S874E, S878E) (Yan and Jin, 2012).

Future biochemical and genetic experiments will be necessary to test if PPM-2 affects the binding of DLK-1L to DLK-1S, or directly regulates DLK-1L activation independent of DLK-1S. Several experiments could be helpful in testing which of the two models is correct. For example, we could perform single phosphomimetic point mutations at S874 or S878 residues of DLK-1L to test if modification of one or both residues affects binding to DLK-1S. If only S878 mediates binding to DLK-1S then we would conclude that phosphorylation of both S874 and S878 are required for DLK-1L activation, but phosphorylation of

each residue mediates an independent mechanism of inhibition.

Furthermore, if experimental evidence indicates that DLK-1L is regulated by phosphorylation at both S874 and S878, it will be critical to understand how DLK-1L is activated and inactivated. Since its identification and characterization, autophosphorylation of mammalian DLK was observed (Holzman et al., 1994; Mata et al., 1996), and later studies showed that dimerization initiates this autophosphorylation and subsequent activation of DLK catalytic activity (Nihalani et al., 2000; Nihalani et al., 2001). Despite this initial progress, the mechanisms that govern activation of DLK remain poorly understood. In addition, recent studies have revealed numerous phosphorylation sites present in mammalian DLK (Huntwork-Rodriguez et al., 2013), suggesting that the complexity of this regulatory system could be significantly expanded in mammals. Our discovery in worms that PPM-2 inhibits DLK-1L by direct dephosphorylation at S874, and the discovery of DLK-1S provide a good start in understanding how DLK-1L is inhibited and how dimerization may occur. However, identification of kinases and other phosphatases that regulate phosphorylation at S874 and/or S878 of DLK-1L will be helpful in further unraveling how DLK-1L is activated and inactivated.

5.2.2 PP2C phosphatase function outside of neuronal development

While DLK-1 plays an important role in neuronal development, it is also essential for axon regeneration in *C. elegans*, Drosophila, and mice (Hammarlund et al., 2009; Itoh et al., 2009; Shin et al., 2012; Xiong et al., 2010; Yan et al., 2009).

Importantly, loss of function in *C. elegans rpm-1* and Drosophila *Highwire*, or overexpression of DLK-1 leads to improved axon regeneration (Hammarlund et al., 2009; Nix et al., 2011; Xiong et al., 2010; Yan et al., 2009). Loss of function in *fsn-1* also results in improved regeneration (Hammarlund et al., 2009). These studies demonstrate that relieving inhibition on or activating the DLK-1 pathway promotes axon regeneration, particularly in older adult *C. elegans* where regeneration is much less robust. Additionally, another MAPK pathway, the MLK-1/MEK-1/KGB-1(JNK), functions together with the DLK-1 pathway to regulate axon regeneration (Nix et al., 2011). These studies suggest that potential therapies aimed at improving recovery after traumatic axotomy could potentially target either of these pathways.

Our findings that PPM-2 specifically regulates the DLK-1 pathway and PPM-1 broadly inhibits both the DLK-1 and MLK-1 pathway during neuronal development (Figure 5-1), suggests that these phosphatases may also play a post-developmental role in axon regeneration. Our findings predict that increased DLK-1 and/or MLK-1 activity in *ppm-2-/-* and/or *ppm-1-/-* animals could result in improved regenerative capacity compared to wild-type animals. In addressing this possibility, several important considerations from our developmental understanding of DLK-1 and MLK-1 signaling should be taken into account. 1) A combination of loss of function in *fsn-1* with either *ppm-2* or *ppm-1* might be necessary to see improved regeneration, as these genes function in parallel pathways to regulate DLK-1. 2) A prior study showed that older animals have

poor regeneration that is more sensitive to increased levels of DLK-1 activity (Hammarlund et al., 2009). Therefore, with PPM-2 being a partial regulator of DLK-1 activity, the possible effects of PPM-2 on regeneration may be more noticeable in older animals. 3) Crosstalk between the DLK-1 and MLK-1 pathways exists (Nix et al., 2011). Therefore, inhibiting a broad regulator of both pathways, such as PPM-1, may be a better therapeutic approach than inhibiting a specific regulator of just one of the MAPK pathways, such as PPM-2. On the other hand, inhibition of the MAP3Ks of the MAPK cascades may prevent signal amplification, therefore limiting the cellular response to axonal injury. In this case, inhibitors of the highest kinases of the MAPK cascades, DLK-1 and/or MLK-1 may prove to be the best therapeutic targets for improving regeneration. Exploring the possible role of the PP2C phosphatases in regeneration is worthwhile, as the enzymatic activity of these phosphatases may be particularly amenable to pharmaceutical intervention.

5.2.3 Crystal structure of the PHR ubiquitin ligase complex

The PHR proteins are larger than 400 kDa, and the large size and complex biochemistry of these proteins has limited structure-function analysis. Some progress was made with the discovery that the F-box protein Fbxo45 binds to a fragment of Pam that was previously shown to bind to Myc (Saiga et al., 2009). This dissertation describes further structure-function analysis in which we showed the conserved FSN-1 binding domain 1 (FBD1) in RPM-1 was sufficient

for binding to FSN-1 *in vivo* in worm neurons and in HEK 293 cells (Figure 5-1). FBD1 is a conserved domain in all PHR proteins suggesting it is likely to be a conserved mechanism by which PHR proteins bind to F-box proteins. We showed that transgenic overexpression of recombinantly expressed FBD1 (RIP) in the neurons of worms results in dominant negative effects on synapse formation and axon termination, which are consistent with *fsn-1* loss of function. RIP represents the first specific inhibitor of the PHR ubiquitin ligase complex. Given the role of PHR proteins in axon degeneration and regeneration, RIP represents a potential therapeutic treatment for neurodegenerative diseases (Babetto et al., 2013; Hammarlund et al., 2009; Nix et al., 2011; Xiong et al., 2012; Xiong et al., 2010). However, further structure-function analysis of the PHR ubiquitin ligase complex will prove valuable for a number of reasons. 1) While FBD1 is sufficient for binding to FSN-1, it is unlikely to be the only site that mediates binding of FSN-1 to RPM-1. Our recent findings indicate that in addition to FBD1, several other sites mediate binding of FSN-1 to RPM-1. These sites were not detected when we used a heterologous expression system, HEK 293 cells, for biochemical mapping of FSN-1 binding to different domains in RPM-1. 2) Previous work has showed that PHR proteins form complexes that include FSN-1 and Skp proteins (Brace et al., 2014; Liao et al., 2004; Saiga et al., 2009). A Cullin has been implicated in the RPM-1/FSN-1 ubiquitin ligase complex, which is absent in the non-canonical Hiw/DFsn and Pam/Fbxo45 ubiquitin ligase complexes. Pursuing further structure-function with Pam, Skp1, and Fbxo45 will

allow us to determine if FBD1 of Pam mediates direct binding to Fbxo45 or Skp1. Further, we will assess whether the FBD1 of Pam is a conserved site of F-box binding for the PHR proteins. Structure-function analysis with Pam, Skp1, and Fbxo45 will ultimately lay the groundwork for generation of crystal structures that definitively address the nature of this non-canonical ubiquitin ligase complex. Hopefully, this type of comprehensive biochemical analysis will allow development of a small molecule that specifically impairs the ubiquitin ligase activity of the Pam/Skp1/Fbxo45 complex, and potential value in treating a range of neurodegenerative diseases.

Bibliography

Abrams, B., Grill, B., Huang, X., and Jin, Y. (2008). Cellular and molecular determinants targeting the Caenorhabditis elegans PHR protein RPM-1 to perisynaptic regions. Dev Dyn *237*, 630-639.

Ahmari, S.E., Buchanan, J., and Smith, S.J. (2000). Assembly of presynaptic active zones from cytoplasmic transport packets. Nat Neurosci *3*, 445-451.

Aitken, A., Cohen, P., Santikarn, S., Williams, D.H., Calder, A.G., Smith, A., and Klee, C.B. (1982). Identification of the NH2-terminal blocking group of calcineurin B as myristic acid. FEBS Lett *150*, 314-318.

Alonso, A., Narisawa, S., Bogetz, J., Tautz, L., Hadzic, R., Huynh, H., Williams, S., Gjorloff-Wingren, A., Bremer, M.C., Holsinger, L.J.*, et al.* (2004). VHY, a novel myristoylated testis-restricted dual specificity protein phosphatase related to VHX. The Journal of biological chemistry *279*, 32586-32591.

Alsina, B., Vu, T., and Cohen-Cory, S. (2001). Visualizing synapse formation in arborizing optic axons in vivo: dynamics and modulation by BDNF. Nat Neurosci *4*, 1093-1101.

Arikkath, J., and Reichardt, L.F. (2008). Cadherins and catenins at synapses: roles in synaptogenesis and synaptic plasticity. Trends Neurosci *31*, 487-494.

Babetto, E., Beirowski, B., Russler, E.V., Milbrandt, J., and DiAntonio, A. (2013). The Phr1 ubiquitin ligase promotes injury-induced axon self-destruction. Cell Rep *3*, 1422-1429.

Baker, S.T., Opperman, K.J., Tulgren, E.D., Turgeon, S.M., Bienvenut, W., and Grill, B. (2014). RPM-1 uses both ubiquitin ligase and phosphatase-based mechanisms to regulate DLK-1 during neuronal development. PLoS genetics *10*, e1004297.

Bargmann, C.I. (1998). Neurobiology of the Caenorhabditis elegans genome. Science *282*, 2028-2033.

Baril, C., Sahmi, M., Ashton-Beaucage, D., Stronach, B., and Therrien, M. (2009). The PP2C Alphabet is a negative regulator of stress-activated protein kinase signaling in Drosophila. Genetics *181*, 567-579.

Bashaw, G.J., and Klein, R. (2010). Signaling from axon guidance receptors. Cold Spring Harb Perspect Biol *2*, a001941.

Ben Fredj, N., Hammond, S., Otsuna, H., Chien, C.B., Burrone, J., and Meyer, M.P. (2010). Synaptic activity and activity-dependent competition regulates axon arbor

maturation, growth arrest, and territory in the retinotectal projection. The Journal of neuroscience : the official journal of the Society for Neuroscience *30*, 10939-10951.

Benson, D.L., and Huntley, G.W. (2012). Building and remodeling synapses. Hippocampus *22*, 954-968.

Berkowitz, L.A., Hamamichi, S., Knight, A.L., Harrington, A.J., Caldwell, G.A., and Caldwell, K.A. (2008). Application of a C. elegans dopamine neuron degeneration assay for the validation of potential Parkinson's disease genes. J Vis Exp.

Bermudez, O., Pages, G., and Gimond, C. (2010). The dual-specificity MAP kinase phosphatases: critical roles in development and cancer. Am J Physiol Cell Physiol *299*, C189-202.

Bloom, A.J., Miller, B.R., Sanes, J.R., and DiAntonio, A. (2007). The requirement for Phr1 in CNS axon tract formation reveals the corticostriatal boundary as a choice point for cortical axons. Genes Dev *21*, 2593-2606.

Brace, E.J., Wu, C., Valakh, V., and DiAntonio, A. (2014). SkpA restrains synaptic terminal growth during development and promotes axonal degeneration following injury. The Journal of neuroscience : the official journal of the Society for Neuroscience *34*, 8398-8410.

Brenner, S. (1974). The genetics of Caenorhabditis elegans. Genetics *77*, 71-94.

Budnik, V., Zhong, Y., and Wu, C.F. (1990). Morphological plasticity of motor axons in Drosophila mutants with altered excitability. The Journal of neuroscience : the official journal of the Society for Neuroscience *10*, 3754-3768.

Burgess, R.W., Peterson, K.A., Johnson, M.J., Roix, J.J., Welsh, I.C., and O'Brien, T.P. (2004). Evidence for a conserved function in synapse formation reveals Phr1 as a candidate gene for respiratory failure in newborn mice. Molecular and cellular biology *24*, 1096-1105.

Caldwell, G.A., and Caldwell, K.A. (2008). Traversing a wormhole to combat Parkinson's disease. Dis Model Mech *1*, 32-36.

Ch'ng, Q., Williams, L., Lie, Y.S., Sym, M., Whangbo, J., and Kenyon, C. (2003). Identification of genes that regulate a left-right asymmetric neuronal migration in Caenorhabditis elegans. Genetics *164*, 1355-1367.

Chalfie, M., and Thomson, J.N. (1979). Organization of neuronal microtubules in the nematode Caenorhabditis elegans. J Cell Biol *82*, 278-289.

Chalfie, M., Tu, Y., Euskirchen, G., Ward, W.W., and Prasher, D.C. (1994). Green fluorescent protein as a marker for gene expression. Science *263*, 802-805.

Charron, F., and Tessier-Lavigne, M. (2005). Novel brain wiring functions for classical morphogens: a role as graded positional cues in axon guidance. Development *132*, 2251-2262.

Chen, S.Y., and Cheng, H.J. (2009). Functions of axon guidance molecules in synapse formation. Curr Opin Neurobiol *19*, 471-478.

Cherra, S.J., 3rd, and Jin, Y. (2015). Advances in synapse formation: forging connections in the worm. Wiley Interdiscip Rev Dev Biol *4*, 85-97.

Chida, T., Ando, M., Matsuki, T., Masu, Y., Nagaura, Y., Takano-Yamamoto, T., Tamura, S., and Kobayashi, T. (2013). N-myristoylation is essential for protein phosphatases PPM1A and PPM1B to dephosphorylate their physiological substrates in cells. Biochem J.

Coleman, M.P., and Perry, V.H. (2002). Axon pathology in neurological disease: a neglected therapeutic target. Trends Neurosci *25*, 532-537.

Collins, C.A., Wairkar, Y.P., Johnson, S.L., and Diantonio, A. (2006). Highwire Restrains Synaptic Growth by Attenuating a MAP Kinase Signal. Neuron *51*, 57-69.

Colon-Ramos, D.A., Margeta, M.A., and Shen, K. (2007). Glia promote local synaptogenesis through UNC-6 (netrin) signaling in C. elegans. Science *318*, 103-106.

Consortium, C.e.S. (1998). Genome sequence of the nematode C. elegans: a platform for investigating biology. Science *282*, 2012-2018.

Couteaux, R. (1963). The Differentiation of Synaptic Areas. Proc R Soc Lond B Biol Sci *158*, 457-480.

Craig, A.M., and Kang, Y. (2007). Neurexin-neuroligin signaling in synapse development. Curr Opin Neurobiol *17*, 43-52.

Culican, S.M., Bloom, A.J., Weiner, J.A., and DiAntonio, A. (2009). Phr1 regulates retinogeniculate targeting independent of activity and ephrin-A signalling. Mol Cell Neurosci *41*, 304-312.

D'Souza, J., Hendricks, M., Le Guyader, S., Subburaju, S., Grunewald, B., Scholich, K., and Jesuthasan, S. (2005). Formation of the retinotectal projection requires Esrom, an ortholog of PAM (protein associated with Myc). Development *132*, 247-256.

Daviau, A., Di Fruscio, M., and Blouin, R. (2009). The mixed-lineage kinase DLK undergoes Src-dependent tyrosine phosphorylation and activation in cells exposed to vanadate or platelet-derived growth factor (PDGF). Cell Signal *21*, 577-587.

Dickson, B.J. (2002). Molecular mechanisms of axon guidance. Science *298*, 1959-1964.

Dickson, B.J., and Senti, K.A. (2002). Axon guidance: growth cones make an unexpected turn. Curr Biol *12*, R218-220.

Dontchev, V.D., and Letourneau, P.C. (2003). Growth cones integrate signaling from multiple guidance cues. J Histochem Cytochem *51*, 435-444.

Du, H., and Chalfie, M. (2001). Genes regulating touch cell development in Caenorhabditis elegans. Genetics *158*, 197-207.

Duda, D.M., Scott, D.C., Calabrese, M.F., Zimmerman, E.S., Zheng, N., and Schulman, B.A. (2011). Structural regulation of cullin-RING ubiquitin ligase complexes. Curr Opin Struct Biol *21*, 257-264.

Eto, K., Kawauchi, T., Osawa, M., Tabata, H., and Nakajima, K. (2010). Role of dual leucine zipper-bearing kinase (DLK/MUK/ZPK) in axonal growth. Neurosci Res *66*, 37-45.

Fannon, A.M., and Colman, D.R. (1996). A model for central synaptic junctional complex formation based on the differential adhesive specificities of the cadherins. Neuron *17*, 423-434.

Feldheim, D.A., and O'Leary, D.D. (2010). Visual map development: bidirectional signaling, bifunctional guidance molecules, and competition. Cold Spring Harb Perspect Biol *2*, a001768.

Feng, J., Zhao, J., Li, J., Zhang, L., and Jiang, L. (2010a). Functional characterization of the PP2C phosphatase CaPtc2p in the human fungal pathogen Candida albicans. Yeast *27*, 753-764.

Feng, Y., Yan, T., He, Z., and Zhai, Q. (2010b). Wld(S), Nmnats and axon degeneration--progress in the past two decades. Protein Cell *1*, 237-245.

Friedman, H.V., Bresler, T., Garner, C.C., and Ziv, N.E. (2000). Assembly of new individual excitatory synapses: time course and temporal order of synaptic molecule recruitment. Neuron *27*, 57-69.

Furukawa, T., Itoh, M., Krueger, N.X., Streuli, M., and Saito, H. (1994). Specific interaction of the CD45 protein-tyrosine phosphatase with tyrosine-phosphorylated CD3 zeta chain. Proc Natl Acad Sci U S A *91*, 10928-10932.

Garbarini, N., and Delpire, E. (2008). The RCC1 domain of protein associated with Myc (PAM) interacts with and regulates KCC2. Cell Physiol Biochem *22*, 31-44.

George, R., and Griffin, J.W. (1994). Delayed macrophage responses and myelin clearance during Wallerian degeneration in the central nervous system: the dorsal radiculotomy model. Exp Neurol *129*, 225-236.

Ghosh, A.S., Wang, B., Pozniak, C.D., Chen, M., Watts, R.J., and Lewcock, J.W. (2011). DLK induces developmental neuronal degeneration via selective regulation of proapoptotic JNK activity. J Cell Biol *194*, 751-764.

Ghosh-Roy, A., Wu, Z., Goncharov, A., Jin, Y., and Chisholm, A.D. (2010). Calcium and cyclic AMP promote axonal regeneration in Caenorhabditis elegans and require DLK-1 kinase. The Journal of neuroscience : the official journal of the Society for Neuroscience *30*, 3175-3183.

Grill, B., Bienvenut, W.V., Brown, H.M., Ackley, B.D., Quadroni, M., and Jin, Y. (2007). C. elegans RPM-1 Regulates Axon Termination and Synaptogenesis through the Rab GEF GLO-4 and the Rab GTPase GLO-1. Neuron *55*, 587-601.

Grill, B., Chen, L., Tulgren, E.D., Baker, S.T., Bienvenut, W., Anderson, M., Quadroni, M., Jin, Y., and Garner, C.C. (2012). RAE-1, a Novel PHR Binding Protein, Is Required for Axon Termination and Synapse Formation in Caenorhabditis elegans. The Journal of neuroscience : the official journal of the Society for Neuroscience *32*, 2628-2636.

Guo, Q., Xie, J., Dang, C.V., Liu, E.T., and Bishop, J.M. (1998). Identification of a large Myc-binding protein that contains RCC1-like repeats. Proc Natl Acad Sci U S A *95*, 9172-9177.

Hallam, S.J., and Jin, Y. (1998). lin-14 regulates the timing of synaptic remodelling in Caenorhabditis elegans. Nature *395*, 78-82.

Hammarlund, M., Nix, P., Hauth, L., Jorgensen, E.M., and Bastiani, M. (2009). Axon regeneration requires a conserved MAP kinase pathway. Science *323*, 802-806.

Han, S., Kim, S., Bahl, S., Li, L., Burande, C.F., Smith, N., James, M., Beauchamp, R.L., Bhide, P., Diantonio, A.*, et al.* (2012). The E3 ubiquitin ligase, protein associated with Myc (Pam) regulates mammalian/mechanistic target of rapamycin complex 1 (mTORC1) signaling in vivo through N- and C-terminal domains. The Journal of biological chemistry.

Han, S., Witt, R.M., Santos, T.M., Polizzano, C., Sabatini, B.L., and Ramesh, V. (2008). Pam (Protein associated with Myc) functions as an E3 ubiquitin ligase and regulates TSC/mTOR signaling. Cell Signal *20*, 1084-1091.

Hanada, M., Ninomiya-Tsuji, J., Komaki, K., Ohnishi, M., Katsura, K., Kanamaru, R., Matsumoto, K., and Tamura, S. (2001). Regulation of the TAK1 signaling pathway by protein phosphatase 2C. The Journal of biological chemistry *276*, 5753-5759.

Hannah, M.J., Schmidt, A.A., and Huttner, W.B. (1999). Synaptic vesicle biogenesis. Annu Rev Cell Dev Biol *15*, 733-798.

Hedgecock, E.M., Culotti, J.G., and Hall, D.H. (1990). The unc-5, unc-6, and unc-40 genes guide circumferential migrations of pioneer axons and mesodermal cells on the epidermis in C. elegans. Neuron *4*, 61-85.

Hendricks, M., and Jesuthasan, S. (2009). PHR regulates growth cone pausing at intermediate targets through microtubule disassembly. The Journal of neuroscience : the official journal of the Society for Neuroscience *29*, 6593-6598.

Hirai, S., Cui de, F., Miyata, T., Ogawa, M., Kiyonari, H., Suda, Y., Aizawa, S., Banba, Y., and Ohno, S. (2006). The c-Jun N-terminal kinase activator dual leucine zipper kinase regulates axon growth and neuronal migration in the developing cerebral cortex. The Journal of neuroscience : the official journal of the Society for Neuroscience *26*, 11992-12002.

Hirano, S., and Takeichi, M. (2012). Cadherins in brain morphogenesis and wiring. Physiol Rev *92*, 597-634.

Holland, S., Coste, O., Zhang, D.D., Pierre, S.C., Geisslinger, G., and Scholich, K. (2011). The ubiquitin ligase MYCBP2 regulates transient receptor potential vanilloid receptor 1 (TRPV1) internalization through inhibition of p38 MAPK signaling. The Journal of biological chemistry *286*, 3671-3680.

Holzman, L.B., Merritt, S.E., and Fan, G. (1994). Identification, molecular cloning, and characterization of dual leucine zipper bearing kinase. A novel serine/threonine protein kinase that defines a second subfamily of mixed lineage kinases. The Journal of biological chemistry *269*, 30808-30817.

Hua, J.Y., Smear, M.C., Baier, H., and Smith, S.J. (2005). Regulation of axon growth in vivo by activity-based competition. Nature *434*, 1022-1026.

Huang, C., Zheng, X., Zhao, H., Li, M., Wang, P., Xie, Z., Wang, L., and Zhong, Y. (2012). A permissive role of mushroom body alpha/beta core neurons in long-term memory consolidation in Drosophila. Curr Biol *22*, 1981-1989.

Huntwork-Rodriguez, S., Wang, B., Watkins, T., Ghosh, A.S., Pozniak, C.D., Bustos, D., Newton, K., Kirkpatrick, D.S., and Lewcock, J.W. (2013). JNK-mediated phosphorylation of DLK suppresses its ubiquitination to promote neuronal apoptosis. J Cell Biol *202*, 747-763.

Itoh, A., Horiuchi, M., Bannerman, P., Pleasure, D., and Itoh, T. (2009). Impaired regenerative response of primary sensory neurons in ZPK/DLK gene-trap mice. Biochem Biophys Res Commun *383*, 258-262.

Jackson, M.D., Fjeld, C.C., and Denu, J.M. (2003). Probing the function of conserved residues in the serine/threonine phosphatase PP2Calpha. Biochemistry *42*, 8513-8521.

Jacoby, T., Flanagan, H., Faykin, A., Seto, A.G., Mattison, C., and Ota, I. (1997). Two protein-tyrosine phosphatases inactivate the osmotic stress response pathway in yeast by targeting the mitogen-activated protein kinase, Hog1. The Journal of biological chemistry *272*, 17749-17755.

Ji, R.R., Gereau, R.W.t., Malcangio, M., and Strichartz, G.R. (2009). MAP kinase and pain. Brain Res Rev *60*, 135-148.

Jin, Y., and Garner, C.C. (2008). Molecular mechanisms of presynaptic differentiation. Annu Rev Cell Dev Biol *24*, 237-262.

Kim, J.H., Wang, X., Coolon, R., and Ye, B. (2013). Dscam expression levels determine presynaptic arbor sizes in Drosophila sensory neurons. Neuron *78*, 827-838.

Klassen, M.P., and Shen, K. (2007). Wnt signaling positions neuromuscular connectivity by inhibiting synapse formation in C. elegans. Cell *130*, 704-716.

Klinedinst, S., Wang, X., Xiong, X., Haenfler, J.M., and Collins, C.A. (2013). Independent Pathways Downstream of the Wnd/DLK MAPKKK Regulate Synaptic Structure, Axonal Transport, and Injury Signaling. The Journal of neuroscience : the official journal of the Society for Neuroscience *33*, 12764-12778.

Kolodkin, A.L. (1996). Growth cones and the cues that repel them. Trends Neurosci *19*, 507-513.

Kolodkin, A.L., and Tessier-Lavigne, M. (2011). Mechanisms and molecules of neuronal wiring: a primer. Cold Spring Harb Perspect Biol *3*.

Lander, E.S., Linton, L.M., Birren, B., Nusbaum, C., Zody, M.C., Baldwin, J., Devon, K., Dewar, K., Doyle, M., FitzHugh, W*., et al.* (2001). Initial sequencing and analysis of the human genome. Nature *409*, 860-921.

Lewcock, J.W., Genoud, N., Lettieri, K., and Pfaff, S.L. (2007). The ubiquitin ligase Phr1 regulates axon outgrowth through modulation of microtubule dynamics. Neuron *56*, 604-620.

Li, D., Wang, F., Lai, M., Chen, Y., and Zhang, J.F. (2005). A protein phosphatase 2calpha-Ca2+ channel complex for dephosphorylation of neuronal Ca2+ channels phosphorylated by protein kinase C. The Journal of neuroscience : the official journal of the Society for Neuroscience *25*, 1914-1923.

Li, H., Kulkarni, G., and Wadsworth, W.G. (2008). RPM-1, a Caenorhabditis elegans protein that functions in presynaptic differentiation, negatively regulates axon outgrowth by controlling SAX-3/robo and UNC-5/UNC5 activity. The Journal of neuroscience : the official journal of the Society for Neuroscience *28*, 3595-3603.

Liao, E.H., Hung, W., Abrams, B., and Zhen, M. (2004). An SCF-like ubiquitin ligase complex that controls presynaptic differentiation. Nature *430*, 345-350.

Locke, C.J., Fox, S.A., Caldwell, G.A., and Caldwell, K.A. (2008). Acetaminophen attenuates dopamine neuron degeneration in animal models of Parkinson's disease. Neurosci Lett *439*, 129-133.

Lu, G., and Wang, Y. (2008). Functional diversity of mammalian type 2C protein phosphatase isoforms: new tales from an old family. Clin Exp Pharmacol Physiol *35*, 107-112.

Maeda, T., Wurgler-Murphy, S.M., and Saito, H. (1994). A two-component system that regulates an osmosensing MAP kinase cascade in yeast. Nature *369*, 242-245.

Margeta, M.A., Shen, K., and Grill, B. (2008). Building a synapse: lessons on synaptic specificity and presynaptic assembly from the nematode C. elegans. Curr Opin Neurobiol *18*, 69-76.

Mata, M., Merritt, S.E., Fan, G., Yu, G.G., and Holzman, L.B. (1996). Characterization of dual leucine zipper-bearing kinase, a mixed lineage kinase present in synaptic terminals whose phosphorylation state is regulated by membrane depolarization via calcineurin. The Journal of biological chemistry *271*, 16888-16896.

McGeachie, A.B., Cingolani, L.A., and Goda, Y. (2011). Stabilising influence: integrins in regulation of synaptic plasticity. Neurosci Res *70*, 24-29.

Mello, C.C., Kramer, J.M., Stinchcomb, D., and Ambros, V. (1991). Efficient gene transfer in C.elegans: extrachromosomal maintenance and integration of transforming sequences. Embo J *10*, 3959-3970.

Meskiene, I., Bogre, L., Glaser, W., Balog, J., Brandstotter, M., Zwerger, K., Ammerer, G., and Hirt, H. (1998). MP2C, a plant protein phosphatase 2C, functions as a negative regulator of mitogen-activated protein kinase pathways in yeast and plants. Proc Natl Acad Sci U S A *95*, 1938-1943.

Meyer, M.P., and Smith, S.J. (2006). Evidence from in vivo imaging that synaptogenesis guides the growth and branching of axonal arbors by two distinct mechanisms. The Journal of neuroscience : the official journal of the Society for Neuroscience *26*, 3604-3614.

Miller, B.R., Press, C., Daniels, R.W., Sasaki, Y., Milbrandt, J., and DiAntonio, A. (2009). A dual leucine kinase-dependent axon self-destruction program promotes Wallerian degeneration. Nat Neurosci *12*, 387-389.

Murthy, V., Han, S., Beauchamp, R.L., Smith, N., Haddad, L.A., Ito, N., and Ramesh, V. (2004). Pam and its ortholog highwire interact with and may negatively regulate the TSC1.TSC2 complex. The Journal of biological chemistry *279*, 1351-1358.

Nakata, K., Abrams, B., Grill, B., Goncharov, A., Huang, X., Chisholm, A.D., and Jin, Y. (2005). Regulation of a DLK-1 and p38 MAP kinase pathway by the ubiquitin ligase RPM-1 is required for presynaptic development. Cell *120*, 407-420.

Nguyen, A.N., and Shiozaki, K. (1999). Heat-shock-induced activation of stress MAP kinase is regulated by threonine- and tyrosine-specific phosphatases. Genes Dev *13*, 1653-1663.

Nihalani, D., Merritt, S., and Holzman, L.B. (2000). Identification of structural and functional domains in mixed lineage kinase dual leucine zipper-bearing kinase required for complex formation and stress-activated protein kinase activation. The Journal of biological chemistry *275*, 7273-7279.

Nihalani, D., Meyer, D., Pajni, S., and Holzman, L.B. (2001). Mixed lineage kinase-dependent JNK activation is governed by interactions of scaffold protein JIP with MAPK module components. EMBO J *20*, 3447-3458.

Nix, P., Hisamoto, N., Matsumoto, K., and Bastiani, M. (2011). Axon regeneration requires coordinate activation of p38 and JNK MAPK pathways. Proc Natl Acad Sci U S A *108*, 10738-10743.

O'Donnell, M., Chance, R.K., and Bashaw, G.J. (2009). Axon growth and guidance: receptor regulation and signal transduction. Annu Rev Neurosci *32*, 383-412.

Ogg, S., Paradis, S., Gottlieb, S., Patterson, G.I., Lee, L., Tissenbaum, H.A., and Ruvkun, G. (1997). The Fork head transcription factor DAF-16 transduces insulin-like metabolic and longevity signals in C. elegans. Nature *389*, 994-999.

Opperman, K.J., and Grill, B. (2014). RPM-1 is localized to distinct subcellular compartments and regulates axon length in GABAergic motor neurons. Neural Dev *9*, 10.

Pack-Chung, E., Kurshan, P.T., Dickman, D.K., and Schwarz, T.L. (2007). A Drosophila kinesin required for synaptic bouton formation and synaptic vesicle transport. Nat Neurosci *10*, 980-989.

Park, E.C., Glodowski, D.R., and Rongo, C. (2009). The ubiquitin ligase RPM-1 and the p38 MAPK PMK-3 regulate AMPA receptor trafficking. PLoS One *4*, e4284.

Pierre, S., Maeurer, C., Coste, O., Becker, W., Schmidtko, A., Holland, S., Wittpoth, C., Geisslinger, G., and Scholich, K. (2008). Toponomics analysis of functional interactions of the ubiquitin ligase PAM (Protein Associated with Myc) during spinal nociceptive processing. Mol Cell Proteomics *7*, 2475-2485.

Pierre, S.C., Hausler, J., Birod, K., Geisslinger, G., and Scholich, K. (2004). PAM mediates sustained inhibition of cAMP signaling by sphingosine-1-phosphate. EMBO J *23*, 3031-3040.

Po, M.D., Hwang, C., and Zhen, M. (2010). PHRs: bridging axon guidance, outgrowth and synapse development. Curr Opin Neurobiol *20*, 100-107.

Poon, V.Y., Klassen, M.P., and Shen, K. (2008). UNC-6/netrin and its receptor UNC-5 locally exclude presynaptic components from dendrites. Nature *455*, 669-673.

Raff, M.C., Whitmore, A.V., and Finn, J.T. (2002). Axonal self-destruction and neurodegeneration. Science *296*, 868-871.

Ranganathan, R., Sawin, E.R., Trent, C., and Horvitz, H.R. (2001). Mutations in the Caenorhabditis elegans serotonin reuptake transporter MOD-5 reveal serotonin-dependent and -independent activities of fluoxetine. The Journal of neuroscience : the official journal of the Society for Neuroscience *21*, 5871-5884.

Refai, O., Rohs, P., Mains, P.E., and Gaudet, J. (2013). Extension of the Caenorhabditis elegans Pharyngeal M1 neuron axon is regulated by multiple mechanisms. G3 (Bethesda) *3*, 2015-2029.

Riddle, D.L., Blumenthal, T., Meyer, B.J., and Priess, J.R. (1997). Introduction to C. elegans. In C elegans II, D.L. Riddle, T. Blumenthal, B.J. Meyer, and J.R. Priess, eds. (Cold Spring Harbor (NY)).

Ruthazer, E.S., Li, J., and Cline, H.T. (2006). Stabilization of axon branch dynamics by synaptic maturation. The Journal of neuroscience : the official journal of the Society for Neuroscience *26*, 3594-3603.

Saha, S., and Wolozin, B. (2011). A simple, quantitative immunoblot protocol using equal numbers of nematodes. Worm Breeder's Gazette *19*, 6-7.

Saiga, T., Fukuda, T., Matsumoto, M., Tada, H., Okano, H.J., Okano, H., and Nakayama, K.I. (2009). Fbxo45 forms a novel ubiquitin ligase complex and is required for neuronal development. Molecular and cellular biology *29*, 3529-3543.

Saito, H., and Tatebayashi, K. (2004). Regulation of the osmoregulatory HOG MAPK cascade in yeast. J Biochem *136*, 267-272.

Sakuma, H., Ikeda, A., Oka, S., Kozutsumi, Y., Zanetta, J.P., and Kawasaki, T. (1997). Molecular cloning and functional expression of a cDNA encoding a new member of mixed lineage protein kinase from human brain. The Journal of biological chemistry *272*, 28622-28629.

Samuels, I.S., Saitta, S.C., and Landreth, G.E. (2009). MAP'ing CNS development and cognition: an ERKsome process. Neuron *61*, 160-167.

Schaefer, A.M., Hadwiger, G.D., and Nonet, M.L. (2000). rpm-1, a conserved neuronal gene that regulates targeting and synaptogenesis in C. elegans. Neuron *26*, 345-356.

Scheiffele, P. (2003). Cell-cell signaling during synapse formation in the CNS. Annu Rev Neurosci *26*, 485-508.

Scholich, K., Pierre, S., and Patel, T.B. (2001). Protein associated with Myc (PAM) is a potent inhibitor of adenylyl cyclases. The Journal of biological chemistry *276*, 47583-47589.

Schwertassek, U., Buckley, D.A., Xu, C.F., Lindsay, A.J., McCaffrey, M.W., Neubert, T.A., and Tonks, N.K. (2010). Myristoylation of the dual-specificity phosphatase c-JUN N-terminal kinase (JNK) stimulatory phosphatase 1 is necessary for its activation of JNK signaling and apoptosis. FEBS J *277*, 2463-2473.

Shapira, M., Zhai, R.G., Dresbach, T., Bresler, T., Torres, V.I., Gundelfinger, E.D., Ziv, N.E., and Garner, C.C. (2003). Unitary assembly of presynaptic active zones from Piccolo-Bassoon transport vesicles. Neuron *38*, 237-252.

Shen, K., and Cowan, C.W. (2010). Guidance molecules in synapse formation and plasticity. Cold Spring Harb Perspect Biol *2*, a001842.

Shen, K., and Scheiffele, P. (2010). Genetics and cell biology of building specific synaptic connectivity. Annu Rev Neurosci *33*, 473-507.

Shi, Y. (2009). Serine/threonine phosphatases: mechanism through structure. Cell *139*, 468-484.

Shin, J.E., Cho, Y., Beirowski, B., Milbrandt, J., Cavalli, V., and Diantonio, A. (2012). Dual leucine zipper kinase is required for retrograde injury signaling and axonal regeneration. Neuron *74*, 1015-1022.

Shin, J.E., and DiAntonio, A. (2011). Highwire regulates guidance of sister axons in the Drosophila mushroom body. The Journal of neuroscience : the official journal of the Society for Neuroscience *31*, 17689-17700.

Siddiqui, T.J., and Craig, A.M. (2011). Synaptic organizing complexes. Curr Opin Neurobiol *21*, 132-143.

Stern, A., Privman, E., Rasis, M., Lavi, S., and Pupko, T. (2007). Evolution of the metazoan protein phosphatase 2C superfamily. J Mol Evol *64*, 61-70.

Sudhof, T.C. (2008). Neuroligins and neurexins link synaptic function to cognitive disease. Nature *455*, 903-911.

Sudhof, T.C. (2012). The presynaptic active zone. Neuron *75*, 11-25.

Sun, H., Charles, C.H., Lau, L.F., and Tonks, N.K. (1993). MKP-1 (3CH134), an immediate early gene product, is a dual specificity phosphatase that dephosphorylates MAP kinase in vivo. Cell *75*, 487-493.

Sundaram, M., and Greenwald, I. (1993). Suppressors of a lin-12 hypomorph define genes that interact with both lin-12 and glp-1 in Caenorhabditis elegans. Genetics *135*, 765-783.

Takekawa, M., Maeda, T., and Saito, H. (1998). Protein phosphatase 2Calpha inhibits the human stress-responsive p38 and JNK MAPK pathways. EMBO J *17*, 4744-4752.

Tian, X., Li, J., Valakh, V., DiAntonio, A., and Wu, C. (2011). Drosophila Rae1 controls the abundance of the ubiquitin ligase Highwire in post-mitotic neurons. Nat Neurosci *14*, 1267-1275.

Tulgren, E.D., Baker, S.T., Rapp, L., Gurney, A.M., and Grill, B. (2011). PPM-1, a PP2Calpha/beta phosphatase, regulates axon termination and synapse formation in Caenorhabditis elegans. Genetics *189*, 1297-1307.

Tulgren, E.D., Turgeon, S.M., Opperman, K.J., and Grill, B. (2014). The Nesprin family member ANC-1 regulates synapse formation and axon termination by functioning in a pathway with RPM-1 and beta-Catenin. PLoS genetics *10*, e1004481.

Valakh, V., Walker, L.J., Skeath, J.B., and DiAntonio, A. (2013). Loss of the spectraplakin short stop activates the DLK injury response pathway in Drosophila. The Journal of neuroscience : the official journal of the Society for Neuroscience *33*, 17863-17873.

Venter, J.C., Adams, M.D., Myers, E.W., Li, P.W., Mural, R.J., Sutton, G.G., Smith, H.O., Yandell, M., Evans, C.A., Holt, R.A.*, et al.* (2001). The sequence of the human genome. Science *291*, 1304-1351.

Wan, H.I., DiAntonio, A., Fetter, R.D., Bergstrom, K., Strauss, R., and Goodman, C.S. (2000). Highwire regulates synaptic growth in Drosophila. Neuron *26*, 313-329.

Wang, X., Kim, J.H., Bazzi, M., Robinson, S., Collins, C.A., and Ye, B. (2013). Bimodal control of dendritic and axonal growth by the dual leucine zipper kinase pathway. PLoS Biol *11*, e1001572.

Watkins, T.A., Wang, B., Huntwork-Rodriguez, S., Yang, J., Jiang, Z., Eastham-Anderson, J., Modrusan, Z., Kaminker, J.S., Tessier-Lavigne, M., and Lewcock, J.W.

(2013). DLK initiates a transcriptional program that couples apoptotic and regenerative responses to axonal injury. Proc Natl Acad Sci U S A *110*, 4039-4044.

White, J.G., Southgate, E., Thomson, J.N., and Brenner, S. (1986). The structure of the nervous system of the nematode *C. elegans*. Philos Trans R Soc Lond B Biol Sci *314B*, 1-340.

Wu, C., Daniels, R.W., and DiAntonio, A. (2007). DFsn collaborates with Highwire to down-regulate the Wallenda/DLK kinase and restrain synaptic terminal growth. Neural Dev *2*, 16.

Wu, C., Wairkar, Y.P., Collins, C.A., and DiAntonio, A. (2005). Highwire function at the Drosophila neuromuscular junction: spatial, structural, and temporal requirements. The Journal of neuroscience : the official journal of the Society for Neuroscience *25*, 9557-9566.

Xiong, X., and Collins, C.A. (2012). A conditioning lesion protects axons from degeneration via the Wallenda/DLK MAP kinase signaling cascade. The Journal of neuroscience : the official journal of the Society for Neuroscience *32*, 610-615.

Xiong, X., Hao, Y., Sun, K., Li, J., Li, X., Mishra, B., Soppina, P., Wu, C., Hume, R.I., and Collins, C.A. (2012). The Highwire ubiquitin ligase promotes axonal degeneration by tuning levels of Nmnat protein. PLoS Biol *10*, e1001440.

Xiong, X., Wang, X., Ewanek, R., Bhat, P., Diantonio, A., and Collins, C.A. (2010). Protein turnover of the Wallenda/DLK kinase regulates a retrograde response to axonal injury. J Cell Biol *191*, 211-223.

Yamagata, M., Sanes, J.R., and Weiner, J.A. (2003). Synaptic adhesion molecules. Curr Opin Cell Biol *15*, 621-632.

Yan, D., and Jin, Y. (2012). Regulation of DLK-1 Kinase Activity by Calcium-Mediated Dissociation from an Inhibitory Isoform. Neuron *76*, 534-548.

Yan, D., Wu, Z., Chisholm, A.D., and Jin, Y. (2009). The DLK-1 kinase promotes mRNA stability and local translation in C. elegans synapses and axon regeneration. Cell *138*, 1005-1018.

Yoshihara, M., Rheuben, M.B., and Kidokoro, Y. (1997). Transition from growth cone to functional motor nerve terminal in Drosophila embryos. The Journal of neuroscience : the official journal of the Society for Neuroscience *17*, 8408-8426.

Zhai, Q., Wang, J., Kim, A., Liu, Q., Watts, R., Hoopfer, E., Mitchison, T., Luo, L., and He, Z. (2003). Involvement of the ubiquitin-proteasome system in the early stages of wallerian degeneration. Neuron *39*, 217-225.

Zhai, R.G., Zhang, F., Hiesinger, P.R., Cao, Y., Haueter, C.M., and Bellen, H.J. (2008). NAD synthase NMNAT acts as a chaperone to protect against neurodegeneration. Nature *452*, 887-891.

Zhao, H., and Nonet, M.L. (2000). A retrograde signal is involved in activity-dependent remodeling at a C. elegans neuromuscular junction. Development *127*, 1253-1266.

Zhao, Y., and Sun, Y. (2013). Cullin-RING Ligases as attractive anti-cancer targets. Curr Pharm Des *19*, 3215-3225.

Zhen, M., Huang, X., Bamber, B., and Jin, Y. (2000). Regulation of presynaptic terminal organization by C. elegans RPM-1, a putative guanine nucleotide exchanger with a RING-H2 finger domain. Neuron *26*, 331-343.

Zheng, N., Schulman, B.A., Song, L., Miller, J.J., Jeffrey, P.D., Wang, P., Chu, C., Koepp, D.M., Elledge, S.J., Pagano, M.*, et al.* (2002). Structure of the Cul1-Rbx1-Skp1-F boxSkp2 SCF ubiquitin ligase complex. Nature *416*, 703-709.

Zito, K., Parnas, D., Fetter, R.D., Isacoff, E.Y., and Goodman, C.S. (1999). Watching a synapse grow: noninvasive confocal imaging of synaptic growth in Drosophila. Neuron *22*, 719-729.

Ziv, N.E., and Garner, C.C. (2004). Cellular and molecular mechanisms of presynaptic assembly. Nat Rev Neurosci *5*, 385-399.